



Universitat Autònoma de Barcelona

ADVERTIMENT. L'accés als continguts d'aquesta tesi queda condicionat a l'acceptació de les condicions d'ús establertes per la següent llicència Creative Commons:  http://cat.creativecommons.org/?page_id=184

ADVERTENCIA. El acceso a los contenidos de esta tesis queda condicionado a la aceptación de las condiciones de uso establecidas por la siguiente licencia Creative Commons:  <http://es.creativecommons.org/blog/licencias/>

WARNING. The access to the contents of this doctoral thesis it is limited to the acceptance of the use conditions set by the following Creative Commons license:  <https://creativecommons.org/licenses/?lang=en>

Novel therapeutic strategy for muscle disorders

Presented by Sara Marmolejo Martínez-Artesero

ACADEMIC DISSERTATION

To obtain the Degree of PhD in Neuroscience of the
Universitat Autònoma de Barcelona, 2020

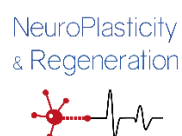
Group of Neuroplasticity and Regeneration

Institut de Neurociències

Departament de Biologia Cel·lular, Fisiologia i Immunologia

Supervised by:

Caty Casas



INDEX

SUMMARY	1
Articles produced from the work of this thesis	2
ABBREVIATIONS	3
INTRODUCTION	4
1. The neuromuscular system	5
1.1 Skeletal muscle	5
1.2 Control of skeletal muscle activity	7
1.2.1 The motor nervous system	7
1.2.2 Excitation-Contraction Coupling	9
1.2.3 Cross-Bridge Cycle	10
1.3 Skeletal Muscle Types	10
2. Skeletal muscle alterations	11
2.1 Muscle wasting	12
2.1.1 Atrophy caused by denervation	12
2.2 Muscle injury	14
2.2.1 Classification	14
2.2.2 Characteristics	16
2.2.3 Therapies	16
2.3 Therapies under study: NeuroHeal	17
3. Molecular mechanisms in muscle metabolism	19
3.1 Molecular mechanisms in muscle atrophy	19
3.1.1 UB-proteasome system	19
3.1.1.1 Atrogenes: MuRF1 and MabF _x /Atrogin-1	20
3.1.2 Autophagy	21
3.2 Molecular mechanisms in muscle regeneration	23
3.3 SIRT1 and skeletal muscle	27
HYPOTHESIS AND OBJECTIVES	29
STUDY DESIGN AND METHODOLOGIES	31
RESULTS	37
Chapter I	38
Chapter II	58
GENERAL DISCUSSION	75
CONCLUSIONS	82
REFERENCES	84
ACKNOWLEDGEMENTS	99

SUMMARY

Skeletal muscle alterations appear due to different reasons, such as chronic diseases, muscular dystrophies, neurodegenerative diseases, traumatic injuries at different levels (nerve, muscle, or bone), and aging. These alterations usually produce muscle atrophy, which is a reduction of muscle mass and muscle function, and is provoked by protein metabolism imbalance consisting in an excessive protein breakdown. Skeletal muscle has limited regenerative capabilities for self-repair after trauma or muscular diseases. That self-repairing ability is derived by satellite cells (SCs), which are a muscle-specific stem cells that are activated and follow a process of differentiation giving newly formed myofibers. All current available pharmacological and biological agents only relieve clinical symptoms and have limited or no effect on the progression of the underlining muscle disease. In some cases, the endogenous process of muscle repair proves insufficient, leading to loss of contractile tissue, fatty degeneration, and fibrotic scar tissue, which cause long-term deficits in muscle structure and strength.

We have recently discovered a neuroprotective drug, termed as NeuroHeal, for peripheral nerve injury (PNI). NeuroHeal is based on the combination of two approved drugs (Acamprosate and Ribavirin), and was discovered using artificial intelligence and systems biology-based networks, which facilitate its readiness for clinical use. Using a model of severe PNI, we observed that NeuroHeal enhanced nerve regeneration and reduced the associated muscle atrophy. Thus, we aimed to decipher the novel therapeutic effect of NeuroHeal for muscle tissue disorders, focusing on *in vivo* models of muscle atrophy and muscle injury. We pursued to elucidate if NeuroHeal also endorsed protective mechanisms against atrophy and regenerative effects to promote muscle tissue recovery after disuse or injury.

In order to know whether NeuroHeal had a direct effect on muscle atrophy, we used two *in vivo* models of atrophy, muscle denervation and a hindlimb immobilization, and *in vitro* model, the cell line C2C12 atrophy-induced by TNF α . We observed that NeuroHeal prevented the reduction of myofibers, reduced the catalytic activity of the UPS, and induced a correct resolution of autophagy. To elucidate whether NeuroHeal modulates muscle regeneration, we used an *in vivo* model of a surgically-induced lesion which mimics the most frequent skeletal muscle lesions observed in human sport clinics. NeuroHeal promoted the regenerative response of the skeletal muscle, enhancing activation and differentiation of the SCs, by the activation of SIRT1. This was accompanied by an increase in muscle contraction and a fast myosin fiber-switch. In both cases, we observed that SIRT1 activity is needed for the protective effects of NeuroHeal.

Overall, we conclude that NeuroHeal could be clinically used to reduce muscle atrophy and accelerate muscle regeneration for different clinical affectations such as neurodegenerative diseases, peripheral nerve injuries, or muscle direct injuries, and probably also as a treatment in various muscle diseases due to its ability to activate protective and myogenic mechanisms via SIRT1.

ARTICLES PRODUCED FROM THE WORK OF THIS THESIS

Published:

- Marmolejo-Martínez-Artesero S., Romeo-Guitart D., Mañas-García L., Barreiro E., Casas C. (2020) **NeuroHeal Reduces Muscle Atrophy and Modulates Associated Autophagy**. *Cells* 9:1575.

In preparation:

- Marmolejo-Martínez-Artesero S., Romeo-Guitart D. Venegas V., Marotta M., Casas C. **NeuroHeal improves Muscle Regeneration after Injury**.

Other publications during the thesis:

- Romeo-Guitart D., Marmolejo-Martínez-Artesero S., Casas C. (2020) **Is it the time of autophagy fine-tuners for neuroprotection?** *Autophagy*.
- Romeo-Guitart D, Marcos-DeJuana C, Marmolejo-Martínez-Artesero S, Navarro X, Casas C. (2020) **Novel neuroprotective therapy with NeuroHeal by autophagy induction for damaged neonatal motoneurons**. *Theranostics* 10:5154–5168.
- Leiva-Rodríguez, T., Romeo-Guitart, D., Marmolejo-Martínez-Artesero, S., Herrando-Grabulosa, M., Bosch, A., Forés, J., Casas, C. (2018) **ATG5 overexpression is neuroprotective and attenuates cytoskeletal and vesicle-Trafficking alterations in axotomized motoneurons**. *Cell Death and Disease* 9: 626.

ABBREVIATIONS

ACA: Acamprosate	MyHC: Myosin heavy chain
ALS: Amyotrophic lateral sclerosis	MyoG: Myogenin
AP: Action potential	NAM: Nicotinamide
ATG: Autophagy-related genes	NH: NeuroHeal
CMAP: Compound muscle action potential	NMJ: Neuromuscular junctions
CNS: Central nervous system	p62: Sequestosome 1
CSA: Cross-sectional area	PBS: Phosphate buffered Saline
CT: Contraction time	PF: Peak force
DHRP: Dihydropyridine receptor	PGC1a: Transcription factors g-coactivator 1a
div: Days of in vitro	PNS: Peripheral nervous system
dpi: Days postinjury	PV: Parvalbumin
DMD: Duchenne muscular dystrophy	RA: Root avulsion
DMEM: Modified Eagle's medium high-glucose	RIB: Ribavirin
ECM: Extracellular matrix	RyR: Ryanodine receptor
EMG: Electromyography	SC: Satellite cell
FoxO: Forkhead box O	SIRT: Sirtuin
GA: Gastrocnemius muscle	SR: Sarcoplasmic reticulum
H&E: Hematoxylin and Eosin	s5α: Proteasome subunit 5 α
HRT: Half-relaxation time	TBS: Tris-buffered saline
IHC: Immunohistochemistry	TetF: Maximum tetanus force
KO: Knock out	TNFα: Tumor Necrosis Factor- α
LC3-I: Microtubule-associated protein 1 light chain 3	TPMS: Therapeutic Performance Mapping System
MAFbx: Muscle atrophy F-box protein	Ulk1: Unc-51-like kinase 1
MN: Motoneuron	Ub: Ubiquitin
mTOR: Mammalian target of Rapamycin	UPS: Ubiquitin-proteasome system
MuRF1: Muscle RING Finger-containing protein 1	WB: Western Blot

INTRODUCTION

1. THE NEUROMUSCULAR SYSTEM

The neuromuscular system is responsible for performing all the body movements, controlling posture, active motions and maintaining respiratory function. To carry out all these activities, a fine interaction between the nervous system and the muscular system is needed.

1.1 Skeletal muscle

Each individual muscle is formed by muscle fascicles and is surrounded by the epimysium, a layer of connective tissue (**Fig. 1**). The connective layer perimysium surrounds each fascicle, where there are vessels, nerves and proprioceptors. Each muscle fascicle is formed by many myofibers, also referred to as muscle cells or muscle fibers. Each myofiber is composed by a membrane or sarcolemma, cytoplasm or sarcoplasm, and numerous peripheral nuclei. Myofibers contain many parallel myofibrils occupying most of the intracellular space. Cell organelles, mitochondria, and nuclei are localized in the periphery of the sarcoplasm. The endomysium surrounds each of these fibers.

To attach the muscle to the skeleton, the connective tissue layers come together to form a tendon. In this region, there is the myotendinous junction where the contraction force is transmitted from the muscle to the tendon.

Each myofibril is subdivided longitudinally into sarcomeres. The sarcomere is a very organized structure with well-defined areas. It constitutes the simplest functional unit of a myofibril, being the basis for the muscle contractile properties. This is composed of two sets of protein filaments: the thin and the thick filaments, which run parallel to the muscle fiber axis (Huxley 1957). Each myofibril in a muscle fiber is surrounded by sarcoplasmic reticulum (SR). The portions of the SR nearest the T tubules, which are invaginations of the sarcolemma, are called the terminal cisternae. The thin filament is formed by the aggregation of actin molecules. Across the entire actin filament there are dimers of tropomyosin which cover the myosin binding-sites. A troponin complex is composed of three subunits, troponin T, troponin I, and troponin C. Additional proteins associated with the thin filament include tropomodulin, α -actinin, and CapZ. The thick myosin filaments are attached to the sarcomere by the cytoskeletal protein Titin. Integrins are linked to the myofibrils by the cytoskeletal protein Desmin. Both cytoskeletal proteins help to organize and align the sarcomere.

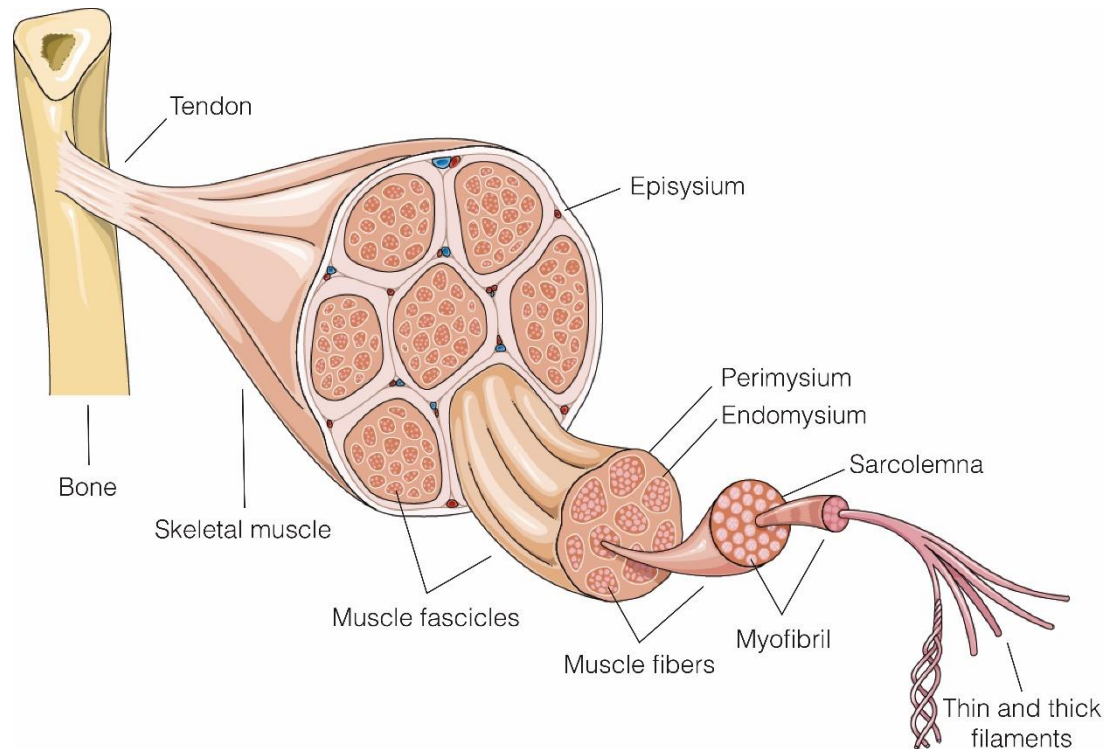


Figure 1. Skeletal muscle gross anatomy and ultrastructure. Skeletal muscle is formed by groups of fascicles. The fascicles are formed by groups of parallel fibers, the unit structure of muscle tissue. The fibers are formed by multiple myofibers, intracellular contractile fibers built from sarcomeres. Skeletal muscles are attached to the bone by tendons composed by connective tissue (Free from Smart Servier Medical Art).

The extracellular matrix (ECM) is the non-contractile section of the muscle. It is formed by fibroblasts, macrophages, and contains capillary and nerve networks. ECM acts as a scaffold distributing and transmitting a force within the muscle, and from the muscle to the tendon. This structure is flexible enough to be adapted to contraction-relaxation cycles. The muscle ECM is formed by three main classes of proteins: collagens, non-collagenous glycoproteins, and proteoglycans. Collagens represent the largest fraction of matrix proteins within the muscle. The predominant collagen is type I, which has high tensile strength and load-bearing properties. Collagen VI forms a network of fine filaments and is the structural component of the basement membrane, integrating laminins, nidogens, and other proteins into a stable structure. Fibroblasts are responsible for ECM synthesis and remodeling (Murphy et al., 2011). When there is an excessive accumulation of ECM production or/and alteration in ECM-degrading activities, it results in a fibrotic phenotype. This accumulation is present in the endomysium and perimysium of skeletal muscle. Muscle fibrosis is closely associated and overlaps with inflammation, sarcopenia, recovery after muscle injury, and atrophy.

1.2 Control of skeletal muscle activity

To carry out all the physical actions performed by the human body, the nervous system needs the precise controlled activation of specific muscles. For each action, the nervous system is in charge of deciding which muscles to activate, when and for how long they have to be activated.

1.2.1 The motor nervous system

The activation signal sent from the nervous system to muscle arises from motoneurons (MNs) present in the spinal cord or brain stem.

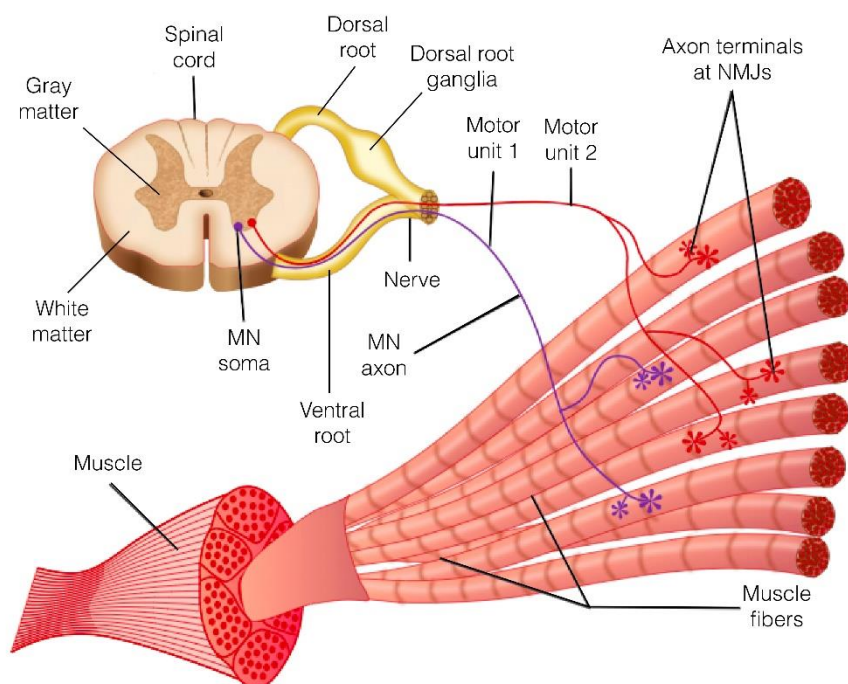


Figure 2. The motor unit. The axon of a MN leaves the spinal cord, near the muscle ramified and innervate several muscle fibers, forming a motor unit. The NMJ is the specialized synapses between the motor nerve terminal and the muscle (Modified from Carlson, 2013).

The spinal cord is transversally divided into the white and the gray matter (**Fig. 2**). The white matter is located outside of the grey matter. It mainly consists of myelinated motor and sensory axons. Internally, there is the gray matter, containing the neuronal cell bodies, with a butterfly-shape. The gray matter is divided into dorsal and ventral horns which are separated by an intermediate zone. The ventral horn is where MNs reside and are group in the motor nuclei. This horn is the main target of descending motor pathways from the brain. In contrast, the dorsal horn is the main source of ascending sensory pathways where there is incoming sensory information.

A MN is a neuron which projects to muscle cells. It represents the only route for central nervous system (CNS) activity to control muscle action. MNs receive inputs from the motor primary cortex, brainstem control nuclei, and inputs of sensory afferents to close reflex arches. Two main classes of somatic MNs are distinguished based on their size and axonal diameter. The α -MNs innervate the contractile muscle fibers and γ -MNs innervate the intrafusal fibers within the muscle spindles. So, the γ -MNs are smaller than α -MNs. The γ -MNs and α -MNs which project to the same muscle, are located in the same region of the ventral horn. γ -MNs synapse on the specialized striated muscle fibers called intrafusal muscle fibers. The function of γ -MNs is to regulate the sensitivity of the spindle receptors.

MNs are surrounded and supported by different cellular types as microglia, astroglia, oligodendrocytes, and ependymal cells. Although they have different functions, they maintain the optimal performance of the nervous system by sustaining, feeding, and ensuring neuronal correct function. They protect MNs from external or internal insults. Indeed, microglia expresses receptors for some neurotransmitters and neuropeptides to monitor the state of the neurons (Pocock and Kettenmann, 2007). The astrocytes reuptake the exceed of neurotransmitter to maintain the CNS homeostasis (Perdan et al., 2009). Microglia secrete different factors to sustain neuronal survival (Colonna and Butovsky, 2017) or support neurons favoring functional recovery after injury (Song et al., 2016). Therefore, microglia have an active role in neuroplasticity. In the same way, the CNS is protected by the blood-brain barrier, helping to maintain a correct homeostatic environment and isolating neurons from damaging compounds.

The MN axons leave the spinal cord through the ventral roots (**Fig. 2**). Then, they are distributed to the appropriate skeletal muscles via peripheral nerves. These nerves are composed of axons, fibroblasts, blood vessels supplying the tissue, and Schwann cells. Schwann cells are responsible for axon myelination to increase their conduction velocity. The peripheral nervous system (PNS) provides an interface between the environment and the CNS. It facilitates the sensory information flowing to the CNS and for motor commands issued from the CNS. The axon terminates by synapsing onto the extrafusal muscle fibers. These synapses are called neuromuscular junctions (NMJ) or endplates. Each extrafusal muscle fiber in mammals is supplied by only one α -MN. Thus, a motor unit can be defined as an α -MN and all of the skeletal muscle fibers that its axon innervates, being the basic unit of movement. Its function allows synchronous contraction in all the muscle fibers when the motor nerve fires an action potential (AP).

MNs are cholinergic neurons which release the neurotransmitter acetylcholine at the NMJs. Acetylcholine controls the gating of a cation-selective channel in the motor endplate of skeletal muscle cells. Acetylcholine is synthesized in the cytoplasm of cholinergic presynaptic terminals. After synthesis, acetylcholine is concentrated in

vesicles. After release, the action of acetylcholine is terminated by the enzyme acetylcholinesterase, which is highly concentrated in the synaptic cleft. Acetylcholinesterase hydrolyzes acetylcholine. When acetylcholine is released from the α -MN at the NMJ, this initiates an AP in the muscle fiber. An AP is a change in the membrane potential by which the cell transmits the nerve impulse. The AP rapidly spreads along the sarcolemma and the T tubules, allowing very rapid contraction of the fiber. When several MNs are excited jointly, the resulting activation of the motor unit can be recorded as a compound muscle action potential (CMAP). When there is a disease or after an injury, this response can be altered. For that reason, CMAPs can be monitored by electrophysiological techniques to study the state of MNs in neuromuscular diseases (Morales et al 1987) or the grade of axon regeneration, and muscle recovery after nerve injury (Navarro, 2016).

1.2.2 Excitation-Contraction Coupling

The AP is transmitted along the sarcolemma of the muscle fiber. When an AP passes down the T tubules, Ca^{2+} is released from the terminal cisternae into the myoplasm. This release causes an increase in intracellular $[\text{Ca}^{2+}]$, which promotes actin-myosin interaction and contraction. This increase in intracellular $[\text{Ca}^{2+}]$ initiates a contraction called twitch.

The elevation in intracellular $[\text{Ca}^{2+}]$ involves an interaction between proteins in the T tubule and the adjacent terminal cisternae of the SR (Fig. 3). This interaction is mediated by the Ca^{2+} released by the channels Ryanodine receptor (RyR). When the AP passes down the T tubule, there is a conformational change in the voltage-gated Ca^{2+} Dihydropyridine receptor (DHPR). This conformational change opens the RyR and releases Ca^{2+} into the myoplasm. Calsequestrin stores at high $[\text{Ca}^{2+}]$ to establish a favorable concentration gradient. This facilitates the efflux of Ca^{2+} from the SR into the myoplasm when the RyR are opened. Triadin and Junctin anchor calsequestrin near the RyR and increase Ca^{2+} buffering capacity. Relaxation of skeletal muscle occurs when intracellular Ca^{2+} is resequenced by the SR. Uptake of Ca^{2+} into the SR is done by the Ca^{2+} pump SERCA and Parvalbumin (PV). PV is a cytosolic calcium buffer which with high affinity to Ca^{2+} being a relaxing factor (Schwaller, 2012). PV is directly correlated with relaxation speeds of mammalian fast muscle (Rall, 1996), being exclusively expressed in fast fibers (Gundersen et al., 1988; Schwaller et al., 1999; Campbell et al., 2001).

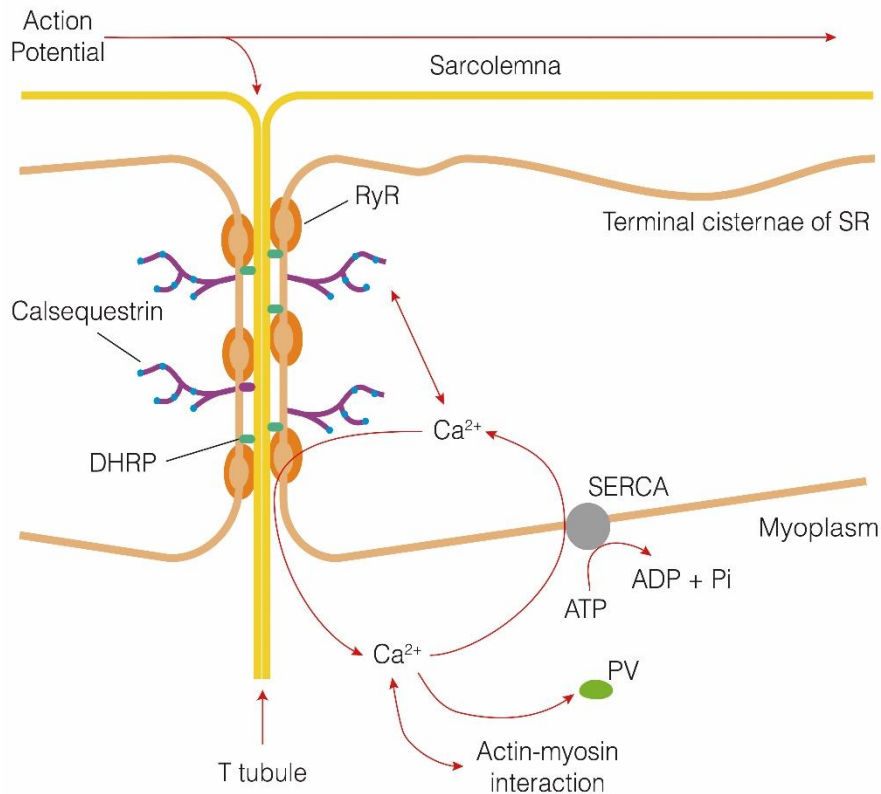


Figure 3. Stimulation of a skeletal muscle fiber and posterior contraction. The initiation of AP in the muscle travels down the T tubule and induces release of Ca^{2+} from the terminal cisternae of the SR. The rise in intracellular $[\text{Ca}^{2+}]$ causes a contraction. As Ca^{2+} is pumped back into the SR by SERCA, relaxation occurs (Based from (Koeppen and Stanton n.d.))

1.2.3 Cross-Bridge Cycle

As noted, the contraction of skeletal muscle requires an increase in intracellular $[\text{Ca}^{2+}]$. The process of contraction is regulated by the thin filament. This process is named Cross-Bridge Cycle and starts when a myosin and an actin are bound. This leads to ATP-dependent conformational changes in the myosin protein, moving the actin filaments toward the center of the sarcomere. Such movement shortens the length of the sarcomere leading to muscle fiber contraction.

1.3 Skeletal Muscle Types

Skeletal muscle fibers can be classified into two main groups according to the speed of contraction: fast-twitch and slow-twitch muscle fibers. The difference in the speed of contraction is correlated with myosin ATPase activity. This reflects the type of myosin present in the muscle fiber. Fast-twitch muscle fibers contain myosin isoforms which hydrolyze ATP quickly, whereas slow-twitch muscle fibers hydrolyze it slowly. The myosin isoforms expressed are distinguished based on Myosin Heavy Chain (MyHC)

composition. Slow-twitch muscle fibers express type I MyHC, whereas fast-twitch skeletal muscle fibers can contain type IIa, type IIx, or type IIb MyHCs. Some fast-twitch muscle fibers may contain a mixture of type II myosin isoforms.

Motor units are generally composed of only one type of muscle fiber, unless the myofibers are undergoing a transition. This fiber change happens in chronic conditions such as microgravity in space flight, denervation, and chronic unloading. These conditions are associated with atrophy. These situations promote the gradual transition from the expression of slow fibers to the expression of fast fibers (types IIa and IIx). Thus, the motor innervation of the muscle fiber plays an important role in determining which type of myosin isoform is expressed in the muscle fiber.

An important function of slow motor units is the maintenance of posture. They resist to fatigue due to smaller diameter and higher capillary density. In contrast, fast muscles participate in activities with faster movements or more force. This extra demand is compensated with an additional recruitment of motor units and a highly developed SR

MNs in slow motor units are more easily excited than in fast units, thus slow motor units are typically recruited first. This is caused by a differential expression of Troponin and Tropomyosin isoforms. Slow fibers begin to develop tension at lower $[Ca^{2+}]$ than fast fibers. This difference is caused by the lower affinity of the troponin C has to Ca^{2+} in slow fibers. Slow-twitch skeletal muscles are also characterized by a high oxidative capacity, which in combination with the low myosin ATPase activity contributes to the fatigue resistance of slow-twitch muscle fibers. The oxidative capacity of the fast-twitch muscle fiber ranges from relatively high (in muscle fibers expressing type IIa MyHC) to low (in muscle fibers expressing type IIb MyHC).

2. SKELETAL MUSCLE ALTERATIONS

Skeletal muscle alterations can be triggered by different reasons. There are many chronic diseases which lead to muscle atrophy, such as cancer or diabetes. Other diseases have alterations in some muscle genes, such as muscular dystrophies. In addition, neurodegenerative diseases such as Amyotrophic lateral sclerosis (ALS) or Spinal muscular atrophy, present a progressive death of the MNs, which eliminates the nervous stimulation of the target muscle. Traumatic injuries at the nerve, muscle or bone level can lead to degeneration of the muscle tissue. Lastly, ageing can lead to muscle disorder called sarcopenia.

2.1 Muscle wasting

Muscle wasting is the result of an imbalance in protein metabolism due to an excess of protein degradation. This protein breakdown excess provokes muscle mass loss. Muscle wasting can be caused by disuse conditions or atrophy, chronic diseases or cachexia, and aging or sarcopenia.

Muscle atrophy can be present in one muscle (bedridden patients or body part immobilization) or can be generalized. This last one is caused by many pathologies with different muscle atrophy degrees, such as obesity, AIDS, aging, alcohol-associated myopathy, cancer, cirrhosis, chronic obstructive pulmonary disease, diabetes, denervation, heart failure, liver or kidney failure, malnutrition, or sepsis.

Muscle wasting is accompanied by histological changes, which present a different pattern depending on the origin. Most of the changes are in myofibers. The most characteristic change is the reduction of the myofiber diameter, although it is accompanied by rounded to angular morphology with hypereosinophilic sarcoplasm. There is an atrophying preference on the myofiber type, which depend on the origin of the muscle wasting. Finally, there is replacement by connective tissue which can lead to a fibrotic phenotype.

2.1.1 Atrophy caused by denervation

Denervation occurs when there is a disconnection between the nervous system and the muscle tissue (Fig. 4). This disconnection can be originated by loss of spinal MNs (MN diseases or spinal cord injury) or by injury to the PNS (nerve injury or neuropathies). This disconnection leads to a loss of the contractile activity and the replacement of the skeletal muscle tissue by connective tissue (fibrosis) and fat. This leads to muscle atrophy (Tower, 1935; Gutmann, 1948). There are three main stages in the atrophy process (Tower, 1935; Lapalombella et al., 2008). During the first stage after the lesion, there is an immediate loss of function, rapid weight loss, and myofiber atrophy. In the second stage, there is an increase in the severity of muscle wasting due to loss of sarcomere organization. In the last, which is the longest, there is general interstitial fibrosis and fat deposits.

During the first phase, lasting two months, the denervated muscle retains a capacity for restoration equal to that of a normal control muscle. The second phase (from 2-7 months), the restorative ability progressively and dramatically declines. The terminal phase (beyond 7 months) is characterized by minimal restorative ability.

During the initial stage there is a preservation of sarcomere structure. In the second stage there is an increase in the ultrastructural changes of the sarcomere (Schmalbruch et al., 1991; Lu et al., 1997; Midrio, 2006). It is observed a loss of myofibrillar alignment

due to a disrupted Z-line registration, and the loss of actin and myosin filaments. All these cause alterations in size, number, and orientation of the SR which change the excitation-coupling system (Takekura et al., 1996). Although there is this disorganization, the muscle spindles are preserved (Lu et al., 1997; Zelena et al., 2017). To compensate this degeneration, satellite cells (SCs) activate the myogenic program (Adams et al., 1995; Batt et al., 2006; Jeng et al., 2009). SCs are resident stem cells which give to the muscle its regenerative capacity. They are quiescent and are activated when there is a metabolic stimulation, such as exercise, or after damage, such as injury or atrophy. This process is observed from the beginning until two months later (de Castro Rodrigues and Schmalbruch, 1995; Viguie et al., 1997; Chen et al., 2010). Regarding tissue level adaptations, there is an increase in the blood flow but with a decrease in capillarity (Carpenter and Karpati, 1982; Borisov et al., 2000; Tysl, 2001). Fibrosis is minimal during the first week (Mochizuki et al., 2005).

The main characteristic of a long-term denervation is fibrosis (Lu et al., 1997; Borisov et al., 2001; Kern et al., 2004; Carraro et al., 2005). There is a replacement of muscle mass by fat and fibrous connective tissue, and a dramatic capillarity loss. Individual atrophic myofibers are embedded in dense mats of collagen fibers. Adipocytes are localized in clumps without any organization (Rodrigues et al., 2007). Besides, there is higher disorganization of the sarcomere with a reduction in the contraction (Squecco et al., 2009). The slow fibers are not altered (Schmalbruch et al., 1991; Lu et al., 1997; Borisov et al., 2001) and there is a decline in mitochondrial number and complexity. Finally, this degeneration is compensated with the appearance of newly forming muscle fibers.

Innervation is crucial for skeletal muscle performance. If the motor nerve is transected, muscle fasciculation occurs. Several days after denervation, muscle fibrillation begins. Fibrillation is characterized by spontaneous, repetitive contractions. The muscle fibrillations reflect supersensitivity to Acetylcholine. Atrophy can be reversed if reinnervation occurs within a few months. Reinnervation is normally achieved by the regrowth of the peripheral stump of motor nerve axons along the old nerve sheath. When formerly fast fibers are reinnervated by slow motoneurons there is a redifferentiation into a slow fiber, and vice versa. This is caused by a chronic low-frequency stimulation which converts the fast motor units into slow. This low-frequency stimulation is caused by reducing the excitatory input. This is provoked by sectioning the spinal or dorsal root or by severing the tendon, which functionally inactivates peripheral mechanoreceptors.

As explained above, there is a different atrophy progress depending on the muscle and the fiber type. Type II fibers present in fast muscles have quick atrophy, whereas type I fibers do not reduce their diameter up to two months beyond injury (Karpati and Engel, 1968; Davis and Kiernan, 1980; Lu et al., 1997; Borisov et al., 2001).

Not only is nerve stimulation involved in myosin-switch. Chronic elevation of intracellular Ca^{2+} induces a change in gene expression from fast myosin isoform to slow. These Ca^{2+} -dependent change is reversible by a reduction of intracellular $[\text{Ca}^{2+}]$.

Currently, there are no approved pharmacological therapies for the prevention or treatment of muscle wasting. For that reason, the current resources to increase muscle mass are an increased protein intake (Zhang et al., 2020), exercise training practice (Daou, 2020), and neuromuscular electrical stimulation.

2.2 Muscle injury

2.2.1 Classification

Muscle injuries are frequent in athletes and no professional, accounting for 10 to 55% (depending on the type of sport) of all acute sport injuries (Chan et al., 2012). The injury depends on the impact intensity, the state of the muscle contraction, the traumatic moment, and the muscle injured (Walton and Rothwell, 1963). Clinically, contraction-induced injuries are often defined as muscle strains and are classified into three categories (Prentice, 2020). Grade 1 or mild in which there is minor damage of muscle fibers and ECM, and patients will often make full recovery from these injuries. Grade 2 or moderate, there are more substantial tears in muscle fibers and damage to the ECM. Grade 3 or severe injuries are complete or near-complete tears across a cross-section of a whole muscle. Most muscle injuries are mainly managed conservatively with excellent results, while surgery is reserved only for larger tears. The most commonly involved muscle groups are the hamstrings, the rectus femoris, and the medial head of the gastrocnemius (GA) muscle. The diagnosis is usually done by imaging tools to identify the extent and site of the lesion (De Smet and Best, 2000). For patients who suffer from moderate and severe injuries, there is often persistent atrophy of muscle fibers, an accumulation of fibrotic scar tissue in the ECM, and a decrease in strength, functional capacity, and athletic ability (Kujala et al., 1997; Järvinen et al., 2007; Smith et al., 2008). These patients are also much more likely to have repeated muscle injuries. For each subsequent injury results in greater muscle atrophy and scar tissue deposition (Kujala et al., 1997; Brockett et al., 2004; Smith et al., 2008). For that reason, preventing muscle atrophy and the scar tissue accumulation could help to restore full strength and prevent re-injuries. Nowadays, the ability to prevent atrophy and fibrosis in medicine is currently limited (Kujala et al., 1997; Brockett et al., 2004; Smith et al., 2008).

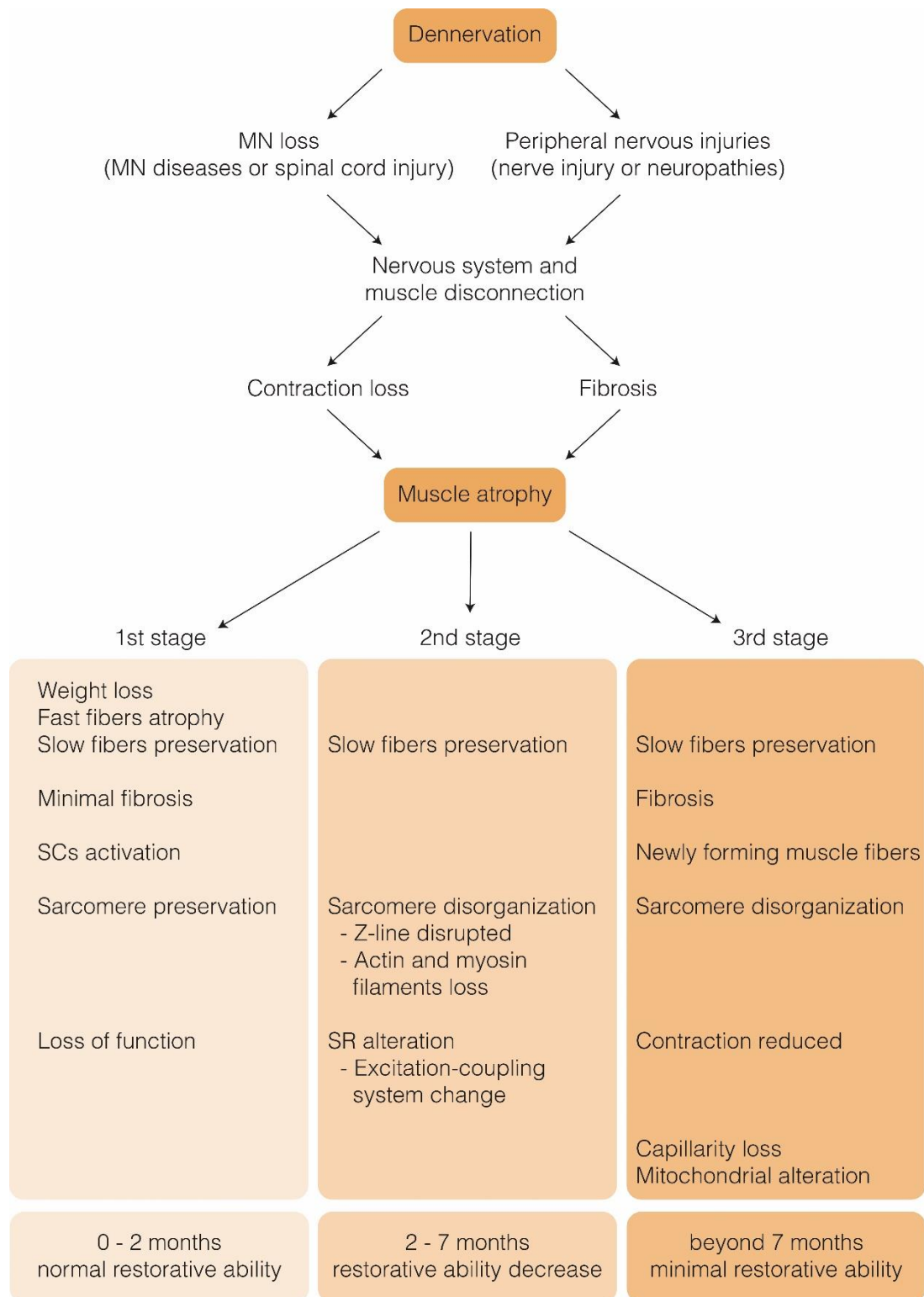


Figure 4. Summary of the progress of muscular atrophy caused by denervation. Denervation leads to the disconnection between the nervous system and the muscle. This leads to a progressive muscle atrophy which is divided into three stages.

2.2.2 Characteristics

Skeletal muscles can be injured when performing eccentric contractions (McCully and Faulkner, 1985). When there is an alteration on the external load after an injury, the forces transmitted to the sarcomere can immediately decrease the force production (Brooks et al., 1995; Devor and Faulkner, 1999; Baumann et al., 2014; Choi, 2014). This process of sarcomere and membrane damage initiates the subsequent muscle regeneration response.

Following a muscle fiber injury, the nuclei from the damaged area undergo apoptosis (Smith et al., 2000). In response to injury, SCs become activated, migrate to the site of damage, proliferate, and fuse with the myotubes (Hawke and Garry, 2001). SCs play an important role in regulating the activity of fibroblasts.

In addition to SCs and fibroblasts, macrophages and neutrophils play important roles in muscle injury and regeneration. Neutrophils appear soon after the muscle is injured. They help to initiate the inflammatory response, contribute to phagocytosis of damaged fibers, and participate in recruiting macrophages to the site of injury. When the number of neutrophils is reduced, macrophages begin to increase in number (Best and Hunter, 2000).

2.2.3 Therapies

Despite the high incidence, the treatment of severely injured muscles remains an unmet clinical need, and the restoration of the original structure and function is a current challenge.

The gold-standard treatment for muscle injuries is often focused on reducing pain, inflammation, and swelling in the acute phase. Despite a lack of evidence of effectiveness in the treatment of these injuries, numerous therapeutic approaches are used in the treatment of muscle strain injuries (Maffulli et al., 2015). Clinical options for the treatment of skeletal muscle injuries can be categorized into conservative management practices or invasive surgical procedures (Järvinen et al., 2007). Minor injuries, for example, muscle strains and contusions, heal spontaneously in healthy adults. In these cases, it is complemented with a conservative treatment to reduce inflammation and post-traumatic pain with non-steroidal anti-inflammatory drugs (NSAIDs). Numerous studies have shown that blocking the COX enzymes after muscle injury generally inhibits biological processes associated with muscle regeneration, leading to long term deficits in muscle function. At the whole muscle level, in animal models of muscle injury, NSAID use can result in an initial reduction in inflammation. In a long term use, it leads to smaller, weaker muscle fibers, and greater connective tissue accumulation (Shen et al., 2005; Mackey et al., 2012). This conservative treatment is

supplemented with the RICE principle, which is quick management of the injured body part. This consists of a sequence of steps which are rest, ice, compression, and elevation. This process tries to reduce blood flow, reducing the hematoma size, and preventing the extension of the actual trauma. Ice and other forms of cryotherapy are commonly used in the acute muscle injury phase to cool muscle tissue and provide analgesia. They are thought to alter cellular metabolism, reduce inflammation, and oxidative stress in the injured tissue (Torres et al., 2012; White and Wells, 2013; Denegar et al., 2016). In addition, training regimes and rehabilitation strategies are often used in sports injuries to allow muscle recovery in relatively short periods (weeks to months). In those patients suffering from volumetric muscle loss is usually recommended a surgical intervention to reconstruct the soft tissue (Sicari et al., 2014; Dziki et al., 2016; Hurtgen et al., 2017).

2.3 Therapies under study: NeuroHeal

Until recently, classical research for new therapeutic strategies have been based on "one drug for one target for one disease". Recent evidence indicates that a disease has to be treated as a complete network instead of address a single pathway. Network models enable an analysis of complex interaction networks between drugs and their targets, and also leads to the elucidation of mechanisms of action of novel drug therapies (Barabási, 2007; Cheng et al., 2012; Woo et al., 2015). To study more holistically, it is necessary the use of systems biology and computational tools for big data analysis.

There are platforms which take profit of artificial intelligence to screen drugs for their capacity to shift the profile of topological molecular maps from pathological to beneficial (Herrando-Grabulosa et al., 2016). This is the case of the Therapeutic Performance Mapping System (TPMS), a platform for drug discovery based on systems biology and artificial intelligence (www.Anaxomics.com). To screen the drugs using TPMS, two molecular maps were built based on a degenerative and a regenerative profiles. The data was obtained from two pre-clinical rat models: root avulsion (RA) model which leads to retrograde degeneration of MNs and distal axotomy and suture model which leads to MN survival and nerve regeneration (Casas et al., 2015). These maps were used to screen neuroprotective combinations of FDA-approved drugs. The selected combinations were validated in the RA model and Acamprosate and Ribavirin were chosen as the one with better results, naming as NeuroHeal (Romeo-Guitart et al., 2018).

All the systems have the availability to trigger endogenous mechanisms to cope with an alteration. In the case of the nervous system, this allows neurons to survive, axons to speedily regenerate, and healthy denervated muscle to be sustained. Thus, potentiating

those mechanisms would result in effective neuroprotection and repair of the damaged nervous system. At the same time, covering all these aspects by influencing multi targets would be easier to achieve.

NeuroHeal accomplishes these goals, because it activates different targets fulfilling the requirements. NeuroHeal is neuroprotective and pro-regenerative, and pre-clinical data indicate that it holds promise as a co-adjuvant treatment to facilitate recovery of nervous system function after traumatic injury to the peripheral nerves.

NeuroHeal is a combination of two repurposed drugs: Acamprosate and Ribavirin. Acamprosate is used for alcohol dependence and Ribavirin is a nucleoside used for treating viral infections such as hepatitis. Drug re-purposing facilitates clinical translation because it drastically reduces the need for preclinical toxicity and efficacy assays and for safety profiling in human volunteers (Ashburn and Thor, 2004).

The mechanism of action of NeuroHeal described in the nervous system showed different targets (Romeo-Guitart et al., 2018) (Fig. 5). Acamprosate is an antagonist of the N-methyl-d-aspartate (NMDA) receptor and acts as a positive modulator of the GABA receptor (A) (GABAR(A)). GABAR(A) activation leads to a hyperpolarization caused by Cl^- entry allowing VGCC activation. With this activation, there is a Ca^{2+} entry. Ribavirin inhibits inosine-5'-monophosphate dehydrogenase 1, an enzyme which catalyzes the conversion of inosine 5'-phosphate to xanthosine 5'-phosphate (Fig. 5). In the skeletal muscle, there are present the targets of Acamprosate (NMDA-R, GABA-R(A), and VGCC-R) and of Ribavirin (IMPDH and SIRT1). All these led us to study NeuroHeal in the skeletal muscle.

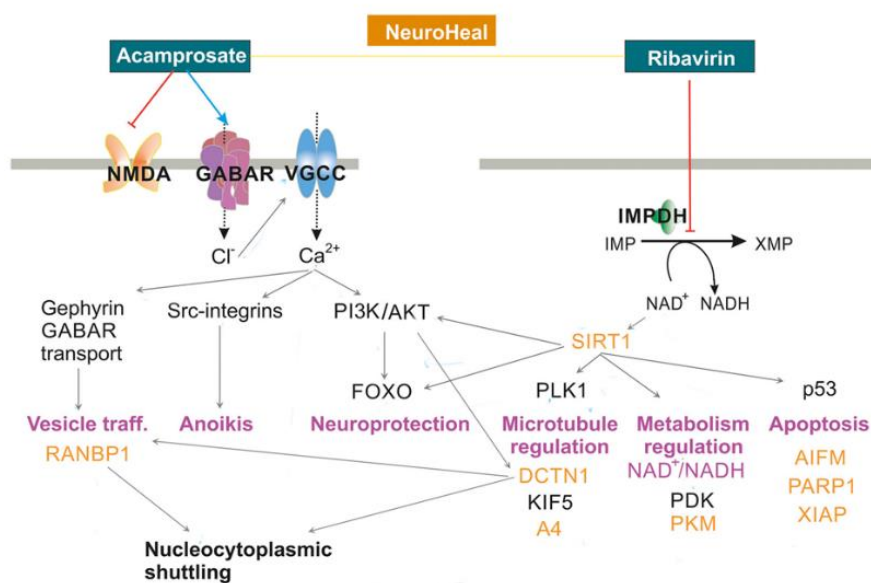


Figure 5. Summary of the mechanism of action of NeuroHeal. Representation of putative NeuroHeal mechanism of action from initial ACA and RIB targets to downstream possible effects

to yield the synergic effects (pink) through its targets (orange). Representation is based on analysis using STRING and IntAct platforms and manual scrutiny of relevant literature. From (Romeo-Guitart et al., 2018)

3. MOLECULAR MECHANISMS IN MUSCLE METABOLISM

3.1 Molecular mechanisms in muscle atrophy

There are several pathways modulating muscle atrophy, the main pathways are the UB-proteasome system and the autophagy machinery.

3.1.1 UB-proteasome system

The ubiquitin-proteasome system (UPS) is over-activated when there is an alteration on the muscle activity. This increase induces the elimination of the sarcomere proteins, leading to a reduction in the muscle mass. Although an extra induction provokes atrophy, UPS is present in normal conditions. For example, UPS recycles amino acids for energy production and has an essential role in myogenesis. Nevertheless, UPS represents the main proteolytic system of dysfunctional proteins in the skeletal muscle (de Theije et al., 2013). Until this date, UPS is the most implicated pathway on denervated muscle atrophy (Bodine et al., 2001a; Beehler et al., 2006).

UPS degradation of proteins depends on their ubiquitination. The ubiquitination process is a post-translational modification. This is formed by a cascade of reactions done by three types of proteins: ubiquitin-activating enzymes (E1), ubiquitin-conjugating enzymes (E2), and ubiquitin-protein ligases (E3s). The first step is the activation of the ubiquitin (Ub) with an E1 enzyme. This Ub is transferred to an E2 enzyme. Finally, the Ub is transferred again to a substrate by an E3 ligase (Fig. 6). This Ub transferring can be added to only one Ub (monoubiquitin) or a chain of variable length (polyubiquitin). Ub is formed by seven Lys (K6, K11, K27, K29, K33, K48, and K63) which can be linked through any one of these seven Lys (Kravtsova-Ivantsiv and Ciechanover, 2012). In skeletal muscle atrophy the K48 and K29 polyubiquitin chains can be joint to MuRF1 and MAFbx/Atrogin-1. These two chains target the substrate to the 26S proteasome for degradation (Passmore and Barford, 2004; Napolitano et al., 2011). When the substrate is tagged with the polyubiquitin chains, this is recognized by the $s5\alpha$ subunit. The 26S proteasome is formed by two large subcomplexes: the 20S proteasome and the 19S regulatory particle (Glickman and Ciechanover, 2002; Pickart and Cohen, 2004; Finley, 2009). The 20S proteasome is formed by four heteroheptameric rings: the inner two are formed by the β subunits and house the peptidase activities, and the outer two are formed by the α subunits, which gate access to the inner chambers (Groll et al., 1997).

muscle function (Boutari and Mantzoros, 2017). Also, Atrogin-1 induces the degradation of MyoD (Tintignac et al., 2005; Lagirand-Cantaloube et al., 2009) and eIF3F, a protein synthesis inductor (Tintignac et al., 2005; Li et al., 2007; Csibi et al., 2010).

MuRF1 (Muscle RING Finger-containing protein 1) is one of the most important UPS components involved in skeletal muscle atrophy. As its name says, has a RING-finger domain in which has the ubiquitin ligase activity and it binds to an E2 enzyme (Borden and Freemont, 1996; Saurin et al., 1996; Joazeiro, 1999). There are three types of MuRF -1, -2, and -3 (Centner et al., 2001) which are localized at the M-line of the sarcomere, although they can be present in other areas. MuRF1 and -3 are localized at the Z-lines (Centner et al., 2001; McElhinny et al., 2002), whereas MuRF1 and -2 are detected in the nucleus. Depending on the development stage, there is more presence of a specific MuRF: MuRF2 acts principally at embryonic stages, whereas MuRF1 and -3 increase their expression after birth (Perera et al., 2012). Nonetheless, MuRF1 is the only involved in muscle atrophy (Bodine, 2001; Labeit et al., 2010; Baehr et al., 2011; Files et al., 2012). MuRF1 is involved in the myofibrils degradation. It ubiquitinates myosin light chains 1 and 2, MyHC (Clarke et al., 2007a; Fielitz et al., 2007), myosin-binding protein C (Cohen et al., 2009, 2012), and troponin I (Kedar et al., 2004). Finally, it was observed that MuRF1 is downregulated in cardiac and skeletal myopathy (Banerjee et al., 2015; Mulder et al., 2015; Baehr et al., 2017). In addition, MuRF1 null mice preserve MyHC during atrophy, and knockdown of MuRF1 shows an increase of MyHC (Clarke et al., 2007b). Inhibiting NF- κ B decreases muscle wasting, by blocking the upregulation of MuRF1 in cachexia (Cai et al. 2004; Moore-Carrasco et al. 2007) (Ramírez et al., 2011; Langen et al., 2012).

Not only is NF- κ B implicated as a proinflammatory process. The p38 MAP kinase also participates on it. Both upregulate MuRF1 and Atrogin-1 expression (Lagirand-Cantaloube et al., 2008; Csibi et al., 2009; Sanchez et al., 2013). Besides, during denervation, the transcription factor Myogenin, is required for the maximal activation of MuRF1 and Atrogin-1 (Moresi et al., 2010). Furthermore, Atrogin-1 knockdown mice prevent muscle loss during fasting (Cong et al., 2011) and MuRF1 KO mice are resistant to dexamethasone-induced muscle atrophy (Baehr et al., 2011).

3.1.2 Autophagy

Autophagy is a highly controlled mechanism in which the cytoplasmic content is degraded through lysosomal degradation by the cell. By activating this process, the cell can control its own protein and organelle homeostasis. Autophagy has an important role in normal conditions because its levels are constant at basal. Nevertheless, under new conditions, such as injury, autophagy helps to fight an insult as a self-protective mechanism.

Depending on the way through the cytosolic content is delivered to lysosomes, there are three types of autophagy. The first type is microautophagy in which there is a direct invagination of the lysosomal membrane to degrade the enfolded material. The second is the chaperon-mediated autophagy, in which the degradation of the soluble protein aggregates is done by the chaperones. The last type is the macroautophagy, hereinafter called autophagy.

This process is highly coordinated by different Autophagy-related (Atg) genes, kinases, and other regulatory proteins. All of them work together for the initiation, nucleation, elongation, closure, and correct fusion of the autophagosome with the lysosomes (Galluzzi et al., 2016).

The initiation step can be started by 2 pathways: dependent or independent of Mammalian target of Rapamycin (mTOR) (Arbogast and Gros, 2018). The first is activated under amino acids deprivation in which mTOR is inhibited, specifically mTORC1 (Dikic and Elazar, 2018), or by AMPK or SIRT1. When mTOR is inhibited, Ulk1 is activated starting the autophagy process. The other pathway, which is independent of mTOR, is mediated by PI3K, in which Ulk1 activates Beclin-1 (Arbogast and Gros, 2018). This initiation can be interrupted blocking PI3K activity by 3-methyladenine or LY294 compounds (Galluzzi et al., 2016). mTOR is found in two distinct protein complexes, mTORC1 and mTORC2, but only mTORC1 regulates directly autophagy (Dikic and Elazar, 2018). The mTOR kinase is a sensor of the nutrient levels. When there is hypertrophy in skeletal muscle, mTOR is required, but when mTOR is inhibited there is myofiber degeneration and muscle growth is blocked (Bodine et al., 2001b). mTOR, Beclin-1, and Unc-51-like kinase 1 (Ulk1) are essential for a correct initiation and nucleation, and for the formation of the double-membrane of the autophagosome (Russell et al., 2013; Galluzzi et al., 2016) (**Fig. 7**).

Atg5 and Atg7 are essential molecules for autophagy induction (**Fig. 7**). During the elongation, Atg7 is implied in the conjugation of the complexes to facilitate autophagosome formation: Atg12-Atg5 and Atg5-Atg16L1-Atg12 (in this case, with Atg10 help). This second complex mediates the conjugation of phosphatidylethanolamine to the microtubule-associated protein 1 light chain 3 (LC3-I) into LC3-II form. This leads the translocation from the cytoplasm to the autophagosome membrane. The cytosolic contents engulfed by the autophagosomes have degradative signals. These are detected by LC-binding domains or other receptors, such as p62. After the elongation step, there is the autophagosome maturation, in which autophagosomes are fused to the lysosome to degrade their contents. Here, autophagosome is trafficked to the cell periphery by dyneins. This induces the fusion of the autophagosome and the lysosomal vesicle, resulting in an autolysosome (Ravikumar et al., 2005; Reggiori and Ungermann, 2017). At that moment, the inside cargo can be

eliminated by the lysosomal hydrolases. The autophagy-derived metabolites can be recycled and released, such as amino acids, glucose, and others (Kaur and Debnath, 2015).

Autophagic flux shows the rate at which lysosomes degrade the substrates of autophagy. This determine the efficiency of the autophagic response (Loos et al., 2014).

The autophagy-lysosome activity is increased during muscle wasting (Bechet et al., 2005), such as fasting (Mizushima et al., 2004, 2008, 2010), atrophy (Mammucari et al., 2007; Sandri, 2008), and denervation (Schiaffino and HanzlíkováVěra, 1972), or it is decreased in age-related sarcopenia (Wohlgemuth et al., 2010). Not only is there an increase in induction, there is also an accumulation of autophagosomes. When there is this unbalance is known as autophagy blockage. At the same, as a constitutive process, correct autophagy flux is fundamental for myofiber survival (Vergne et al., 2009; Grumati et al., 2010). Unbalanced autophagy leads to a pathophysiology system in which overactivation causes excessive cytosolic content leading to muscle atrophy. Insufficient autophagy causes an accumulation of damaged or dysfunctional cell components. In both cases are impairing the myofiber homeostasis. Therefore, a fine-tuning of autophagy is essential for a correct muscle state.

Atg7 is the unique E1 enzyme of the autophagic machinery. Atg7-null mice model presents sarcomere disorganization and UPS activation. This leads to myofiber degeneration, abnormal mitochondria, oxidative stress, and accumulation of polyubiquitylated proteins. All this is caused by a complete inhibition of autophagosome formation (Masiero et al., 2009; Masiero and Sandri, 2010). Another model, the Atg5-null mice shows a similar phenotype (Raben et al., 2008).

All these genes are controlled by Forkhead box O 3 (FoxO3) transcription factor (Mammucari et al., 2007; Zhao et al., 2007). FoxO3a is fundamental to modulate protein breakdown by lysosome in skeletal muscle (Mammucari et al., 2007; Romanello et al., 2010). FoxO3 is able to regulate independently the UPS and the autophagy-lysosome machinery *in vivo* and *in vitro* (Mammucari et al., 2007; Zhao et al., 2007). Akt is the most representative inhibitor of autophagy flux in muscle. Akt is able to regulate autophagy by dependent and independent from mTOR (Sandri et al., 2004; Mammucari et al., 2007; Zhao et al., 2007).

3.2 Molecular mechanisms in muscle regeneration

Muscle has regenerative potential. It is able to manage conservatively the majority of muscle injuries obtaining a good functional outcomes.

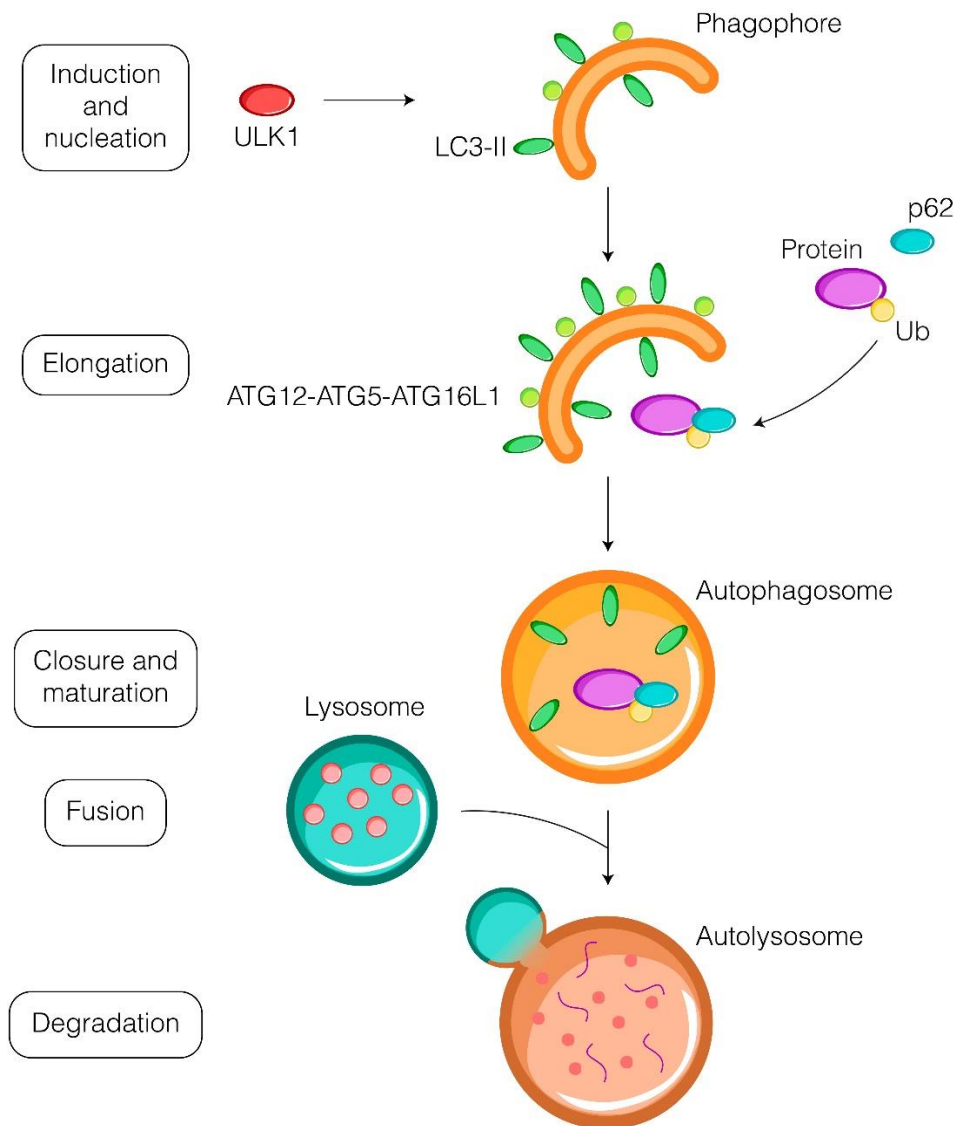


Figure 7. Overview of the autophagy process. Summary of the principal genes involved in each of the stages (based from (Parzych and Klionsky, 2014)).

Muscle healing is a process with different stages (Fig. 8). These include a brief destructive stage of hemorrhage and necrosis (0–2 days); an inflammatory stage of phagocytosis of necrotic tissue and angiogenesis (2–5 days); a repair stage of regeneration and revascularization (3–60 days); and a remodeling stage (3–60 days). This last stage includes maturation of regenerating fibers, reintegration of newly formed tissue with native muscle and tendon, and organization of scar tissue (Järvinen et al., 2005).

At the beginning, damaged myofibers start a necrotic process. This releases molecules to stimulate an inflammatory response. Mastocytes, immune cells from the connective tissue, are the first to be activated releasing cytokines such as TNF- α . This leads to SC

activation and proliferation (Chen et al., 2007; Serrano et al., 2008; Duchesne et al., 2011).

After the necrosis and the inflammatory response, there is the regenerative process. This is performed by myogenesis and maturation of the SCs (Mauro, 1961; Scharner and Zammit, 2011). Through this process, the skeletal muscle is capable to reestablish the injured contractile apparatus. The muscle regeneration process is divided into stages which are defined by the different Myogenic Regulatory Factors (MRFs) expression and by the modulation and the expression of specific molecular markers. For each stage of differentiation, there is an up- or downregulation of proliferative-associated genes and cell-cycle withdrawal (Zammit et al., 2006; Yablonka-Reuveni et al., 2008; Boldrin et al., 2010).

As said previously, the main protagonist is the SC. SCs are quiescent and are activated under two conditions: in response to a physiological stimulus, such as exercise, or under pathological conditions, such as lesions or degenerative diseases. SCs are localized around the myofibers between the basal lamina and the sarcolemma. When a SC is activated, it starts differentiation through the inhibition of Notch (Kuang et al., 2007; Bjornson et al., 2012; Mourikis et al., 2012).

A quiescent or activated SCs is characterized by the expression of Pax7 and Myf5 (except for the Myf5^{neg} satellite stem cell population). Once a SC is activated can follow two pathways depending on MyoD levels. A downregulation of MyoD leads to a self-renew, guaranteeing the maintenance of a pool of quiescent. A maintaining of MyoD expression with a downregulation of Pax7 induces the activation of Myogenin (MyoG) expression. This MyoG activation commits to SC differentiation (Nagata et al., 2006; Day et al., 2007; Boldrin et al., 2010; Relaix and Zammit, 2012).

SCs are distributed all along the length of myofibers. After muscle injury, activated SCs first migrate from their original location to the damaged area. This migration capacity is mediated by several physical and chemical guidance cues. Besides, molecules released after muscle injury drive SCs to the site of the injury (Germani et al., 2003; Lafreniere et al., 2006). There, they increase their mitotic activity at the site of injury (Schultz et al., 1985). Activated myogenic progenitors undergo several rounds of proliferation to increase the myogenic pool needed for tissue repair. The majority of the growth factors known to participate in activate SCs also facilitates cell division. These factors can directly promote myoblast proliferation through NF- κ B pathway (Otis et al., 2014) and JNK pathway (Guttridge et al., 1999; Perdiguero et al., 2007; Alter et al., 2008). At this stage, committed SCs are termed myoblasts and express the myogenic markers Pax7, and/or Myf5, and/or MyoD.

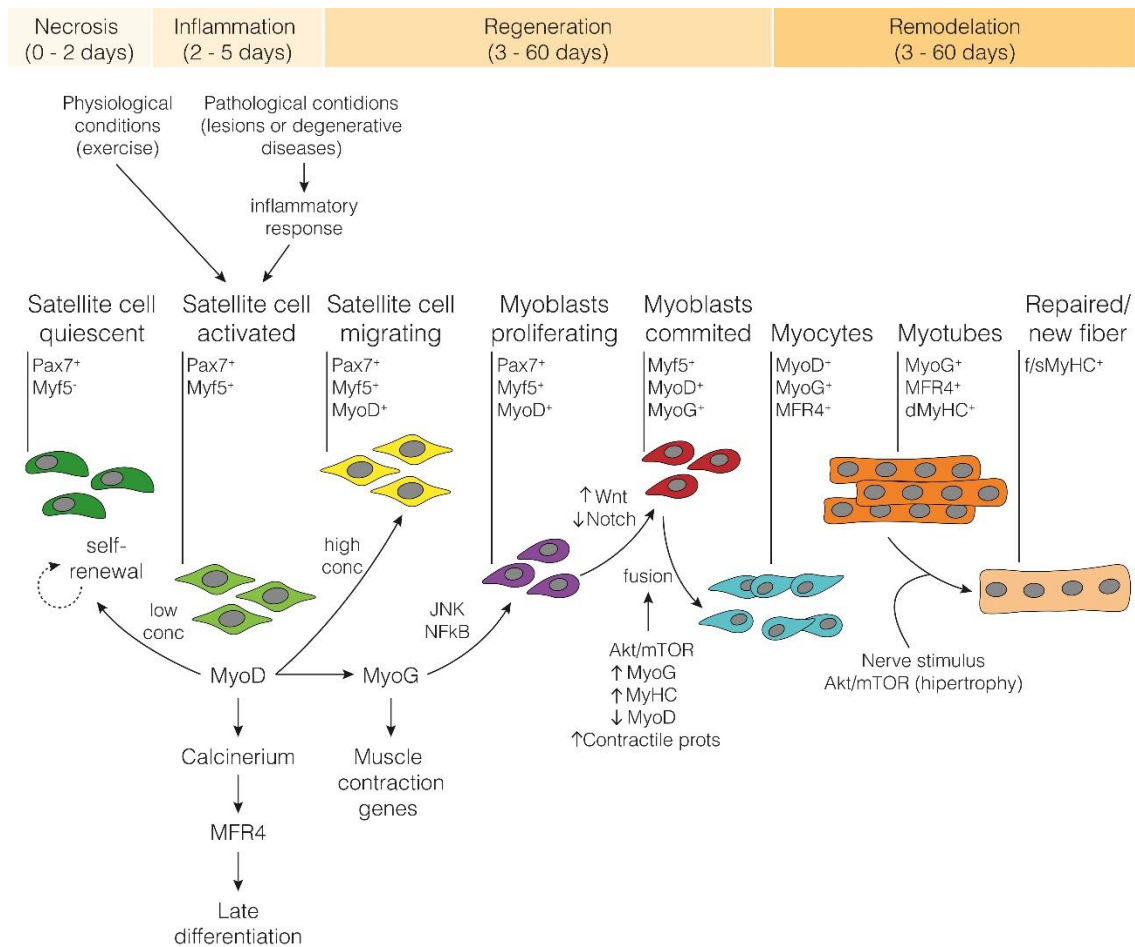


Figure 8. The process of muscle regeneration after muscle injury and the behavior of SCs. It is shown the steps of SC activation, migration, and proliferation, as well as those of myocyte differentiation, maturation, and hypertrophy.

Following several rounds of proliferation, myogenic cells exit the cell cycle and start to differentiate. Thereafter, myogenic cells fuse together to form multinuclear myotubes or fuse to an existing damaged fiber. Once activated the myogenic differentiation, MyoG triggers the expression of genes involved in muscle contractility (Davie et al., 2007) and MRF4 is involved in the late differentiation, under MEF2 control (Rawls et al., 1998). The activation of Wnt signaling pathway and the inhibition of the Notch pathway are critical for the transition to myoblast differentiation (Brack et al., 2008). In addition, calcium-activated pathways are involved. Calcineurin activates MyoD through MEF2C (Friday et al. 2003). Myoblasts exit the cell cycle and differentiate into mature myocytes. This differentiation process is accompanied by a decreased in the expression of Pax7 and Myf5, and by an increase in MyoG and MRF4 levels.

Following the induction of the differentiation program, myogenic cells undergo a cell-cell fusion process which strongly modifies cell shape and function. To fuse, myocytes must first recognize and adhere to each other. MyoD levels become reduced while MyHC and other contractile proteins start to be expressed. Nascent myotubes need to

undergo a maturation process to become fully functional myofibers. Mature muscle fibers are highly specialized and need to acquire competent excitation-contraction and metabolic machineries. The Akt/mTOR pathway has a pivotal role in myotube maturation and hypertrophy (Park and Chen, 2005; Park et al., 2005). To reestablish the total complex, there is a reorganization of the connective tissue and angiogenesis (Mutsaers et al., 1997; Pelosi et al., 2007; Grounds, 2008; Mann et al., 2011). The ECM is activated to overproduce to act as a scaffold for the new fibers and to guide the formation of NMJs (Mutsaers et al., 1997; Lluri et al., 2006). This fibrotic response is initially beneficial because it is quick, adds support, increases strength, and helps to protect the injury site. However, the overproduction of collagens within the injured area often leads to heavy scarring and the loss of muscular function. The reparative process is completed when injured myofibers rescue their functional performance and contractile apparatus (Pelosi et al., 2007). Thus, the regeneration of damaged or diseased muscles is only beneficial if the regenerated muscles become effectively innervated. Within two weeks of damage, newly formed NMJs between the surviving axons and the regenerated muscle fibers can be identified. The initial phases of muscle regeneration do not necessarily depend on the nervous system. The subsequent growth and maturation requires the nerve activity. This nerve stimulation influences directly on the protein turnover and the gene expression. Indirectly, the nervous system affects the proliferation and differentiation of the SC. (Mozdziak et al., 2001; Mitchell and Pavlath, 2004). Regenerating innervated myofibers can be monitored by analyzing the expression of different MyHC isoforms. Regenerating muscle fibers initially express developmental MyHC forms and later on adult fast and slow MyHC forms (Sartore et al., 1982; Whalen et al., 1990; Esser et al., 1993).

3.3 SIRT1 and skeletal muscle

Sirtuins (SIRT) have been identified as a major players linking changes in metabolism to transcription. There are different types of SIRT but the most expressed and studied on the skeletal muscle is SIRT1, although is not muscle-exclusive (Ryall, 2012; Tonkin et al., 2012).

SIRT1 is a class III histone deacetylase which is dependent on NADH to deacetylate its targets (Haigis and Sinclair, 2010). This dependence makes SIRT1 highly sensitive to changes in metabolism, acting as a sensor and regulator of the energetic status of the cell.

SIRT1 has been found to target a range of histone and protein targets, including among others the histone H3 lysine 9 (H3k9) and H4k16, and the transcription factors g-coactivator 1a (PGC1a), MyoD, and FoxO1/3a (Vinciguerra et al., 2010; Tonkin et al., 2012). SIRT1 has different functions in the muscle, but the two main functions are block

the reduction in mass and the derive the regenerative ability upon injury. Regarding muscle mass control, SIRT1 deacetylates NF- κ B, which is involved in the activation of atrogenes and is induced by TNF α (Ghosh and Karin, 2002; Lin et al., 2002; Yeung et al., 2004; Salminen and Kaarniranta, 2009; Schug et al., 2010). During intermittent fasting, SIRT1 deacetylates FoxO1 and FoxO3, inhibiting their transcription, which inhibits the atrophy of slow fibers (Lee and Goldberg, 2013; Brandon et al., 2015; Dugdale et al., 2017)). This slow fiber protection is also mediated by the SIRT1 deacetylation of PGC1 α . PGC1 α regulates mitochondrial biogenesis and allows skeletal muscle fibers to adapt to energetic demands (Gerhart-Hines et al., 2007; Cantó et al., 2010). The slow fiber survival is induced by modulating their metabolism, increasing the number of mitochondrias (Lin et al., 2002). Besides, PGC1 α mediates key responses of skeletal muscle to motor nerve activity (Sandri et al., 2006).

SIRT1 influences the regenerative potential of skeletal muscle by affecting the activation, proliferation, and differentiation of the SCs. In the skeletal muscle, SIRT1 is implicated in the differentiation of the fibers because cellular energy requirements are tightly linked to the contractile and force-generating activities (Fulco et al., 2003a, 2008a; Amat et al., 2009; Vinciguerra et al., 2010; Zorzano et al., 2010). When there are high NAD $^{+}$ levels, SCs are under a proliferative state. This high concentration of NAD $^{+}$ activates SIRT1 and it maintains MyoD in a deacetylated state, which inhibits its transcriptional activity. However, when NAD $^{+}$ levels drop, SCs start their differentiation. This reduction leads to MyoD became acetylated and transcriptionally active. This suggest that SIRT1 is a negative regulator of MyoD activity, and its activation inhibits the differentiation process (Fulco et al., 2003b, 2008b; Cerletti et al., 2012).

HYPOTHESIS AND OBJECTIVES

We hypothesize that endorse endogenous mechanisms of cellular protection in the muscle by NeuroHeal could promote tissue homeostasis.

The general objective of this doctoral thesis is to validate the therapeutic effect of NeuroHeal on muscle tissue, specifically on muscle atrophy and on acute muscle injury.

To that end, the thesis has been divided in two different chapters with the following specific objectives:

Chapter I. NeuroHeal reduces Muscle Atrophy and modulates Associated Autophagy

- To assess if NeuroHeal treatment reduces muscle atrophy in two *in vivo* models, chronic denervation and disuse models.
- To perform if NeuroHeal treatment reduces myotube diameter atrophy *in vitro* using the C2C12 cell line.
- To characterize the molecular effects of NeuroHeal in reducing muscle atrophy.

Chapter II. NeuroHeal improves Muscle Regeneration after Injury

- To evaluate the potential of NeuroHeal treatment after a muscle injury *in vivo*.
- To assess the effect of NeuroHeal on satellite cells *in vivo*.
- To perform if NeuroHeal treatment effects myogenesis *in vitro* using the C2C12 cell line.

STUDY DESIGN AND METHODOLOGIES

CHAPTER I: NeuroHeal reduces Muscle Atrophy and modulates Associated Autophagy

The first chapter of this thesis focuses on whether NeuroHeal has an effect on the skeletal muscle in order to prevent muscle atrophy due to denervation or immobilization.

1. Experimental model

To achieve this goal, we used two *in vivo* models and one *in vitro* model:

In vivo model

Denervation model: we transected the sciatic nerve of adult rats and treated them orally from the day of the surgery with vehicle, NeuroHeal, or NeuroHeal plus Nicotinamide. Samples were obtained at 7 days postinjury (dpi) for molecular biology studies and at 28 dpi for histology.

Hindlimb immobilization model: one limb was immobilized for 7 days, and later the splint was removed for 7 days more. Animals were treated intraperitoneally from the day of the immobilization with vehicle or NeuroHeal. The grip strength was evaluated with the grip test at 0, 7, and 14 days post immobilization. Samples obtained at 7 days were used for histological analyses.

In vitro model

TNF α induced atrophy in the C2C12 cell line, in which after 24h of seeding, cells started the differentiation process, and, at 6 days of *in vitro* (div), cells were induced the atrophy by the addition of TNF α . At 6 div, myotubes were treated with NeuroHeal or NeuroHeal plus Ex-527.

2. Muscle atrophy evaluation

To determine the atrophied muscle fibers, we used Hematoxylin and Eosin (H-E) staining to visualize the muscle fibers and evaluate their diameter. We evaluated the myofiber cross-sectional area (CSA) at 28 dpi in the denervation model and at 14 dpi in the hindlimb immobilization model. *In vitro*, we calculated the myotube diameter under light microscopy at 7 div. In addition, we evaluated *in vivo* in the hindlimb immobilization model the grip strength by the grip test.

3. Muscle atrophy modulation by NeuroHeal

To elucidate the mechanisms by which NeuroHeal reduces or prevents muscle atrophy in the experiment models, we used a SIRT1 inhibitor drug (*in vivo* NAM and *in vitro* Ex-527) to treat an experimental group to corroborate NeuroHeal target and its implication. In addition, by immunohistochemistry in the denervation model, we determined the modulation of SIRT1 by NeuroHeal by labeling H4K16. Besides, by western blot, we analyzed the main pathway of protein synthesis (AKT-mTOR) and protein degradation (ubiquitin-proteasome system and autophagy) *in vivo* in the denervation model. This ubiquitin-proteasome system was also analyzed *in vitro*.

	IN VIVO		IN VITRO
	DENERVATION MODEL	HINDLIMB IMMOBILIZATION MODEL	C2C12 CELL LINE ATROPHY-INDUCED
EXPERIMENTAL MODEL	<p>NeuroHeal +/- NAM treatment</p> <p>Day 0 Day 7 Samples Western Blot Day 28 Samples Histology</p> <p>Control uninjured rats Untreated vehicle NeuroHeal treatment</p> <p>NeuroHeal + NAM treatment</p>	<p>NeuroHeal treatment</p> <p>Day 0 Day 7 Grip test Samples Day 14 Grip test</p> <p>Control uninjured mice Untreated vehicle NeuroHeal treatment</p>	<p>Growing medium Differentiation medium TNFα NH/Ex-527</p> <p>Seed Day 0 Day 6 Day 7</p> <p>Control TNFα TNFα + NeuroHeal</p> <p>TNFα + Ex-527 TNFα + NeuroHeal + Ex-527</p>
MUSCLE ATROPHY EVALUATION	<p>Myofiber diameter evaluation</p> <p>H-E stain</p>	<p>Myofiber diameter evaluation</p> <p>H-E stain</p> <p>Muscle function evaluation</p> <p>Grip test</p>	<p>Myotube diameter evaluation</p> <p>Light microscope</p>
MUSCLE ATROPHY MODULATION BY NEUROHEAL	<p>SIRT1 effect evaluation</p> <p>NAM treatment</p> <p>IHC: anti-H4K16</p> <p>Muscle atrophy modulation</p> <p>WB protein synthesis/ degradation Autophagy</p>		<p>SIRT1 effect evaluation</p> <p>Ex-527 treatment</p> <p>Muscle atrophy modulation</p> <p>WB protein synthesis/ degradation</p>

CHAPTER II: NeuroHeal Improves Muscle Regeneration after Injury

The second chapter of this thesis investigates whether NeuroHeal has a potential effect on muscle regeneration after injury.

1. Experimental model

To achieve this goal, we have used an *in vivo* model and an *in vitro* model:

In vivo model

Muscle injury model in which a transversal biopsy procedure was performed at the myotendinous junction level of the gastrocnemius muscle. Animals were treated by gavage from the day of the surgery with vehicle or NeuroHeal until 14 dpi. We performed electrophysiological tests at 0, 3, 7, and 14 dpi, and muscle force testing at 14dpi.

In vitro model

In the C2C12 cell line, after 24h of seeding, cells started the differentiation process and were treated with NeuroHeal or NeuroHeal plus Ex-527. We obtained samples at different time points: before differentiation, and after 1, 3, and 5 div.

2. Muscle function recovery

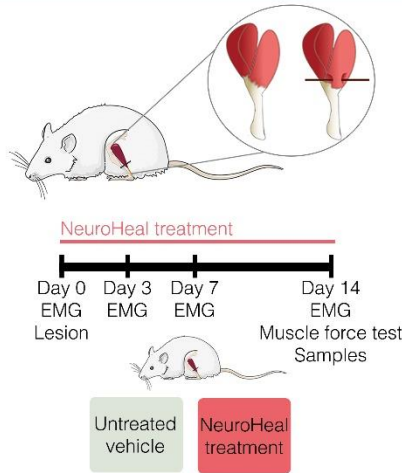
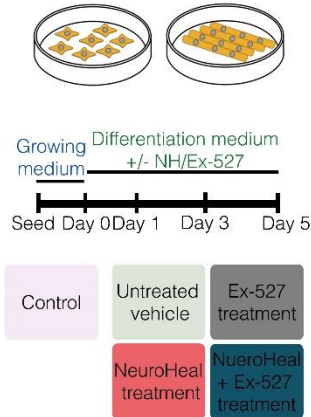

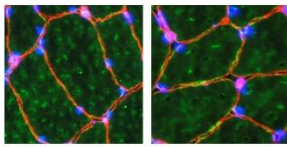
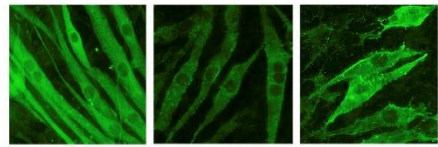
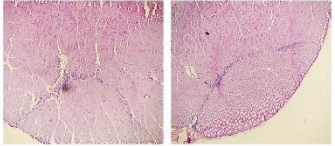
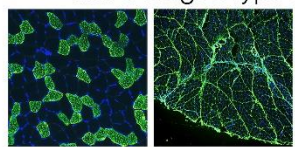
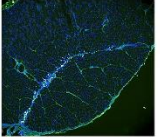

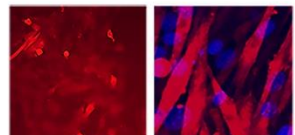
To assess the impact of muscle injury and recovery, we evaluated by electrophysiology tests at different time points (0, 3, 7, and 14 dpi), since these tests are the most important tool for monitoring muscle response. Furthermore, we measured the muscle force to validate functional recovery at 14 dpi.

3. Muscle fiber regeneration

To confirm myofiber recovery by immunohistochemistry, we labeled development MyHC to observe the regenerative myofibers and the amount of slow or fast MyHC positive fibers. In addition, we labeled with collagen type I to assess the effect on fibrosis.

4. Myogenesis

Regarding the regenerative effect of NeuroHeal, we evaluated if NeuroHeal can activate or modulate muscle SCs. By immunohistochemistry, we labeled with different cell markers the myofibers at 14 dpi and the myotubes at different time points (1, 3, and 5 div).

	IN VIVO MUSCLE INJURY MODEL	IN VITRO C2C12 CELL LINE
EXPERIMENTAL MODEL	 <p>NeuroHeal treatment</p> <p>Day 0 Day 3 Day 7 Day 14</p> <p>EMG EMG EMG EMG</p> <p>Lesion Muscle force test Samples</p> <p>Untreated vehicle NeuroHeal treatment</p>	 <p>Growing medium Differentiation medium +/- NH/Ex-527</p> <p>Seed Day 0 Day 1 Day 3 Day 5</p> <p>Control Untreated vehicle Ex-527 treatment</p> <p>NeuroHeal treatment NeuroHeal + Ex-527 treatment</p>
MUSCLE FUNCTION RECOVERY	<p>Muscle function evaluation</p> <p>EMG Muscle force</p>  <p>IHC: anti-Parvalbumin</p> 	<p>Muscle function evaluation</p> <p>IHC: anti-Parvalbumin</p> 
FIBER REGENERATION	<p>Lesion area localization</p> <p>H&E stain</p>  <p>Fiber evaluation</p> <p>IHC: anti-MyHC anti-collagen type I</p> 	
MYOGENESIS	<p>IHC: anti-dMyHC anti-Pax7 anti-MyoD anti-MyoG</p>  	<p>IHC: anti-Pax7 anti-MyoD anti-MyoG Coeficient fussion</p> 

RESULTS

CHAPTER I

NeuroHeal reduces Muscle Atrophy and Modulates associated Autophagy

Article

NeuroHeal Reduces Muscle Atrophy and Modulates Associated Autophagy

Sara Marmolejo-Martínez-Artesero ^{1,†}, David Romeo-Guitart ^{1,*;†,‡}, Laura Mañas-García ², Esther Barreiro ² and Caty Casas ^{1,*}

¹ Institut de Neurociències (INc) and Department of Cell Biology, Physiology and Immunology, Universitat Autònoma de Barcelona (UAB), Bellaterra, 08193, Barcelona, Spain; Sara.Marmolejo@uab.cat

² Pulmonology Department-Muscle Wasting and Cachexia in Chronic Respiratory Diseases and Lung Cancer Research Group, IMIM-Hospital del Mar, Parc de Salut Mar, Health and Experimental Sciences Department (CEXS), Universitat Pompeu Fabra (UPF), Barcelona Biomedical Research Park (PRBB), Barcelona, and Centro de Investigación en Red de Enfermedades Respiratorias (CIBERES), Instituto de Salud Carlos III (ISCIII), 08003, Barcelona, Spain; lauramgarcia9@gmail.com (L.M.-G.); ebarreiro@imim.es (E.B.)

* Correspondence: david.romeo-guitart@inserm.fr (D.R.-G.); Tel: +33-01 40 61 53 57 (D.R.-G.); Caty.Casas@uab.cat (C.C.); Tel: +34-935811324 (C.C.)

† These authors contributed equally to this work.

‡ Current address: Institut Necker Enfants-Malades (INEM), INSERM U1151, Laboratory “Hormonal regulation of brain development and functions” – Team 8, Université Paris Descartes, Sorbonne Paris Cité, 75015 Paris, France

Received: 15 May 2020; Accepted: 24 June 2020; Published: date

Abstract: Muscle wasting is an unmet medical need which leads to a reduction of myofiber diameter and a negative impact on the functional performance of daily activities. We previously found that a new neuroprotective drug called NeuroHeal reduced muscle atrophy produced by transient denervation. Aiming to decipher whether NeuroHeal has a direct role in muscle biology, we used herein different models of muscle atrophy: one caused by chronic denervation, another caused by hindlimb immobilization, and lastly, an in vitro model of myotube atrophy with Tumor Necrosis Factor- α (TNF α). In all these models, we observed that NeuroHeal reduced muscle atrophy and that SIRT1 activation seems to be required for that. The treatment downregulated some critical markers of protein degradation: Muscle Ring Finger 1 (MuRF1), K48 poly-Ub chains, and p62/SQSTM1. Moreover, it seems to restore the autophagy flux associated with denervation. Hence, we envisage a prospective use of NeuroHeal at clinics for different myopathies.

Keywords: NeuroHeal; skeletal muscle atrophy; sirtuin 1; autophagy; proteasome

1. Introduction

Skeletal muscle atrophy or muscle wasting can occur due to several causes, from short periods of muscle disuse due to primary degenerative processes within the skeletal muscle fibers or to secondary neurogenic atrophy and inflammation or spontaneously during aging [1]. The hallmark histopathological feature of skeletal muscle atrophy is the loss or reduction of myofiber diameter. Loss of muscle mass results in reduced muscle function, and this can have a direct negative impact on functional performance, such as the ability to carry out activities of daily living. Muscle wasting has also been associated with poor prognosis and mortality [2]. Medications that treat or prevent muscle atrophy remain mostly unavailable, with exercise and/or physical therapy being the only remaining options.

Optimal muscle state depends on the balance between protein synthesis and protein degradation. Muscle atrophy is initially provoked by an excessive protein breakdown, followed by a reduction in protein synthesis [3]. Several reports describe that increasing protein synthesis could be beneficial and sufficient to block muscle weight loss. Moreover, it is widely described that an overactivation of proteasome or autophagic-degradative pathways hampers muscle tissue. Although this is true regarding proteasome-mediated protein degradation, recent studies suggest that macroautophagy, hereafter autophagy, could have a muscle-protective effect instead. Specifically, the blockade of autophagy has been related to exacerbated atrophy, indicating some beneficial effects of this self-protective mechanism [4].

We have recently discovered a novel neuroprotective drug, NeuroHeal, for peripheral nerve injury (PNI). The drug, discovered using artificial intelligence, is based on the combination of two approved drugs, Acamprosate and Ribavirin, which facilitate its readiness for clinical use [5]. Using a model of severe PNI with delay reimplantation of the damaged nerve roots, we observed that the treatment with NeuroHeal enhanced nerve regeneration and reduced the associated muscle atrophy [6]. Considering the neuroprotective effect of NeuroHeal, the expected reduction of muscle atrophy might be correlated. In order to know whether NeuroHeal might have a direct effect on muscle biology, we set up a series of experiments with specific models of muscle atrophy in the present report. The findings obtained opened exciting possibilities for its use at clinics for different types of myopathies.

2. Materials and Methods

2.1. Denervation Model

All the procedures involving animals were approved by the ethics committee of the Universitat Autònoma de Barcelona and Generalitat de Catalunya and followed the European Community Council Directive 2010/63/EU. Female Sprague–Dawley rats weighted at 220–250 g at 10 weeks old were purchased from Harlan Laboratories (Indianapolis, IN, USA). For surgical intervention, animals were under anesthesia by intraperitoneal injection of 90 mg/kg ketamine (Ketaset) and 10 mg/kg xylazine (Rompun) [6]. Upon exposure of the sciatic nerve freed of connections, a 2 cm of nerve section was transected above the sciatic nerve trifurcation. The wounds were sutured by planes and disinfected with povidone iodine, and the animals were allowed to recover in a warm environment.

2.2. Hindlimb Immobilization Model

All animal experiments were conducted in the animal facilities at Barcelona Biomedical Research Park (PRBB). This study was designed in accordance with the ethical standards on animal experimentation (EU 2010/63 CEE, Real Decreto 53/2013 BOE 34, Madrid, Spain). Ethical approval was obtained by the animal research committee (Animal welfare department in Catalonia, Spain, EBP-13-1485, 2015/04/20). Female C57BL/6J mice (10 weeks old and weight approximately 20 g) were obtained from Harlan Interfauna Ibérica SL (Barcelona, Spain). Mice were exposed to unilateral hindlimb immobilization as previously described to reproduce a model of disuse-induced muscle atrophy [7–9]. Briefly, the left hindlimb was shaved with clippers and was enveloped using surgical tape. The hindlimb was introduced in a 1.5 mL microcentrifuge tube with a cover and the bottom lids were removed, while maintaining the foot in a plantar-flexed position to induce the maximal atrophy of the target limb muscle. As the weight of the tube was approximately 0.6 g, it did not interfere with the usual mobility of the mice. The left hindlimb of the mice was immobilized for 7 consecutive days, with the time at which the splint was removed to let the animals move freely in their cages to evaluate muscle recovery being 7 days later.

2.3. Drug Treatment

The NeuroHeal mixture is composed of acamprosate and ribavirin. For the rat treatment, we ground acamprosate (Merck, Darmstadt, Germany) and ribavirin (Normon, Madrid, Spain) pills into fine powders and added both to drinking water at final concentrations of 2.2 mM and 1 mM,

respectively. The groups treated with NeuroHeal and 5 mM nicotinamide (NAM) (Sigma-Aldrich, Saint Louis, MO, USA) were given water-containing drugs from the day of the surgery. Fresh drug solutions were made every 3 days. For the in vivo experiments with mice, we ground acamprosate (Merck, Darmstadt, Germany) and ribavirin (Normon, Madrid, Spain) pills into fine powder and administered intraperitoneally daily 40 mg/kg and 26 mg/kg, respectively.

2.4. Grip Test

In all mice, limb strength was determined on day 0, day 7, and day 14, using a specific grip strength meter for rodents (Bioseb, Vitrolles Cedex, France) following previously published methodologies [10–13]. In all mice, the four limbs equally contributed to the evaluation of grip strength. In all the animals, limb strength gain was calculated as the percentage of measurements performed at the end of the study period with respect to the same measurements obtained at baseline (grip strength at the end of the study-period grip strength on day 0)/grip strength on day 0 \times 100).

2.5. Histology

Rats were euthanized with Dolethal (Veotquinol, Madrid, Spain), and mice were euthanized with 0.1 mL sodium pentobarbital (60 mg/kg, intraperitoneally). In all cases, the pedal and blink reflexes were evaluated in order to verify total anaesthetic depth. Rats were perfused with a transcardial infusion of a saline solution containing heparin (10 U/mL) followed by 4% paraformaldehyde in 0.1 M Phosphate Buffered Saline (PBS). Gastrocnemius (GA) muscles (ipsi- and contralateral) were obtained from all the animals after perfusion and were weighted. From mice, the muscle samples were weighted and directly fixed in 4% paraformaldehyde solution. All samples were embedded thereafter into a 30% sucrose solution for cryopreservation at 4 °C until needed.

We transversally cut the GA in the middle, placed them in Tissue-tek for serial cutting (10 μ m sections) in a cryotome (Leica, Heidelberg, Germany) to obtain 20 slides with 5 cuts, and stored them at -20 °C until analysis. The distance between the sections of each slide was 100 μ m, covering a total of 500 μ m of each muscle. Histology and immunohistochemistry of the sections to be compared between them were processed together the same day within the same slide, and image analyses for all groups were also performed the same day. Transversal GA muscle sections were stained with Hematoxylin and Eosin (H&E). Briefly, nuclei were stained with Harris hematoxylin for 6 min followed by differentiation with acid solution of 0.01% HCl in ethanol. Cytoplasm was stained with eosin for 1 min. Sections were dehydrated by graded ethanol (50%, 70%, 96%, and 100% and xylene twice, 5 min each solution) and mounted with DPX mounting medium. For mice tissue analysis, we randomly took images under light microscopy at 20 \times (Nikon Eclipse Ni-E, Nikon, Tokyo, Japan) equipped with a digital camera (Nikon DS-RiE, Nikon, Tokyo, Japan) and Nikon NIS-Element BR software (version 5.11.03, Nikon, Tokyo, Japan). For rat tissue analysis, we randomly took images under light microscopy at 20 \times (Olympus BX51, Olympus, Hamburg, Germany) equipped with a digital camera (Olympus DP50, Olympus, Hamburg, Germany) and CellSens Digital Imaging software (version 1.9, Olympus, Hamburg, Germany). For cross-sectional area (CSA) determination, at least 100 muscle fibers from three different images per muscle were measured. The mean and area distribution for each animal was analyzed ($n = 4$ per group) using Image J software (version 1.46; National Institutes of Health; available at <http://rsb.info.nih.gov/ij/>), and the minimum diameter and the circular area were calculated based on a ratio of calibrated pixels to actual size (mm).

For immunofluorescence labeling, the slices were pretreated with 10 mg/mL NaBH₄ to reduce autofluorescence for 80 min at 4 °C. After washing with standard Phosphate Buffered Saline (PBS), the tissue was incubated in a blocking solution (0.3% Triton-X-100 and 10% fetal bovine serum in PBS) for 1 h at room temperature. Samples were then incubated overnight at 4 °C with primary antibody rabbit anti-acetyl H4K16 (H4K16Ac; 1:1000, Millipore, Burlington, MA, USA) and mouse anti-laminin (1:100, DSHB, Iowa City, IA, USA) After several washes with 0.3% Triton-X-100 in PBS, we added Alexa Fluor 488 against the primary antibody (1:200; Jackson ImmunoResearch, Cambridge, UK) and incubated for 1 h at room temperature. Counterstaining was performed with DAPI (Sigma-Aldrich), and mounting was performed with Mowiol mounting medium (Southern Biotech,

Birmingham, UK). Images of the muscle samples from different groups were taken under the same exposure time, sensibility, and resolution for each marker analyzed with the aid of a digital camera (Nikon D5-Ri2) attached to the microscope (Nikon ECLIPSE Ni) and NIS-Elements BR software (version 5.11.03). Co-labeled fibers were determined as positive using a pseudocolor display by Image J software (version 1.46; National Institutes of Health).

2.6. Immunoblotting

For immunoblotting, denervated rats were euthanized with Dolethal (60 mg/kg, intraperitoneally) at 7 days post-injury (dpi), and the right GA muscle was obtained, snap-frozen in liquid nitrogen, and stored at -80°C . GA half-quarter was added to the lysis buffer (50 mM Tris, pH 6.8, 2 mM EDTA, 0.5% Triton-X-100, and a cocktail of proteases (Sigma-Aldrich) and phosphatase inhibitors (Roche, Basel, Switzerland)), homogenized with a Pellet pestle (Sigma-Aldrich) on ice, and sonicated with an Ultrasonic homogenizer (Model 3000, Biologics Inc., Manassas, VA, USA). Samples were centrifuged for 10 min at 13,000g at 4°C , and protein in supernatants were quantified by BCA assay (Pierce Chemical Co., Dallas, TX, USA). Proteins (20 $\mu\text{g}/\text{well}$) were resolved by SDS-PAGE and transferred to a PVDF membrane in a BioRad cuvette system in 25 mM Tris, pH 8.4, 192 mM glycine, and 20% (*v/v*) methanol. We blocked the membrane with 6% milk solution in 0.1% Tween-TBS (TBS-T) for 1 h at room temperature and incubated it overnight with primary antibodies: rabbit anti-phospho-Ulk1 (Ser 555) (pUlk1; 1:1000; Millipore), mouse anti-Atg5 (1:1000; Nanotools, Teningen, Germany), rabbit anti-LC3 (1:1000; Abcam, Cambridge, UK), mouse anti-p62 (1:100; BD Transduction Laboratories New Jersey, USA), rabbit anti-phospho-AKT (Ser 473) (pAKT; 1:1000; Cell Signaling Technology, Danvers, MA, USA), rabbit anti-AKT (1:1000; Cell Signaling Technology), rabbit anti-phospho-S6 kinase (Thr389) (pP70S6k; 1:1000, Antibodies Online, USA), mouse anti-Muscle Ring Finger 1 (MuRF1) (1:100, Santa Cruz Biotechnology, Dallas, TX, USA), mouse anti-Atrogin-1 (1:100 Santa Cruz Biotechnology), mouse anti-Ub-k48 (1:100), rabbit anti-s5 α (1:1000), and mouse anti-GAPDH (1:5000; Sigma-Aldrich). After washing in TBS-T, the membrane was incubated with an appropriate secondary antibody conjugated with horseradish peroxidase (1:5000, Vector Laboratories, Burlingame, CA, USA) for 1 h. The membrane was visualized using a chemoluminescent method (ECL Clarity Kit, Bio-Rad Laboratories, Hércules, CA, USA), and the images were captured and quantified with Image Lab Software (Bio-Rad Laboratories).

2.7. In Vitro Experiments

The C2C12 myoblast cell line was grown in medium composed by modified Eagle's medium high-glucose (DMEM, Life Technologies, Carlsbad, CA, USA) supplemented with 10% fetal bovine serum (Sigma-Aldrich) and 1% penicillin/streptomycin solution (Sigma-Aldrich). Cells were kept in a humidified incubator at 37°C under 5% CO_2 . To initiate the experiments, we seeded the cells at a density of 8.5×10^3 cell/mL, and after 24 h of culture, the medium was changed to a differentiation medium (DMEM supplemented with 2% horse serum (Sigma-Aldrich) with 1% penicillin/streptomycin solution), which was changed every 2 days. After 6 days of in vitro culture, these cells differentiated and fused to form myotubes. At this time, we added different drugs (acamprosate, ribavirin, Ex-527 (Sigma-Aldrich), and Tumor Necrosis Factor- α (TNF α , Sigma-Aldrich) at 55 μM , 1 μM , 10 μM , and 100 ng/mL, respectively) to the cells for 24 h. Thereafter, cells were fixed using 4% tamponed formaldehyde for 30 min and then washed out with TBS for cytology observations. For immunoblotting, we added RIPA buffer (50 mM tris-HCl, 1% triton-X-100, 0.5% Na-deoxycholate, 0.1% SDS, 150 mM NaCl, and 2 mM EDTA) with inhibitor phosphatases 20 \times and inhibitor proteases 100 \times buffer to the cultured cells ($n = 4-5$). For the fiber diameter evaluation, we randomly took images under light microscopy at 20 \times (Olympus CKX41, model U-LH50HG) equipped with a digital camera (Olympus U-TV1x-2) and an Olympus DP20-5 device from three wells for each condition for at least 100 myotubes for each condition. The area distribution for each condition was analyzed ($n = 3$ per group) using Image J software (version 1.46; National Institutes of Health), was calculated using the circle area equation and using the length between two points from

the myotubes width below the nucleus using the “straight” tool based on a ratio of calibrated pixels to actual size (mm).

2.8. Statistics

The normality and homoscedasticity of the data were studied for each parameter to apply the correct statistical method (parametric or nonparametric) using the Shapiro–Wilk test. For all the data, we performed an unpaired Student’s t-test to compare two groups, one-way analysis of variance (ANOVA) to compare three or more groups, and two-way analysis of variance (ANOVA) to compare grouped data followed by Tuckey’s multiple comparison test. Data are presented as means \pm standard error of the mean (SEM). Statistical analyses were conducted using GraphPad Prism 8 software (San Diego, CA, USA). The myofiber and myotube distributions did not present normality, and we performed Kuskal–Wallis test with Benjamin, Krieger and Yekutieli post hoc. Data are presented as mean, and statistical analyses were conducted using GraphPad Prism 8 software. Differences were assumed to be significant for $p \leq 0.05$.

3. Results

3.1. NeuroHeal Reduces Atrophy-Related Histological Parameters

First, we attempted to decipher the adverse effects of NeuroHeal on healthy animals, so we treated control rats with it for 14 days and analyzed muscle weight and cross-sectional area (CSA). Healthy muscles treated with NeuroHeal did not show changes in muscle weight or fiber size, indicating that NeuroHeal does not have a detrimental impact on healthy muscles (Figure A1). Then, we analyzed the effect of NeuroHeal on muscle atrophy using a model of chronic denervation by sciatic nerve transection. The experimental design consists of 4 groups of animals, as shown in Figure 1A: control-uninjured animals, injured animals treated with vehicle, injured animals treated with NeuroHeal, and injured animals treated with NeuroHeal plus nicotinamide (NAM). Some animals per group were sacrificed at 7 days post-injury (dpi) for western blot analyses, and others were sacrificed at terminus 28 dpi. The last group was included using NAM, which inhibits SIRT1, in order to know whether this protein is involved in any effect promoted by NeuroHeal. Indeed, we verified that the abundance of one of the substrates deacetylated by SIRT1, the histone H4 at lysine 16 (H4K16ac), was modulated in the injured muscles by the treatment (Figure A2). Denervation did not significantly affect the number of H4K16ac-positive nuclei per area at the GA, whereas this number significantly decreased in the group treated with NeuroHeal, as expected by an inducer of SIRT1 activity. In agreement, co-treatment with NAM abolished the effect of NeuroHeal (Figure A2).

Muscle wasting of $26\% \pm 1.31\%$, depicted by a reduced muscle mass, was observed in the ipsilateral GA compared to the contralateral side at 28 dpi (Figure 1B). A similar reduction was observed in the groups of animals treated with acamprostate and ribavirin per separate, the compounds of NeuroHeal (Acamprostate (ACA) $26\% \pm 1.54\%$; Ribavirin (RIB) $25.47\% \pm 0.71\%$). In contrast, the NeuroHeal group presented significantly reduced muscle weight loss ($33.63\% \pm 1.14\%$) compared with untreated animals. This attenuation in muscle wasting was not achieved when adding NAM to the treatment ($29.3\% \pm 1.6\%$), suggesting that SIRT1 activity was involved in the action of NeuroHeal in muscle.

The skeletal muscle atrophy was also apparent at the single fiber level measured by myofiber CSA in all the denervated groups compared to the control group (Figure 1C). However, the distribution of fibers depending on their size varied among groups with a clear leftward shift due to denervation (Figure 1D). The untreated group showed a clustering of smaller fibers being mostly ($49.23\% \pm 10.16\%$) below $200 \mu\text{m}^2$. The shift was less pronounced in the group of animals treated with NeuroHeal which presented the most abundant fibers in the range between 200 and $400 \mu\text{m}^2$ ($48.31\% \pm 5.06\%$). Moreover, the prevalence of the bigger fibers with $>800 \mu\text{m}^2$ CSA were significantly more abundant in the NeuroHeal group with respect to the untreated one. All these effects promoted by NeuroHeal treatment were not observed in the NeuroHeal plus NAM group which had a superior percentage of small fibers, $<200 \mu\text{m}^2$, and less of the gross fibers, $>1000 \mu\text{m}^2$, than the NeuroHeal

group. Altogether, these results suggested that NeuroHeal treatment reduced or prevented myotrophy in a model of muscle chronic denervation.

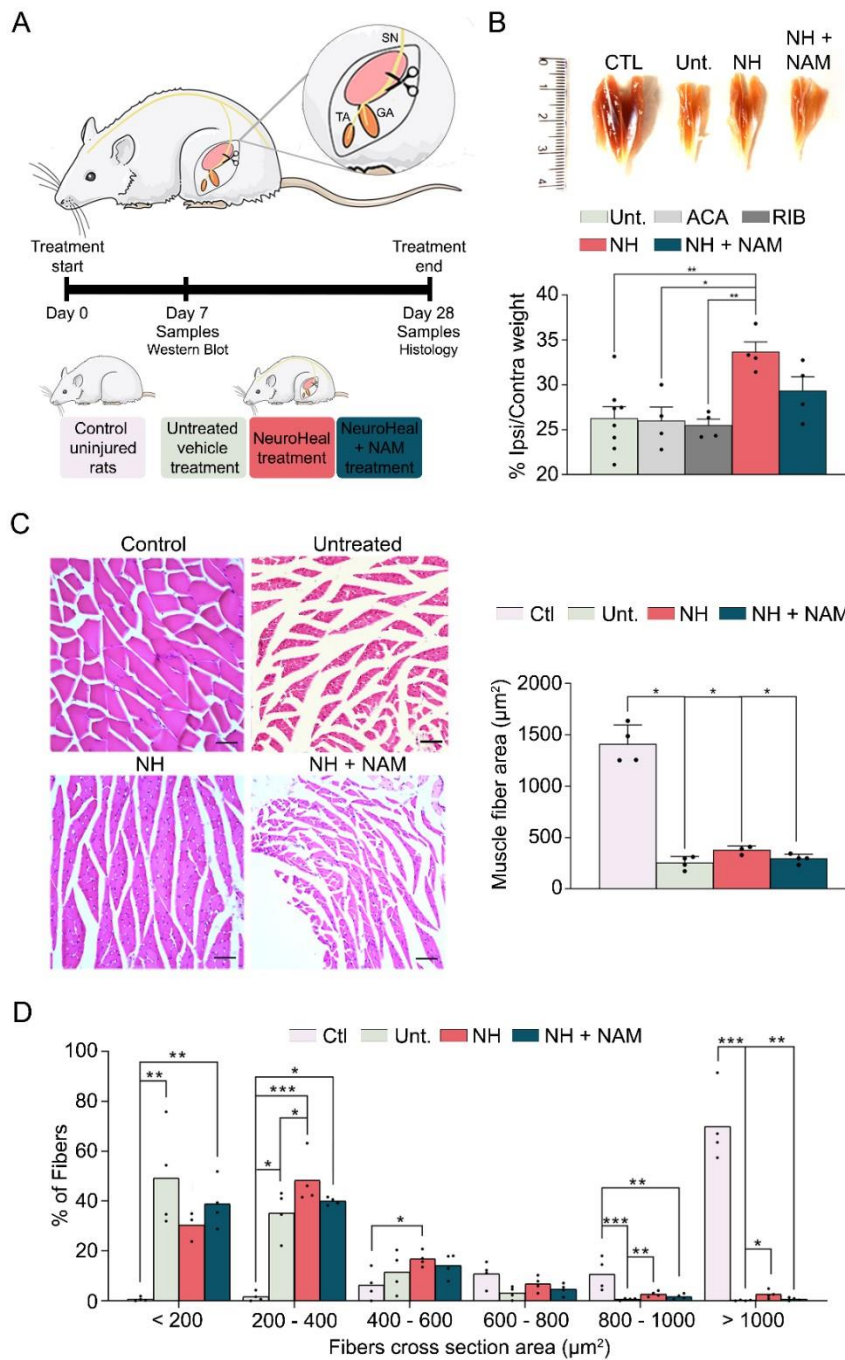


Figure 1. NeuroHeal treatment reduces muscle atrophy by denervation. **(A)** Schematic workflow and experimental groups and **(B)** representative photographs of the gastrocnemius (GA) muscles removed from different experimental groups: control (CTL), injured untreated (Unt.), injured treated with NeuroHeal (NH), and injured treated with NH plus nicotinamide (NAM). Bar graph of the relative average weight of the ipsilateral muscle with respect to the contralateral one from different groups including those animals treated with acamprosate (ACA) or ribavirin (RIB) alone at 28 days post-injury (dpi) ($n = 4$; one-way ANOVA, $*p < 0.05$) is shown. **(C)** Left, representative microphotographs of cross GA muscle sections with Hematoxylin and Eosin (H&E) staining at 28 dpi (scale bar = 100 μm) and, right, representation of cross-sectional area (μm^2) mean of all fibers in the GA muscle ($n = 4$; one-way ANOVA $*p < 0.0001$). **(D)** Histogram of the cross-sectional area (μm^2) distribution of fibers in the GA muscle of different groups ($n = 4$; Kruskal-Wallis, Benjamin, Krieger, and Yekutieli post hoc $*p < 0.05$).

3.2. NeuroHeal Reduces Muscle Atrophy in a Model of Mechanical Unloading

We wanted to discern whether NeuroHeal was attenuating muscle atrophy only in cases with neurogenic origin or whether it may act similarly in those of non-neurogenic origin. Therefore, we used a different model to cause muscle atrophy based on short-term (one-week) hindlimb immobilization with the workflow experimentation schedule depicted in Figure 2A. After one week of recovery time, muscle wasting was evident with a reduction of up 86.82% ± 2.77% in the GA weight ratio of the ipsilateral muscle compared to the non-immobilized contralateral side. In contrast, animals treated with NeuroHeal maintained muscle weight to 94.88% ± 2.25%, significantly higher than untreated animals (Figure 2B). Accordingly, disuse caused a drastic reduction of the mean myofiber CSA in the immobilized and untreated with respect to the non-immobilized muscles although this was not so evident in the group treated with NeuroHeal (Figure 2C). Detailed examination of the distribution of the CSA showed a leftward shift in the fiber diameter distribution, with more prevalence of the smaller fibers, from 400 to 1200 μm² (CTL 23.33%; Unt. 45.92%; NH 32.47%), and less abundance of those bigger than 1800 μm². This shift was significantly less pronounced in the animals treated with NeuroHeal, with more abundance of the bigger sized fibers, >1800 μm² (24.63%), than in the untreated animals (12.33%) (Figure 2D).

Finally, we performed a functional test using the grip test to evaluate the limb strength (Figure 2E). After 1 week of immobilization, the untreated group showed a decrease in strength in the four limbs, which was the worst after 1 week of recovery (Figure 2E; day 7, 87.15% ± 3.08%; day 14, 85.92% ± 1.84%). In contrast, the group treated with NeuroHeal showed a significantly higher strength in the immobilization week and even superior strength after the recovery week (Figure 2E; day 7, 96.7% ± 4.27%; day 14, 112.3% ± 8.95%).

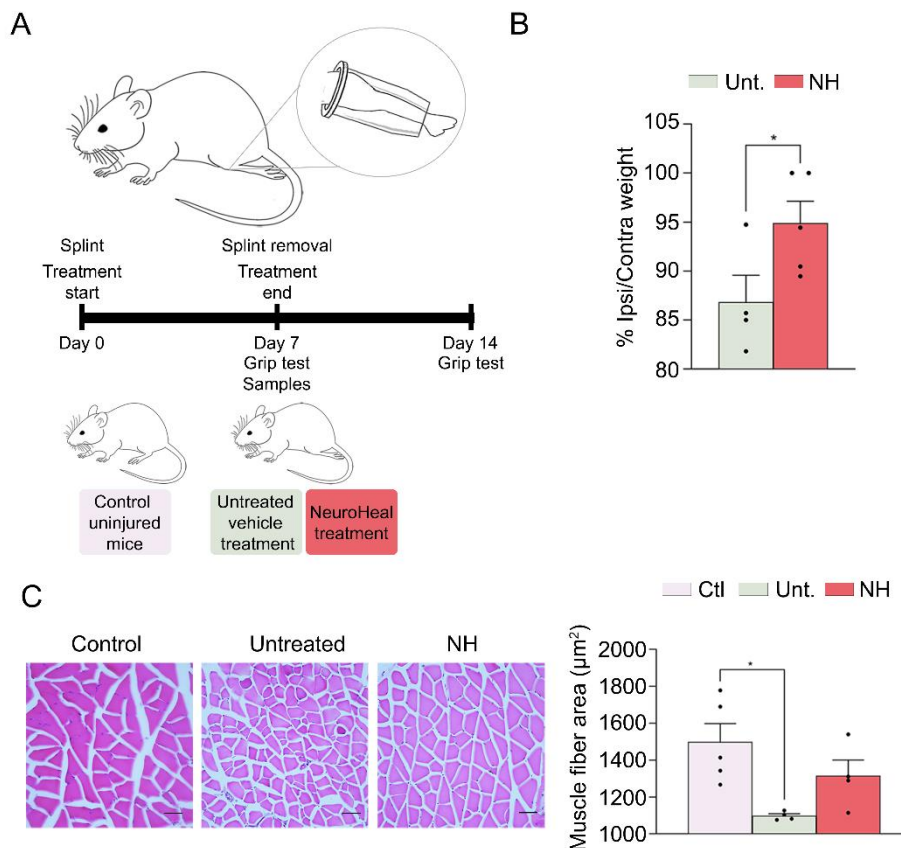


Figure 2. Cont.

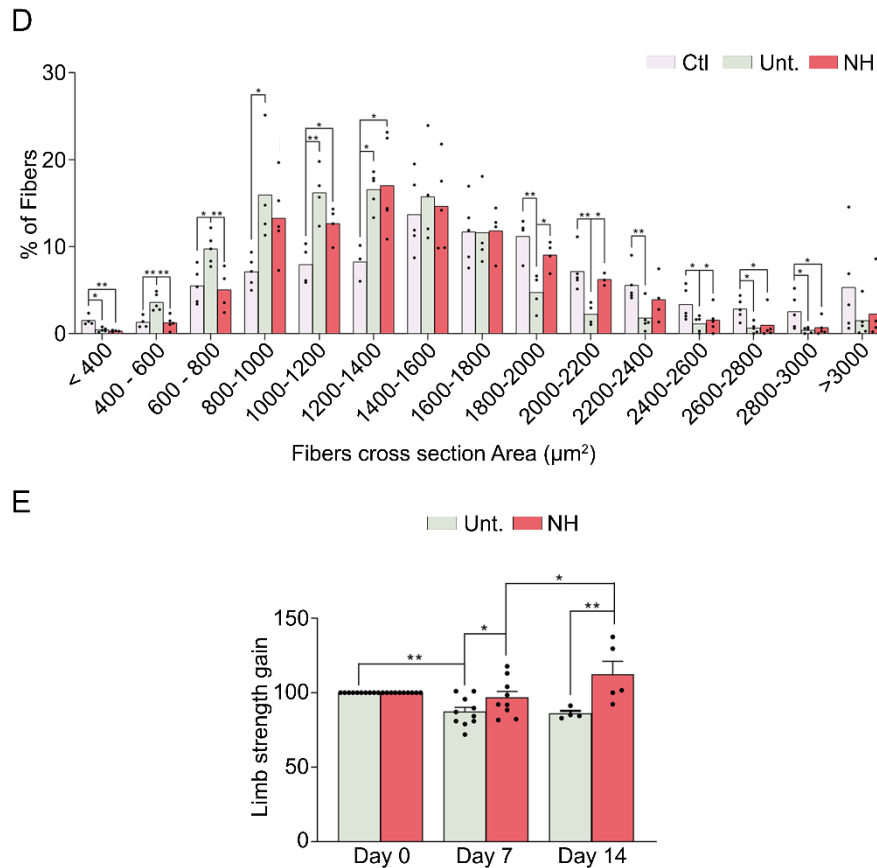


Figure 2. NeuroHeal treatment reduces muscle atrophy by disuse. (A) Schematic workflow and experimental groups and (B) a bar graph of the gastrocnemius (GA) muscle weight ratio between ipsilateral and contralateral sites at day 7 ($n = 3-4$; t-test, $* p < 0.05$). (C) Left, representative microphotographs of cross GA muscle sections with H&E staining at day 7 (scale bar = 100 μm) and, right, representation of cross-sectional area (μm^2) mean of all fibers in the GA muscle ($n = 5$; one-way ANOVA $* p < 0.05$). (D) Histogram of the distribution of the cross-sectional area (μm^2) of GA fibers ($n = 3-4$; Benjamin, Krieger, and Yekutieli post hoc $* p < 0.05$). (E) Bar graph of the grip strength of the immobilized hindlimb from NeuroHeal treated (NH) and untreated groups (Unt.) obtained at day 0, day 7, and day 14 ($n = 5-10$; one-way ANOVA, $* p < 0.05$).

3.3. NeuroHeal Preserved Fiber Diameter in Atrophied Myotubes Cells In Vitro

To confirm that the action of NeuroHeal was produced on the muscular cells independently of a nervous compound, we used a model of myoblast C2C12 cells which form myotubes after 7 days of culture in differentiation medium in vitro [14]. We treated the differentiated myotubes with 10 $\mu\text{g/mL}$ TNF α for 24 h, with or without NeuroHeal or Ex-527, a specific SIRT1 inhibitor. Analyzing the diameter of the formed myotubes, we observed that TNF α caused a shift in the diameter of fibers, increasing the amount of smaller fibers, those $<200 \mu\text{m}^2$ ($81.05\% \pm 12.49\%$ vs $53.93\% \pm 14.68\%$ in the control, non-atrophied cells), and diminishing the amount of the bigger ones, $>400 \mu\text{m}^2$ ($7.86\% \pm 7.04\%$ vs $23.1\% \pm 18\%$ in the control, non-atrophied cells) (Figure 3A). In contrast, the treatment addition of NeuroHeal for the same time as TNF α sustained most of the fibers in its median size (between 200 and 400 μm^2) ($43.5\% \pm 12.01\%$) or bigger sizes ($18.02\% \pm 7.9\%$). The addition of the SIRT1 inhibitor abolished these effects promoted by NeuroHeal. Thus, in agreement with what was observed in vivo, NeuroHeal reduces atrophy-induced in muscle cells. We also observed that NeuroHeal treatment reduced the levels of the Muscle Ring Finger 1 (MuRF1), an E3 ligase used as a marker of atrophy in muscle (Figure 3B).

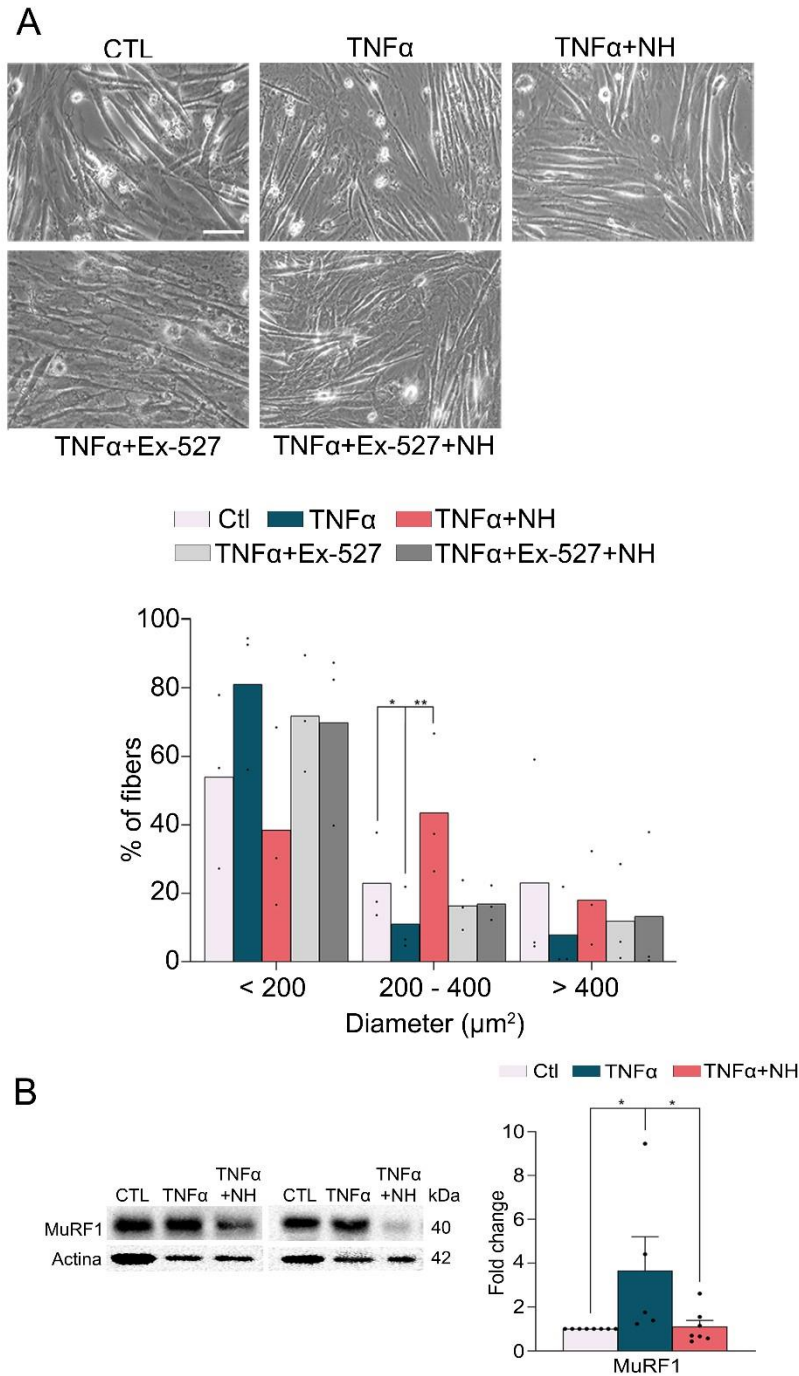


Figure 3. NeuroHeal reduces fiber atrophy produced by Tumor Necrosis Factor- α (TNF α) in vitro. (A) Representative microphotographs of myotubes derived from a C2C12 myoblast cell line culture at day 7 and treated during the last 24 h with different components (control (CTL), NeuroHeal (NH), and Ex-527 as a specific SIRT1 inhibitor (scale bar = 50 μm)). Histogram of the distribution of myotubes diameter ($n = 3-6$; Kruskal–Wallis, Benjamin, Krieger, and Yekutieli post hoc, * $p < 0.05$) and (B) a Western blot and the corresponding bar graph showing the analyses of Muscle Ring Finger 1 (MuRF1) protein levels in the different experimental groups at day 7 ($n = 3$; one-way ANOVA, * $p < 0.05$).

3.4. NeuroHeal Reduced Proteasome Markers

Since muscle atrophy is the result of a protein degradation rate which exceeds protein synthesis [15], we examined how NeuroHeal affected the balance between catabolism and anabolism. PI3K/Akt signaling stimulates the rate of protein synthesis via p70S6Kinase and p90 ribosomal S6 kinase and

negatively regulates protein degradation, predominantly by its inhibiting effect on proteasomal and lysosomal protein degradation [1]. We observed that the ratio of phospho-AKT (Ser 473) isoform was reduced due to denervation at 7 dpi (Figure 4A). In agreement with a reduced activity of AKT, the levels of p70s6k were also reduced. The presence of NeuroHeal, with or without NAM, did not significantly change these effects.

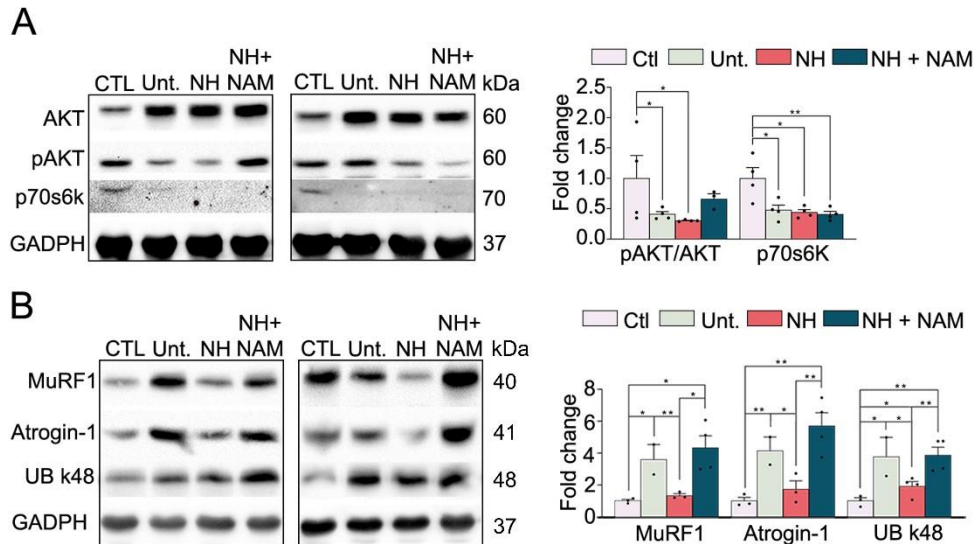


Figure 4. Ubiquitin-proteasomal degradation is modulated by NeuroHeal in the denervated muscle model. (A) Western blots and associated bar graphs showing the analyses of phosphorylated AKT, AKT, and pP70s6k protein levels in different experimental groups at 7 dpi (control (CTL), injured untreated (Unt.), injured treated with NeuroHeal (NH), and injured treated with NH plus nicotinamide (NAM)) ($n = 3-4$; one-way ANOVA, $* p < 0.05$) and (B) Western blots and associated bar graphs showing the analyses of Atrogin-1, MuRF1, and K-48 polyubiquitin chain protein levels in different experimental groups at 7 dpi ($n = 3-4$; t-test, $* p < 0.05$).

On the other side, the prime system for muscle protein degradation is the ubiquitin-proteasome system [1]. During protein degradation, contractile proteins are ubiquitinated by the consecutive actions of the E1, E2, and E3 enzymes which can then be recognized and subsequently degraded by proteasomes. The gene expression as well as their function in muscle atrophy of two E3 ligases, MuRF1 and muscle atrophy F-box (MAFbx, also known as Atrogin-1), have been extensively examined. Both E3 ligases are particularly involved in the degradation of contractile proteins. During several atrophic conditions, MuRF1 and Atrogin-1 expression levels are increased [16]. Accordingly, we observed that MuRF1 and Atrogin-1 levels were raised in the injured untreated animals (Figure 4B). In contrast, the levels of both proteins were diminished in the NeuroHeal group which was abolished in the group with NAM. These results are in agreement with the reduced atrophy observed in denervated muscles.

In light of these differences, we further investigate the proteasome function by analyzing the K48-polyubiquitin chains which are the most abundant linkage in cells and are thought to be the major signal for proteasome-mediated degradation [17]. There was an increase in K-48 polyubiquitin chains in the lesioned untreated animals which was modified by NeuroHeal administration. In contrast, the addition of NAM considerably increased the levels of this factor (Figure 4B). At the same time, untreated injured animals showed an increase in the proteasome subunit 5 α (s5 α) [18], while NeuroHeal-treated animals presented normalized levels of it (Figure A3). These effects were reverted when the animals were co-treated with NeuroHeal and NAM.

Altogether, these results suggested that NeuroHeal did not substantially affect the protein synthesis, but NeuroHeal modulates the proteasome, which might lead to reduced atrophy.

3.5. NeuroHeal Modulates Atrophy Associated Autophagy

Autophagy is another key mechanism for muscle protein degradation [19]. Autophagy concerns the engulfment of cellular particles into autophagosomes, which subsequently fuse with lysosomes to be degraded in the acid intralysosomal environment. In cells undergoing autophagy, phagophore formation initiates after the Unc-51-like autophagy-activating kinase 1 (ULK1) activation, and its elongation is regulated by two ubiquitin-like reactions: the first leading to the formation of the complex ATG12-ATG5-ATG16L1 and the second involving the conjugation of the microtubule-associated protein light chain 3 (MAP-LC3/ATG8/LC3) to phosphatidylethanolamine at the autophagosome membrane to form autophagosome-associated LC3-II. Once the autophagosome is formed, it acquires the ability to bind autophagic substrates and/or proteins which mediate cargo selectivity (including sequestosome 1 (p62/SQSTM1)). We recently observed that NeuroHeal neuroprotects neonatal axotomized motoneurons and promotes autophagy [20]. Thus, we aimed to analyze whether this process was also involved in the observed reduction of muscle atrophy by NeuroHeal. All the protein levels of the markers analyzed, pULK1 (phosphorylation at Ser 555), LC3-II, ATG5-ATG12 conjugate, and p62/SQSTM1, were increased due to denervation as expected [21] (Figure 5). The activation of pULK1 was sustained in the NeuroHeal group; however, the levels of LC3-II were reduced and those of ATG5-ATG12 conjugate and p62/SQSTM1 were normalized. The addition of NAM did not promote differences in these markers with respect to NeuroHeal treatment alone except for a striking increase in p62/SQSTM1 levels (Figure 5). Altogether, these results suggested that denervation caused an activation of autophagy characterized by LC3II and p62/SQSTM1 levels which may suggest autophagy flux blockade, whereas the reduction promoted by NeuroHeal pointed to a better resolution of this process. SIRT1 activation by NeuroHeal may be involved particularly in the diminution of p62/SQSTM1.

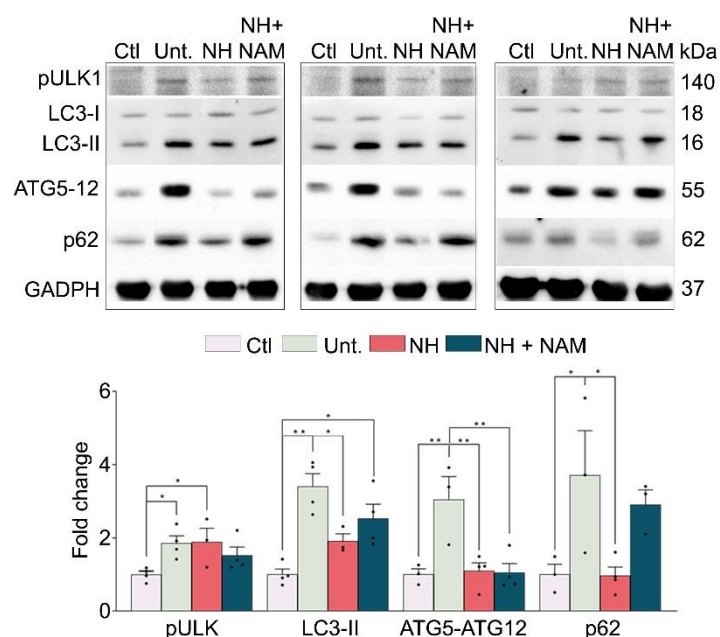


Figure 5. Autophagy flux is modulated by NeuroHeal in the denervated muscle model. Western blots and the associated bar graphs showing the analyses of phosphorylated ULK1, LC3-II, the ATG5-ATG12 complex, p62, and protein levels in different experimental groups at 7 dpi (control (CTL), injured untreated (Unt.), injured treated with NeuroHeal (NH), and injured treated with NH plus nicotinamide (NAM)) ($n = 3-4$; one-way ANOVA, $* p < 0.05$).

4. Discussion

Herein, we have demonstrated that NeuroHeal reduces neurogenic and non-neurogenic myopathy using diverse models: a model of chronic denervation, a disuse model, and an in vitro model without the influence of neuronal components. Analyzing the anabolic/catabolic unbalance

which leads to muscle atrophy, we found that NeuroHeal sustained a normal activation of protein synthesis after denervation, although with significant differences in protein degradation: downregulation of MuRF1, K48 poly-Ub chains, and p62/SQSTM1. These differences suggested that NeuroHeal promotes a diminution in proteasomal activity and amelioration of the autophagy flux. Moreover, SIRT1 activation by NeuroHeal was necessary to prevent muscle atrophy. These results are in agreement with a recent article describing the protective effect of SIRT1 activity on muscle atrophy [22].

The control of mass in adult skeletal muscle is determined by a dynamic balance between anabolic and catabolic processes triggered by changes in activity or pathological conditions. Muscle hypertrophy is associated with increased protein synthesis induced by activated AKT and mammalian target of rapamycin complex 1 (mTORC1) pathways. Unlike muscle hypertrophy, muscle atrophy always involves a proteostatic shift in favor of catabolic versus anabolic processes. Skeletal muscle protein degradation is executed by several proteolytic systems, including calpains [23], caspases [24], the proteasomal system [25], and the autophagy-lysosomal system [26]. Although, importantly, the selective removal of cellular proteins in muscle largely relies on their ubiquitination followed by proteasomal or autophagy-lysosomal degradation [27–29].

The ubiquitin pathway and specific ubiquitin pathway enzymes have been directly implicated in the progression of muscle atrophy. The ubiquitin E3 ligase Muscle-specific RING Finger E3 ligase (MuRF1) is upregulated and increases protein degradation and muscle wasting in numerous muscle atrophy models. MuRF1 knockout mice (MuRF1^{-/-}) is resistant to skeletal muscle atrophy under starvation conditions, post-denervation, and in hindlimb suspension models [30,31], and the use of MuRF1 inhibitors reduces atrophy in cellular models [32]. Although the mechanisms underlying this effect should be analyzed in further detail, we have demonstrated that NeuroHeal downregulates the MuRF1 protein level after denervation, which positioned this agent as a good candidate for clinics.

Autophagy regulates muscle homeostasis, removing protein aggregates and abnormal organelles which otherwise lead to muscle toxicity and dysfunction [4]. Although initially controverted [33–35], the use of more specific techniques to analyze the autophagy flux have demonstrated the importance of autophagy to reduce atrophy and its malfunction is associated with muscle wasting. For instance, deficiency in the autophagy-related genes Atg5 or Atg7 is lethal in neonatal mice due to disruption of the supply of transplacental nutrients [4,36]. These findings suggest that autophagy deficiency plays a role in various forms of hereditary muscular dystrophy, including Bessler myopathy, Ullrich congenital muscular dystrophy, and Duchenne muscular dystrophy (DMD) [37]. More recently, Odeh and collaborators demonstrated that autophagy flux was slowed down or even blocked in denervated muscles [38]. Moreover, it has been reported that a correct autophagy flux is fundamental for myofiber survival [39,40] and satellite cells stemness [41]. A key marker to study autophagy flux is the accumulation of both LC3-II and p62, which indicates the blockade of autophagy flux [19]. Our observations are in agreement with the presence of autophagy flux blockade after denervation. Moreover, NeuroHeal, while sustained, increased pULK1 levels and diminished significantly those markers suggesting a deblockade of the flux and thus a promising agent in this area.

Both the ubiquitin-proteasomal system and autophagy degradative pathways are interconnected. Misfolded ubiquitinated proteins are normally degraded via the ubiquitin-proteasomal system, but when this is overloaded or malfunctioning, these proteins are accumulated and are subsequently sequestered into larger structures which become targets for aggrephagy [42–44]. The autophagic cargo receptor p62/SQSTM1 is required for the nucleation of such structures [45,46] and is a key factor for both degradative pathways [47,48]. On one side, the accumulation of protein aggregates results in an upregulation of p62, which in turn negatively affects the ubiquitin-proteasomal system, promoting a switch towards aggrephagy. On the other side, high concentrations of K48-linked ubiquitin chains, one of the canonical proteasomal degradation signals [49,50], which can be accumulated upon proteasome deficiency [51], inhibits p62-induced clustering [52]. After denervation, we observed accumulation of both p62 and K48-linked ubiquitin chains, suggesting that both systems are dysfunctional or probably overloaded. With NeuroHeal, both systems are less active

or less likely to function correctly probably because the good resolution of autophagy flux may engulf also overloaded proteasomes.

Finally, the effects observed by the addition of NAM were also informative. It has been reported recently that p62 specifically undergoes acetylation, which is required for the formation and subsequent autophagic clearance of p62 clusters [53]. p62 requires acetylation by TIP60 on K420 and K435 to significantly enhance its binding to ubiquitin and p62 clustering during cell starvation. p62 is deacetylated by HDAC6, which is not affected by NAM. However, TIP60 activity is modulated negatively by SIRT1 [54,55]. NeuroHeal increases SIRT1 activity and hence would probably diminish the acetylation activity of TIP60 and consequently slow down p62 clustering. In the presence of NAM, p62 might be overacetylated and might shift toward the avid formation of p62 bodies. Somehow, these observations indicate that softening the autophagy process favors a good resolution. This challenging hypothesis would be very interesting to be tested in the near future. Probably, the controversy of whether to boost autophagy is not the issue to tackle, but its fine-tune activation may yield protective effects. Indeed, we have recently reported that NeuroHeal-fine-tuned autophagy promotes neuroprotection of neonatal motoneurons, improves motor axonal regeneration, and has a role in neuropathic pain [20,56–58].

Altogether, our results suggested that NeuroHeal might be an interesting drug to be used in several clinical affectations and leads to muscle atrophy such as neurodegenerative diseases, to peripheral nerve injuries prolonging medical hospitalization, or even to patients with Covid-19 due to the SARS-Cov-2 virus infection.

5. Study Limitations and Future Research

The first limitation of this study was to analyze autophagy in a single muscle, in an atrophy model, and in a fixed time window. The flow of autophagy differs widely among tissues, and since it is a dynamic process, it would be interesting to describe its state in different paradigms. However, due to the largely different experimental groups, we had to focus on a muscle at a specific time point after injury. Another limitation of this study was that we did not investigate the involvement of mitochondria in our models, as they are known to play an important role in maintaining muscle homeostasis.

Future studies will determine which cell type is the target of NeuroHeal and will analyze whether NeuroHeal affects the shift in fiber type which occurs during muscle loss. Finally, this work has opened new lines of research to test the therapeutic effect of NeuroHeal on other muscle disorders, such as those triggered by food deprivation.

6. Patents

NeuroHeal is currently under patent review.

Author Contributions: S.M.-M.A. and D.R.-G. conceived research, performed the experiments, analyzed the results, and wrote the paper. L.M.-G. and E.B. designed and performed the experiment in the mice model. C.C. conceived the research, analyzed the results, and wrote the paper. All the authors approved the final version of the manuscript.

Funding: This work was funded by the Ministerio de Economía y Competitividad of Spain under the grant number SAF 2014-59701. We are also grateful for the support of TERCEL and CIBERNED from the Instituto de Salud Carlos III of Spain.

Acknowledgments: We are sincerely grateful to Dr. Diego Ruano (Universidad de Sevilla, Spain) and Dr. Alejandro Vaquero (IDIBELL, Barcelona, Spain) for gifting us the UB k48, s5 α and H4K16Ac antibodies. The 2E-8 antibody was obtained from the Developmental Studies Hybridoma Bank developed under the auspices of the NICHD and maintained by the University of Iowa, Department of Biology.

Conflicts of Interest: The authors declare no conflict of interest. NeuroHeal use for muscle disorders is under patent review.

References:

1. Cohen, I.R.; Lambris, J.D. Advances in Experimental Medicine and Biology. *Springer Singapore* **2018**, *1088*, 1434–1436.
2. Legrand, D.; Vaes, B.; Matheï, C.; Adriaensen, W.; Van Pottelbergh, G.; Degryse, J.-M. Muscle Strength and Physical Performance as Predictors of Mortality, Hospitalization, and Disability in the Oldest Old. *J. Am. Geriatr. Soc.* **2014**, *62*, 1030–1038.
3. Cohen, S.; Nathan, J.a.; Goldberg, A.L. Muscle wasting in disease: Molecular mechanisms and promising therapies. *Nat. Rev. Drug Discov.* **2015**, *14*, 58–74.
4. Masiero, E.; Agatea, L.; Mammucari, C.; Blaauw, B.; Loro, E.; Komatsu, M.; Metzger, D.; Reggiani, C.; Schiaffino, S.; Sandri, M. Autophagy is required to maintain muscle mass. *Cell Metab.* **2009**, *10*, 507–515.
5. Romeo-Guitart, D.; Forés, J.; Herrando-Grabulosa, M.; Valls, R.; Leiva-Rodríguez, T.; Galea, E.; González-Pérez, F.; Navarro, X.; Petegnief, V.; Bosch, A.; et al. Neuroprotective Drug for Nerve Trauma Revealed Using Artificial Intelligence. *Sci. Rep.* **2018**, *8*, 1–15.
6. Romeo-Guitart, D.; Forés, J.; Navarro, X.; Casas, C. Boosted Regeneration and Reduced Denervated Muscle Atrophy by NeuroHeal in a Pre-clinical Model of Lumbar Root Avulsion with Delayed Reimplantation. *Sci. Rep.* **2017**, *7*, 1–12.
7. Vargas, R.; Lang, C.H. Alcohol Accelerates Loss of Muscle and Impairs Recovery of Muscle Mass Resulting From Disuse Atrophy. *Alcohol. Clin. Exp. Res.* **2007**, *32*, 128–137.
8. Magne, H.; Savary-Auzeloux, I.; Vazeille, E.; Claustre, A.; Attaix, D.; Anne, L.; Véronique, S.-L.; Philippe, G.; Dardevet, D.; Combaret, L. Lack of muscle recovery after immobilization in old rats does not result from a defect in normalization of the ubiquitin-proteasome and the caspase-dependent apoptotic pathways. *J. Physiol.* **2011**, *589*, 511–524.
9. Lang, S.M.; Kazi, A.A.; Hong-Brown, L.; Lang, C.H. Delayed Recovery of Skeletal Muscle Mass following Hindlimb Immobilization in mTOR Heterozygous Mice. *PLoS One* **2012**, *7*, e38910.
10. Barreiro, E.; Marín-Corral, J.; Sanchez, F.; Mielgo, V.; Alvarez, F.J.; Gáldiz, J.B.; Gea, J. Reference values of respiratory and peripheral muscle function in rats. *J. Anim. Physiol. Anim. Nutr. (Berl.)* **2010**, *94*, e393–e401x.
11. Barreiro, E.; Bustamante, V.; Cejudo, P.; Gáldiz, J.B.; Gea, J.; de Lucas, P.; Martínez-Llorens, J.; Ortega, F.; Puente-Maestu, L.; Roca, J.; et al. Normativa SEPAR sobre disfunción muscular de los pacientes con enfermedad pulmonar obstructiva crónica. *Arch. Bronconeumol.* **2015**, *51*, 384–395.
12. Chacon-Cabrera, A.; Fermoselle, C.; Urtreger, A.J.; Mateu-Jimenez, M.; Diament, M.J.; de Kier Joffé, E.D.B.; Sandri, M.; Barreiro, E. Pharmacological Strategies in Lung Cancer-Induced Cachexia: Effects on Muscle Proteolysis, Autophagy, Structure, and Weakness. *J. Cell. Physiol.* **2014**, *229*, 1660–1672.
13. Chacon-Cabrera, A.; Fermoselle, C.; Salmela, I.; Yelamos, J.; Barreiro, E. MicroRNA expression and protein acetylation pattern in respiratory and limb muscles of Parp-1 $^{-/-}$ and Parp-2 $^{-/-}$ mice with lung cancer cachexia. *Biochim. Biophys. Acta - Gen. Subj.* **2015**, *1850*, 2530–2543.
14. Wang, D.T.; Yin, Y.; Yang, Y.J.; Lv, P.J.; Shi, Y.; Lu, L.; Wei, L.B. Resveratrol prevents TNF- α -induced muscle atrophy via regulation of Akt/mTOR/FoxO1 signaling in C2C12 myotubes. *Int. Immunopharmacol.* **2014**, *19*, 206–213.
15. Schiaffino, S.; Dyar, K.A.; Ciciliot, S.; Blaauw, B.; Sandri, M. Mechanisms regulating skeletal muscle growth and atrophy. *FEBS J.* **2013**, *280*, 4294–4314.
16. Lagirand-Cantaloube, J.; Offner, N.; Csibi, A.; Leibovitch, M.P.; Batonnet-Pichon, S.; Tintignac, L.A.; Segura, C.T.; Leibovitch, S.A. The initiation factor eIF3-f is a major target for Atrogin1/MAFbx function in

- skeletal muscle atrophy. *EMBO J.* **2008**, *27*, 1266–1276.
17. Grice, G.L.; Nathan, J.A. The recognition of ubiquitinated proteins by the proteasome. *Cell. Mol. Life Sci.* **2016**, *73*, 3497–3506.
 18. Tanaka, K. The proteasome: Overview of structure and functions. *Proc. Japan Acad. Ser. B* **2009**, *85*, 12–36.
 19. Klionsky, D.J.; Abdelmohsen, K.; Abe, A.; Abedin, M.J.; Abeliovich, H.; Arozena, A.A.; Adachi, H.; Adams, C.M.; Adams, P.D.; Adeli, K.; et al. Guidelines for the use and interpretation of assays for monitoring autophagy (3rd edition). *Autophagy* **2016**, *12*, 1–222.
 20. Romeo-Guitart, D.; Marcos-DeJuana, C.; Marmolejo-Martínez-Artesero, S.; Navarro, X.; Casas, C. Novel neuroprotective therapy with NeuroHeal by autophagy induction for damaged neonatal motoneurons. *Theranostics* **2020**, *10*, 5154–5168.
 21. Zhao, J.; Braut, J.J.; Schild, A.; Cao, P.; Sandri, M.; Schiaffino, S.; Lecker, S.H.; Goldberg, A.L. FoxO3 Coordinately Activates Protein Degradation by the Autophagic/Lysosomal and Proteasomal Pathways in Atrophying Muscle Cells. *Cell Metab.* **2007**, *6*, 472–483.
 22. Lee, D.; Goldberg, A.L. SIRT1 protein, by blocking the activities of transcription factors FoxO1 and FoxO3, inhibits muscle atrophy and promotes muscle growth. *J. Biol. Chem.* **2013**, *288*, 30515–30526.
 23. Glass, D.J. Molecular mechanisms modulating muscle mass. *Trends Mol. Med.* **2003**, *9*, 344–350.
 24. Glass, D.J. Skeletal muscle hypertrophy and atrophy signaling pathways. *Int. J. Biochem. Cell Biol.* **2005**, *37*, 1974–19848.
 25. Lecker, S.H.; Jagoe, R.T.; Gilbert, A.; Gomes, M.; Baracos, V.; Bailey, J.; Price, S.R.; Mitch, W.E.; Goldberg, A.L. Multiple types of skeletal muscle atrophy involve a common program of changes in gene expression. *FASEB J.* **2004**, *18*, 39–51.
 26. Heszele, M.F.C.; Price, S.R. Insulin-Like Growth Factor I: The Yin and Yang of Muscle Atrophy. *Endocrinology* **2004**, *145*, 4803–4805.
 27. Li, H.; Malhotra, S.; Kumar, A. Nuclear factor-kappa B signaling in skeletal muscle atrophy. *J. Mol. Med.* **2008**, *86*, 1113–1126.
 28. Mammucari, C.; Milan, G.; Romanello, V.; Masiere, E.; Rudolf, R.; Del Piccolo, P.; Burden, S.J.; Di Lisi, R.; Sandri, C.; Zhao, J.; et al. FoxO3 Controls Autophagy in Skeletal Muscle In Vivo. *Cell Metab.* **2007**, *6*, 458–471.
 29. Sandri, M.; Sandri, C.; Gilbert, A.; Skurk, C.; Calabria, E.; Picard, A.; Walsh, K.; Schiaffino, S.; Lecker, S.H.; Goldberg, A.L. Foxo Transcription Factors Induce the Atrophy-Related Ubiquitin Ligase Atrogin-1 and Cause Skeletal Muscle Atrophy. *Cell* **2004**, *117*, 399–412..
 30. S C Bodine 1, E Latres, S Baumhueter, V K Lai, L Nunez, B A Clarke, W T Poueymirou, F J Panaro, E Na, K Dharmarajan, Z Q Pan, D M Valenzuela, T M DeChiara, T N Stitt, G D Yancopoulos, D.J.G. Identification of Ubiquitin Ligases Required for Skeletal Muscle Atrophy. *Science (80-)*. **2001**, *294*, 1704–1708.
 31. Labeit, S.; Kohl, C.H.; Witt, C.C.; Labeit, D.; Jung, J.; Granzier, H. Modulation of Muscle Atrophy, Fatigue and MLC Phosphorylation by MuRF1 as Indicated by Hindlimb Suspension Studies on MuRF1-KO Mice. *J. Biomed. Biotechnol.* **2010**, *2010*, 1–9.
 32. Eddins, M.J.; Marblestone, J.G.; Suresh Kumar, K.G.; Leach, C.A.; Sterner, D.E.; Mattern, M.R.; Nicholson, B. Targeting the Ubiquitin E3 Ligase MuRF1 to Inhibit Muscle Atrophy. *Cell Biochem. Biophys.* **2011**, *60*, 113–118.
 33. Quy, P.N.; Kuma, A.; Pierre, P.; Mizushima, N. Proteasome-dependent Activation of Mammalian Target of Rapamycin Complex 1 (mTORC1) Is Essential for Autophagy Suppression and Muscle Remodeling Following Denervation. *J. Biol. Chem.* **2013**, *288*, 1125–1134.
 34. Sala, D.; Ivanova, S.; Plana, N.; Ribas, V.; Duran, J.; Bach, D.; Turkseven, S.; Laville, M.; Vidal, H.; Karczewska-Kupczewska, M.; et al. Autophagy-regulating TP53INP2 mediates muscle wasting and is repressed in diabetes. *J. Clin. Invest.* **2014**, *124*, 1914–1927.
 35. Kim, J.; Won, K.-J.; Lee, H.M.; Hwang, B.-Y.; Bae, Y.-M.; Choi, W.S.; Song, H.; Lim, K.W.; Lee, C.-K.; Kim, B. p38 MAPK Participates in Muscle-Specific RING Finger 1-Mediated Atrophy in Cast-Immobilized Rat Gastrocnemius Muscle. *Korean J. Physiol. Pharmacol.* **2009**, *13*, 491.
 36. Xia, H.-G.; Zhang, L.; Chen, G.; Zhang, T.; Liu, J.; Jin, M.; Ma, X.; Ma, D.; Yuan, J. Control of basal autophagy by calpain1 mediated cleavage of ATG5. *Autophagy* **2010**, *6*, 61–66.
 37. Sandri, M.; Coletto, L.; Grumati, P.; Bonaldo, P. Misregulation of autophagy and protein degradation systems in myopathies and muscular dystrophies. *J. Cell Sci.* **2013**, *126*, 5325–5333.
 38. Odeh, M.; Tamir-Livne, Y.; Haas, T.; Bengal, E. P38 α MAPK coordinates the activities of several metabolic pathways that together induce atrophy of denervated muscles. *FEBS J.* **2020**, *287*, 73–93.
 39. Vergne, I.; Roberts, E.; Elmaoued, R.A.; Tosch, V.; Delgado, M.A.; Proikas-Cezanne, T.; Laporte, J.; Deretic, V. Control of autophagy initiation by phosphoinositide 3-phosphatase jumpy. *EMBO J.* **2009**, *28*, 2244–2258.
 40. Grumati, P.; Coletto, L.; Sabatelli, P.; Cescon, M.; Angelin, A.; Bertaggia, E.; Blaauw, B.; Urciuolo, A.;

- Tiepolo, T.; Merlini, L.; et al. Autophagy is defective in collagen VI muscular dystrophies, and its reactivation rescues myofiber degeneration. *Nat. Med.* **2010**, *16*, 1313–1320.
41. García-Prat, L.; Martínez-Vicente, M.; Perdiguero, E.; Ortet, L.; Rodríguez-Ubreva, Javier; reboallo, E.; Ruiz-Bonilla, V.; Gutarra, S.; Ballestar, E.; Serrano, A.L.; et al. Autophagy maintains stemness by preventing senescence. *Nature* **2016**, *529*, 37–42.
 42. Rusmini, P.; Polanco, M.J.; Cristofani, R.; Cicardi, M.E.; Meroni, M.; Galbiati, M.; Piccolella, M.; Messi, E.; Giorgetti, E.; Lieberman, A.P.; et al. Aberrant Autophagic Response in The Muscle of A Knock-in Mouse Model of Spinal and Bulbar Muscular Atrophy. *Sci. Rep.* **2015**, *5*, 15174.
 43. Korolchuk, V.I.; Menzies, F.M.; Rubinsztein, D.C. Mechanisms of cross-talk between the ubiquitin-proteasome and autophagy-lysosome systems. *FEBS Lett.* **2010**, *584*, 1393–1398.
 44. Waite, K.A.; De-La Mota-Peynado, A.; Vontz, G.; Roelofs, J. Starvation Induces Proteasome Autophagy with Different Pathways for Core and Regulatory Particles. *J. Biol. Chem.* **2016**, *291*, 3239–3253.
 45. Kageyama, S.; Sou, Y.; Uemura, T.; Kametaka, S.; Saito, T.; Ishimura, R.; Kouno, T.; Bedford, L.; Mayer, R.J.; Lee, M.-S.; et al. Proteasome Dysfunction Activates Autophagy and the Keap1-Nrf2 Pathway. *J. Biol. Chem.* **2014**, *289*, 24944–24955.
 46. Galluzzi, L.; Baehrecke, E.H.; Ballabio, A.; Boya, P.; Bravo-San Pedro, J.M.; Cecconi, F.; Choi, A.M.; Chu, C.T.; Codogno, P.; Colombo, M.I.; et al. Molecular definitions of autophagy and related processes. *EMBO J.* **2017**, *36*, 1811–1836.
 47. Demishtein, A.; Fraiberg, M.; Berko, D.; Tirosch, B.; Elazar, Z.; Navon, A. SQSTM1/p62-mediated autophagy compensates for loss of proteasome polyubiquitin recruiting capacity. *Autophagy* **2017**, *13*, 1697–1708.
 48. Dikic, I.; Wakatsuki, S.; Walters, K.J. Ubiquitin-binding domains — from structures to functions. *Nat. Rev. Mol. Cell Biol.* **2009**, *10*, 659–671.
 49. Yau, R.G.; Doerner, K.; Castellanos, E.R.; Haakonsen, D.L.; Werner, A.; Wang, N.; Yang, X.W.; Martinez-Martin, N.; Matsumoto, M.L.; Dixit, V.M.; et al. Assembly and Function of Heterotypic Ubiquitin Chains in Cell-Cycle and Protein Quality Control. *Cell* **2017**, *171*, 918–933.e20.
 50. Yau, R.; Rape, M. The increasing complexity of the ubiquitin code. *Nat. Cell Biol.* **2016**, *18*, 579–586.
 51. Kaiser, S.E.; Riley, B.E.; Shaler, T.A.; Trevino, R.S.; Becker, C.H.; Schulman, H.; Kopito, R.R. Protein standard absolute quantification (PSAQ) method for the measurement of cellular ubiquitin pools. *Nat. Methods* **2011**, *8*, 691–696.
 52. Zaffagnini, G.; Savova, A.; Danieli, A.; Romanov, J.; Tremel, S.; Ebner, M.; Peterbauer, T.; Sztacho, M.; Trapannone, R.; Tarafder, A.K.; et al. p62 filaments capture and present ubiquitinated cargos for autophagy. *EMBO J.* **2018**, *37*, 1–21.
 53. You, Z.; Jiang, W.-X.; Qin, L.-Y.; Gong, Z.; Wan, W.; Li, J.; Wang, Y.; Zhang, H.; Peng, C.; Zhou, T.; et al. Requirement for p62 acetylation in the aggregation of ubiquitylated proteins under nutrient stress. *Nat. Commun.* **2019**, *10*, 5792.
 54. Peng, L.; Ling, H.; Yuan, Z.; Fang, B.; Bloom, G.; Fukasawa, K.; Koomen, J.; Chen, J.; Lane, W.S.; Seto, E. SIRT1 Negatively Regulates the Activities, Functions, and Protein Levels of hMOF and TIP60. *Mol. Cell. Biol.* **2012**, *32*, 2823–2836.
 55. Yamagata, K.; Kitabayashi, I. Sirt1 physically interacts with Tip60 and negatively regulates Tip60-mediated acetylation of H2AX. *Biochem. Biophys. Res. Commun.* **2009**, *390*, 1355–1360.
 56. Romeo-Guitart, D.; Leiva-Rodriguez, T.; Forés, J.; Casas, C. Improved Motor Nerve Regeneration by SIRT1/Hif1a-Mediated Autophagy. *Cells* **2019**, *8*, 1354.
 57. Romeo-Guitart, D.; Casas, C. NeuroHeal Treatment Alleviates Neuropathic Pain and Enhances Sensory Axon Regeneration. *Cells* **2020**, *9*, 808.
 58. Romeo-Guitart, D.; Casas, C. Network-centric medicine for peripheral nerve injury: Treating the whole to boost endogenous mechanisms of neuroprotection and regeneration. *Neural Regen. Res.* **2019**, *14*, 1122.



Supplementary Materials

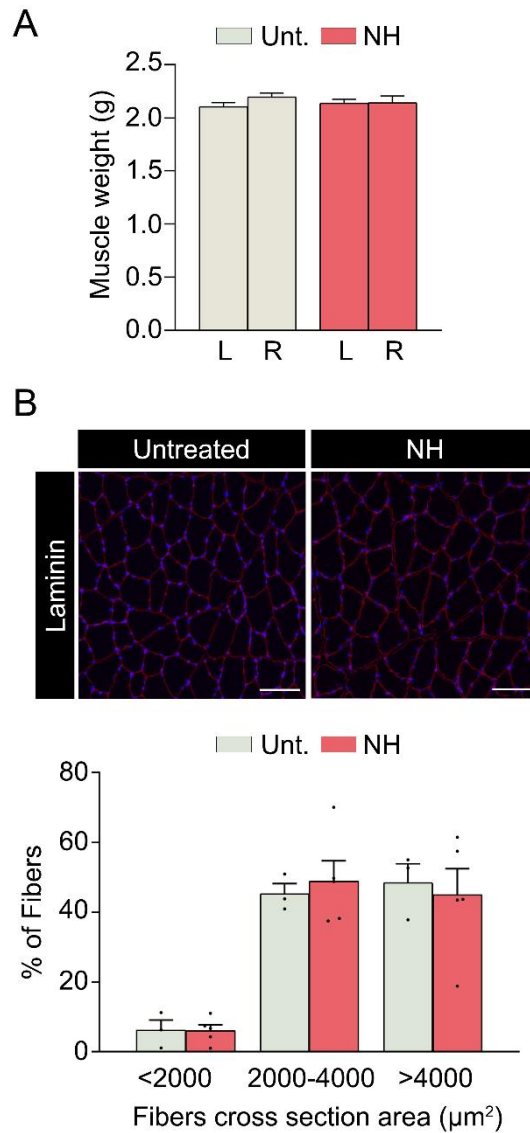


Figure S1. NeuroHeal does not affect the diameter of the uninjured myofibers. **(A)** Bar graph of the relative average weight of the ipsilateral and contralateral gastrocnemius (GA) muscle from the different experimental groups: uninjured animals treated for 14 days with vehicle (untreated) or NeuroHeal ($n = 4$; one-way ANOVA). **(B)** *Up*, representative microphotographs of GA muscle sections stained with laminin (red) and DAPI (blue) from different experimental groups. *Down*, histogram of the cross-sectional area (μm^2) distribution of fibers in GA muscle of different groups ($n = 4$; Kruskal–Wallis, Benjamin, Krieger, and Yekutieli post hoc).

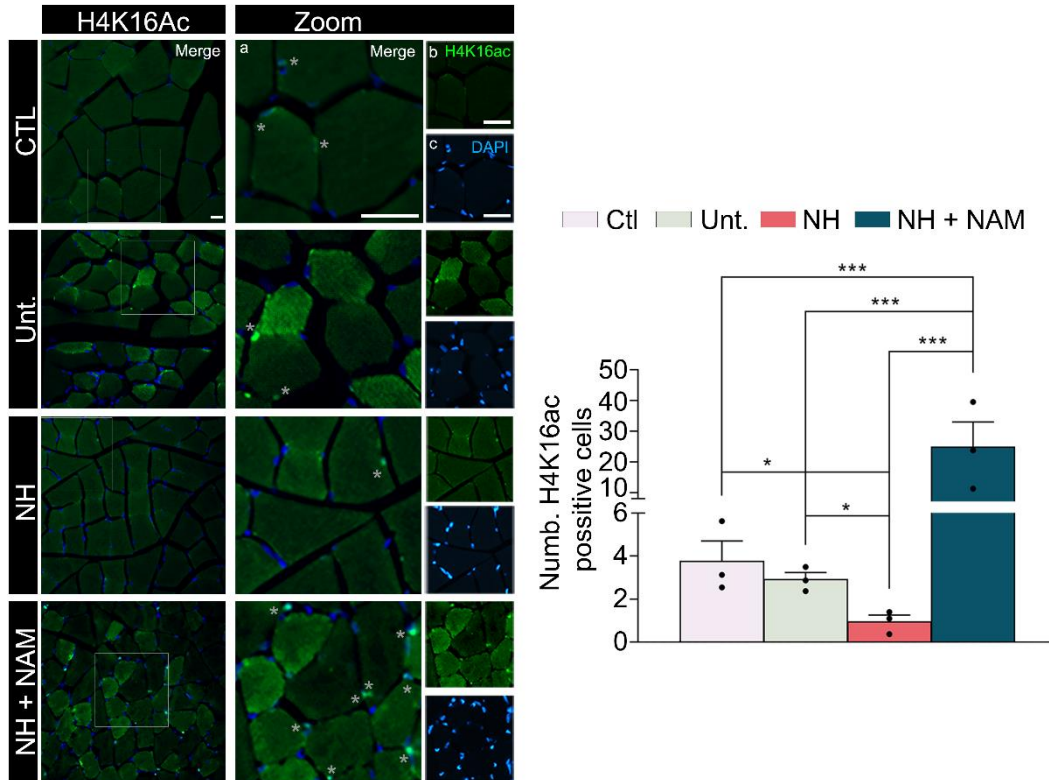


Figure S2. SIRT1 activity is modulated by NeuroHeal and nicotinamide. *Left*, representative microphotographs of the ipsilateral lesioned gastrocnemius muscle sections revealing the presence of acetylated histone 4 (H4K16Ac, green) and stained with DAPI (blue) from the different experimental groups at 28 dpi: control (CTL), injured untreated (Unt.), injured treated with NeuroHeal (NH), and injured treated with NH plus nicotinamide (NAM). At each condition, panels (a–c) are zoomed-in images from the squared region of the images of the left. The scale bar is 500 μ m and identical for all corresponding microphotographs as represented in the first image panel, the control condition. *Right*, bar graph of the average number of positive nuclei for H4K16Ac (n = 4 per group, two-way ANOVA, * p < 0.05).

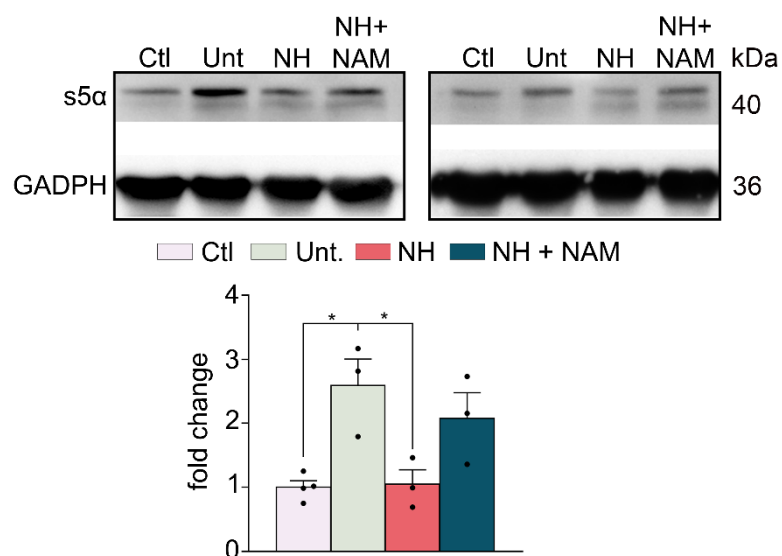


Figure S3. Proteasomal subunit 5 α is modulated by NeuroHeal in the denervated muscle. Western blots and the associated bar graphs showing the analyses of proteasome subunit 5 α (s5 α) protein levels in different experimental groups at 7 dpi (control (CTL), injured untreated (Unt), injured treated with NeuroHeal (NH), and injured treated with NH plus nicotinamide (NAM)) ($n = 3-4$; one-way ANOVA, $*p < 0.05$).

CHAPTER II

NeuroHeal improves Muscle Regeneration after Injury

NeuroHeal improves Muscle Regeneration after Injury

Sara Marmolejo-Martínez-Artesero ¹, David Romeo-Guitart ^{1,2,*}, Vanesa Venegas ^{3,4}, Mario Marotta ^{3,4}, Caty Casas ^{1,5}

¹ Institut de Neurociències (INc) and Department of Cell Biology, Physiology and Immunology, Universitat Autònoma de Barcelona (UAB), Bellaterra, Barcelona, Spain.

² Present address: Institut Necker Enfants-Malades (INEM), INSERM U1151, Laboratory "Hormonal regulation of brain development and functions"—Team 8, Université Paris Descartes, Sorbonne Paris Cité, 75015 Paris, France.

³ Leitat Technological Center, Carrer de la Innovació 2, Terrassa, Barcelona, Spain

⁴ Bioengineering, Cell therapy and Surgery in Congenital Malformations Laboratory. Vall d'Hebron Institut de Recerca (VHIR). Universitat Autònoma de Barcelona (UAB), Barcelona, Spain.

⁵ Died June 29, 2020.

ABSTRACT

Musculoskeletal injuries represent a challenging medical problem. Although the skeletal muscle is able to regenerate and recover after injury, the process engaged with conservative therapy can be inefficient, leading to a high re-injury rate. In addition, the formation of scar tissue implies an alteration of mechanical properties in muscle. There is still a need for new treatments of the injured muscle. NeuroHeal may be one option. Published studies demonstrated that it reduces muscle atrophy due to denervation and disuse. The main objective of the present work was to assess the potential of NeuroHeal to improve muscle regeneration after traumatic injury. Secondary objectives included characterizing the effect of NeuroHeal treatment on satellite cell biology. We used a rat model of sportive-like gastrocnemius injury and analyzed the effects of NeuroHeal on functional recovery by means of electrophysiology and tetanic force analysis. These studies were accompanied by immunohistochemistry of the injured muscle to analyze fibrosis, satellite cell state, and fiber type. In addition, we used an in vitro model to determine the effect of NeuroHeal on satellite cell biology and partially decipher its mechanism of action. The results showed that NeuroHeal treatment advanced muscle fiber recovery after injury in a preclinical model of muscle injury, and significantly reduced the formation of scar tissue. In vitro, we observed that NeuroHeal promoted the formation of myotubes. The results pave the way for novel therapeutic avenues for muscle/tendinous disorders.

INTRODUCTION

Musculoskeletal injuries represent a challenging problem, being the most common cause of severe long-term injuries, accounting for 10 to 55 % of all sports-related injuries (Chan et al., 2012). Muscle injuries are classified by cause of trauma and grade: an acute lesion caused by a direct trauma, as muscle lacerations, or an indirect trauma, such as strains, or by chronic disease or degenerative diseases, such as muscular dystrophies (Huard et al., 2002). Skeletal muscle has regenerative capabilities to self-repair after trauma or muscular dystrophies. This muscle reparative mechanism is divided into different phases: degeneration, inflammation, regeneration, remodeling, and innervation (Canata et al., 2017). The regenerative process is mainly mediated by a specific type of stem cell, the satellite cell (SC) (Starkey et al., 2011; Pallafacchina et al., 2013), which, after being activated, follows a process of differentiation giving a new recovered myofiber (Rocheteau et al., 2015). Recent reports have provided evidence that SCs are essential for the regenerative process, which is directly dependent on the microenvironmental niche (Lepper et al., 2011; Sambasivan et al., 2011).

Current therapies for most muscle injuries are mainly directed to decrease pain and inflammation by NSAIDs drugs, supplemented with immobilization and external physical stimulation. In severe cases, surgery is required to restore the anatomic continuity and function. In some cases, the endogenous process of muscle repair proves insufficient, leading to loss of contractile tissue, fatty degeneration, and fibrotic scar tissue, which can cause long-term deficits in muscle structure and strength. Although in those cases medical need is unsolved, some promising therapies are under study. The use of molecular therapies, such as growth factors or platelet-rich-plasma (PRP), which releases growth factors, structural proteins, and interleukins and chemokines, try to foster a beneficial microenvironment to boost regenerative biological processes (Canata et al., 2017). Although there is controversy regarding the clinical effects of PRP in humans (Grassi et al., 2018), it was shown to promote beneficial effects on muscle recovery in a rat injury model (Contreras-Muñoz et al., 2017a). Besides, cell therapy is a promising approach to treat skeletal muscle injuries in pre-clinical settings (Qazi et al., 2019), but not for all types of injuries. Therefore, all current available pharmacological and biological agents only relieve clinical symptoms and have limited or no effect on the progression of the underlining muscle disease.

In this study, we evaluated the therapeutic potential of NeuroHeal, a combination of two repurposed drugs (Acamprosate plus Ribavirin), previously designed using artificial intelligence (Romeo-Guitart et al., 2017; Romeo-Guitart and Casas, 2019), which facilitates its readiness for clinical use. We have previously reported its neuroprotective effects in different neurodegenerative models (Romeo-Guitart et al., 2017, 2019, 2020; Romeo-Guitart and Casas, 2020). In addition, we recently observed that NeuroHeal

protects the muscle by reducing atrophy induced by denervation or by immobilization (Marmolejo-Martínez-Artesero et al., 2020), suggesting it may have also protective effects in other types of myopathies. Herein, we aimed to elucidate whether NeuroHeal has an effect on muscle regeneration by using an in vivo model of surgically-induced lesion which mimics the most frequent skeletal muscle lesions observed in human sports clinics. We also provide insight into the possible mechanism involved in the pro-regenerative effect of NeuroHeal.

METHODS

Muscle injury model

All the experimental procedures were performed in accordance with Spanish (Real Decreto 53/2013) and European (2010/63/UE) legislation, approved. The funder played no role in the design, conduct, or reporting of this study by the Departament d'Agricultura, Ramaderia, Pesca, Alimentació i Medi Natural of the Catalan Government (Generalitat de Catalunya) and followed the ethical standards in sport and exercise science research (Harriss and Atkinson, 2013; Contreras-Muñoz et al., 2016, 2017a). Adult male Wistar rats of 8 weeks of age (Harlan Laboratories) were used for the in vivo studies. Rats were anesthetized by an intraperitoneal injection of a mixture of ketamine (90 mg/kg, Ketaset) and xylazine (10 mg/kg, Rompun). The surgical procedure was performed as previously described (Contreras-Muñoz et al., 2016, 2017b) inserting an 18 G biopsy needle in the right medial gastrocnemius (GA) muscle at 3 mm from the muscle-tendon junction. Post-surgical analgesia (0.01 mg/kg buprenorphine) was administered to all operated animals.

Drug treatment

NeuroHeal mixture is composed of Acamprosate and Ribavirin. For in vivo experiments, we grounded Acamprosate (Merck, Darmstadt, Germany) and Ribavirin (Normon, Madrid, Spain) pills into a fine powder and daily administered 40 mg/kg and 26 mg/kg respectively by gavage, dissolved in 1 mL of water at a concentration of 2.2 mM Acamprosate and 1 mM Ribavirin. To test whether NeuroHeal may accelerate muscle regeneration after damage, we used a model of injured GA muscle, comparing a group of rats treated with NeuroHeal (n = 5) and a group of rats receiving vehicle (n = 5).

Electrophysiology

Rats were anesthetized by intraperitoneal administration of ketamine and xylazine, and maintained warm by a thermostated blanket. The sciatic nerve was stimulated with

single pulses of increasing intensity by means of transcutaneous electrodes placed at the sciatic notch. The compound muscle action potential (CMAP) of the GA muscle was recorded to measure the maximum CMAP amplitude. The tests were performed using an electromyography (EMG) apparatus (Synergy Medelec, Viasys HealthCare). The CMAP amplitude from baseline to peak was used as a readout of the GA muscle integrity. The percentage of CMAP recovery was calculated as the ratio of injured / uninjured contralateral values. The nerve conduction test was performed before surgical injury and at 3, 7, and 14 days post-injury (dpi).

Measurement of muscle force

To measure contractile muscle force, rats were anesthetized by intraperitoneal injection of ketamine and xylazine. Animals were placed in a prone position and the limbs were immobilized. The Achilles tendon was separated from the calcaneus and attached to a force transducer (Wide Range Force Transducer, MLT 1030/D; ADInstruments) connected to a PowerLab/16SP data acquisition hardware (ADInstruments). The sciatic nerve was exposed by lateral incision and an electrode placed around the nerve and connected in turn to a stimulator (Stimulus Isolator, FE180; ADInstruments). The GA muscles were covered with mineral oil (Sigma-Aldrich) to prevent drying, and the room temperature was set at 25 °C. Muscle force was measured for right (injured) and left (control) GA muscles of each rat. Repeated isometric muscle twitches were induced at a frequency of 1 Hz (5 pulses) and a voltage of 5 V. The twitch response was analyzed by contraction time (CT) and half-relaxation time (HRT). Following twitch stimulation or peak force (PF), maximum tetanus force (TetF) was induced by a train of stimuli with a frequency of 100 Hz, a pulse width of 0.1 ms and a voltage of 5 V. Animals were euthanized by anesthetic overdose immediately after finishing muscle force measurements and muscle samples were excised and processed for further histological analysis.

Histology

For histology studies, animals were euthanized by intraperitoneal injection of an anesthetic overdose. The GA muscles were carefully excised, weighed, and immediately frozen in 2-methylbutane (Alfa Aesar), which was previously supercooled in liquid nitrogen, and were stored at -80 °C until further analysis.

To locate the area of injury, 10 µm serial cross sections were made from the myotendinous junction. Muscle samples were embedded in Tissue-tek, sectioned in a cryotome (Leica), and preserved at -20 °C until analysis. Hematoxylin and Eosin (H&E) staining was performed in each series, which were formed by 5 slices, having discarded

50 μm between them. The samples to be compared were processed together the same day within the same slide, and image analysis for all groups was also performed the same day using the same microscope setting.

For the H&E, nuclei were stained with Harris hematoxylin for 6 min followed by differentiation with an acid solution of 0.01 % HCl in ethanol. The cytoplasm was stained with eosin for 1 min. Sections were dehydrated by graded ethanol (50 %, 70 %, 96 % and 100 %, and xylene twice, 5 min in each solution) and mounted with DPX mounting solution.

For immunofluorescence labeling, the slices were pre-treated with frozen acetone, to fix the samples, and with 10 mg/ml NaBH_4 , to reduce autofluorescence for 80 min at 4 °C. After washing with standard Phosphate Buffered Saline (PBS), the tissue was incubated in blocking solution (0.3 % Triton-X-100 and 10 % fetal bovine serum in PBS) for 1 h at room temperature. Samples were then incubated at 4 °C with primary antibodies containing solution (PBS with 0.15 % triton X-100, 5 % FBS) overnight. The antibodies used were mouse anti-collagen type 1 (1:100, DBSH), mouse anti-developmental myosin heavy chain (dMyHC. 1:100, DSHB), mouse anti-fast myosin heavy chain (fMyHC. 1:100, DSHB), mouse anti-laminin (1:100, DSHB), mouse anti-MyoD (1:150; Santa Cruz), mouse anti-Myogenin (1:100; Abcam), rabbit anti-parvalbumin (1:100, Swant), mouse anti-Pax7 (1:100; DSHB) and mouse anti- $\alpha\beta$ slow myosin heavy chain (sMyHC. 1:100, DSHB). After several washes with 0.3% Triton-X-100 in PBS, we added Alexa Fluor 488 and 594 conjugated secondary antibodies against the primary antibody (1:100; Jackson Immunoresearch) and incubated for 1 h at room temperature. Counterstaining was performed with DAPI (Sigma) and mounted with Fluoromont (SouthernBiotech) mounting solution. Images from different groups were taken under the same exposure time, sensibility, resolution, and microscope for each analyzed marker. Images were taken using a Nikon Eclipse Ni-E microscope equipped with a digital camera (Nikon DS-RiE) and Nikon NIS-Element BR software (version 5.11.03). Co-labeled fibers were determined as positive using a pseudocolor display by Image J software (version 1.46; National Institutes of Health), using images at 4 \times (fiber type markers) and 10 \times (myogenesis markers). For signal intensity analysis, randomly selected images were selected at 10 \times (collagen I) and 20 \times (parvalbumin), which were transformed to grayscale and analyzed immunoreactivity by calculating the integrated density of a region of interest (ROI) after defining a threshold for background correction. For collagen I, the ROI was 1.49 mm^2 and the ROI of parvalbumin was myofiber area for a total of 20 myofibers.

Myoblast differentiation and analysis

C2C12 myoblast cell line was grown in a medium composed of modified Eagle's medium high-glucose (DMEM) supplemented with 10 % fetal bovine serum (Sigma-Aldrich), and 1% penicillin/streptomycin solution (Sigma-Aldrich). Cells were kept in a humidified incubator at 37 °C under 5 % CO₂. To initiate the experiments, cells were seeded at a density of 8.5×10³ cell/ml, and after 24 h of culture, the medium was changed to a differentiation medium (DMEM supplemented with 2 % horse serum (Sigma-Aldrich) with 1 % penicillin/streptomycin solution), which was changed every 2 days. Then, the differentiation medium was added with or without NeuroHeal (55 μM acamprosate and 1 μM ribavirin) and Ex-527 (Sigma-Aldrich) at 10 μM until the end of the experiment. At 0 (before changing to differentiation medium), 1, 3, and 5 div (days of in vitro) cells were fixed using 4 % formaldehyde for 30 min and then washed out with TBS. For immunofluorescence labeling, cells were incubated in a blocking solution (0.3 % Triton-X-100 and 10 % normal donkey serum in TBS) for 1 h at room temperature. Samples were then incubated for 4h at room temperature with primary antibodies containing solution (TBS with 0.3 % triton X-100, 5 % FBS). The antibodies used were rabbit anti-ki67 (1:100; Abcam), mouse anti-MyoD (1:150; Santa Cruz), and mouse anti-Myosin heavy chain (all fast isoforms) (MyHC, 1:20, DSHB), rabbit anti-parvalbumin (1:100, Swant), and mouse anti-Pax7 (1:100; DSHB). After several washes in TBS-0.1 % tween-20, we added Cy2 and Cy3 (1:200; Jackson Immunoresearch) during 50 min at room temperature. Counter-staining was performed with DAPI (Sigma) and mounting with Mowiol mounting medium (Southern Biotech). Images of C2C12 cells from different groups were taken at 20× under the same exposure time, sensibility, and resolution for each marker analyzed with the same microscope system as above. Co-labeled fibers were determined as positive using a pseudocolor display by Image J software. For the fusion coefficient, a mature myotube was considered having 3 or more MyHC positive nuclei. For signal intensity analysis, images were transformed to grayscale and analyzed immunoreactivity by calculating the integrated density of a ROI, after defining a threshold for background correction. For MyoD, the ROI used was DAPI to analyze nuclei area and for parvalbumin, the ROI used was 5615.103 μm² for 15-20 myotubes for each condition.

Statistical analysis

We performed an unpaired Student's t-test to compare two groups, an one-way analysis of variance (ANOVA) to compare three or more groups, and two-way analysis of variance (ANOVA) to compare grouped data followed by Tuckeys' multiple comparison test, as appropriate. Data are presented as means ± standard error of the mean (SEM)

and differences were assumed to be significant for $p \leq 0.05$. Statistical analyses were conducted using GraphPad Prism 8 software.

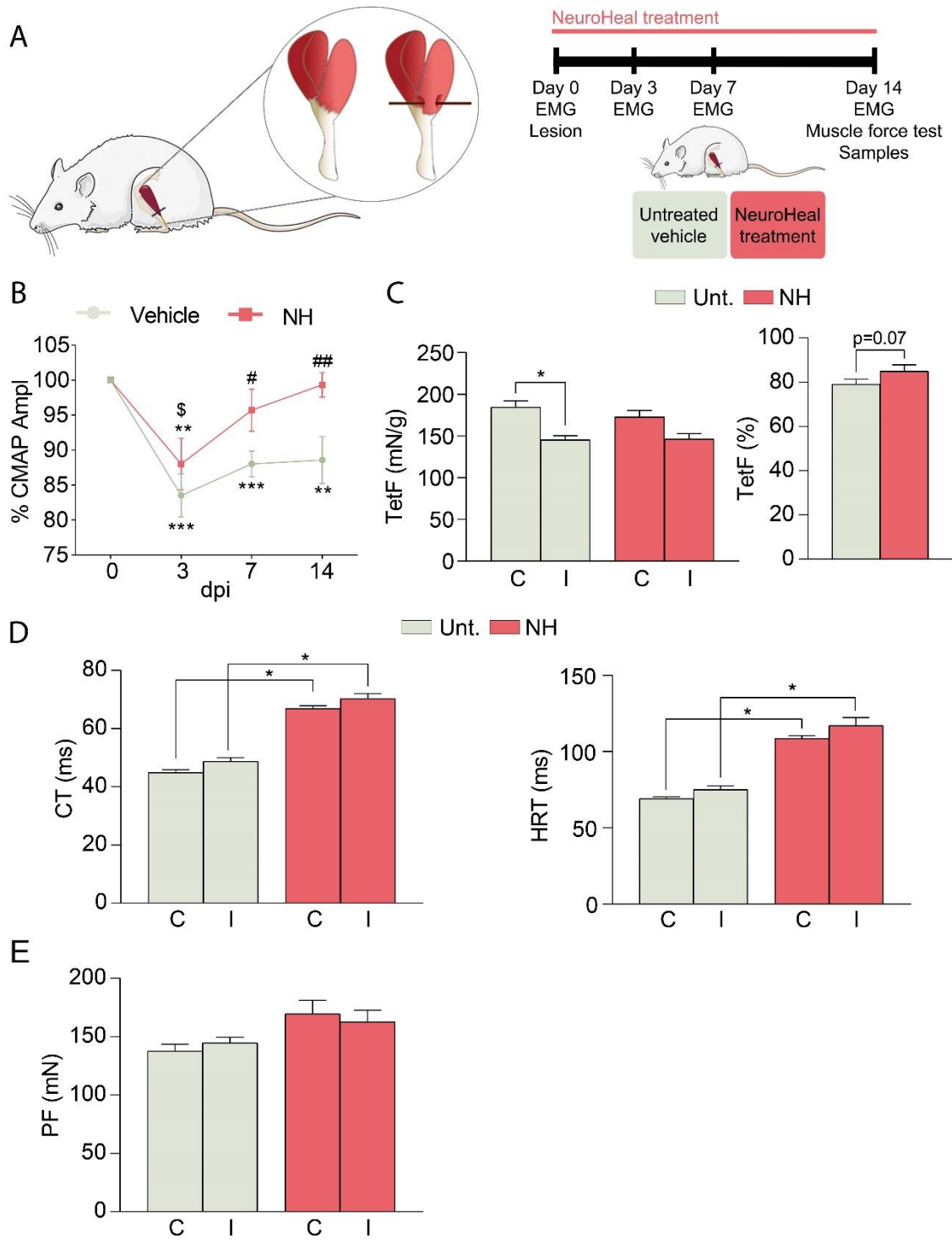
RESULTS

NeuroHeal accelerates muscle fiber function recovery

The lesion caused a reduction of the CMAP amplitude in the GA muscle ($83.5 \% \pm 3.1 \%$) compared to the contralateral non-injured muscle at 3 dpi (**Fig. 1B**). Weekly follow-up of the injured animals showed a progressive recovery of the CMAP amplitude until normal values by 14 dpi in the NeuroHeal group. These results evidenced that the treatment with NeuroHeal significantly improved muscle fiber recovery.

No significant differences were detected in GA muscle weight between the two groups and between ipsi- and contralateral GA muscle for each group at the end of follow-up (**Fig. S1**). Regarding muscle force recovery, untreated animals showed an approximate 20 % decrease in TetF of the injured versus contralateral leg ($79.1 \% \pm 2.3 \%$), whereas the animals treated with NeuroHeal exhibited higher values of TetF ($84.9 \% \pm 2.9 \%$) (**Fig. 1C**). Besides, the untreated group showed a shorter CT and HRT in comparison to the NeuroHeal treated group (**Fig. 1D**), coinciding with a PF non-significant increase on this group (**Fig. 1E**). All these data suggested that NeuroHeal may be altering the muscle contractile properties regardless of injury.

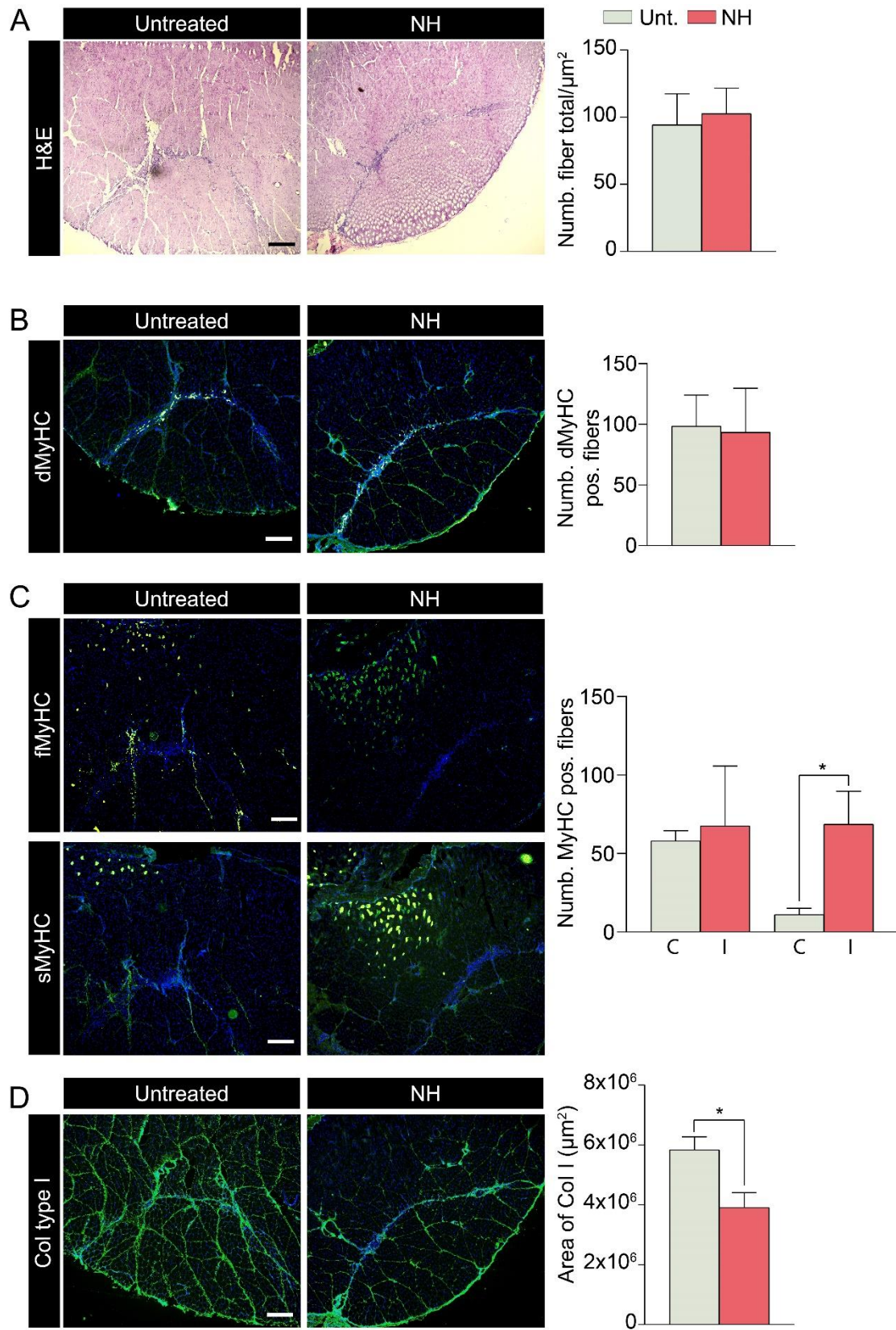
Figure 1. NeuroHeal-treated animals show a better functional recovery after muscle injury. (A) Schematic workflow and experimental groups. (B) Percentage of the compound muscle action potential (CMAP) amplitude of the ipsilateral gastrocnemius (GA) muscle with respect to the contralateral one from injured untreated (Unt., $n = 13$) and injured treated with NeuroHeal (NH, $n = 11$) groups (two-way ANOVA, $*p < 0.05$ vs. 0 dpi for each respective group; $\#p < 0.05$ vs. Unt. for each dpi; $\$p < 0.05$ vs. 3 dpi in NH group). (C) *Left*, bar graph of the average of the maximum tetanus force (TetF) from ipsi- and contralateral GA muscle from Unt. and NH at 14 dpi ($n=5$; one-way ANOVA, $*p < 0.01$). *Right*, bar graph of the percentage of TetF of the ipsilateral GA muscle respect to the contralateral one from Unt. and NH at 14 dpi ($n = 5$; t-test, $*p = 0.07$). (D) *Left*, bar graph of the average of the contraction time (CT) from ipsi- and contralateral GA muscle from GA from Unt. and NH at 14 dpi ($n = 5$; one-way ANOVA, $*p < 0.0001$). *Right*, bar graph of the average of the half-relaxion time (HRT) from ipsi- and contralateral GA muscle from Unt. and NH at 14 dpi ($n = 5$; one-way ANOVA, $*p < 0.0001$). (E) Bar graph of the average of the peak force (PF) from ipsi- and contralateral GA muscle from GA from Unt. and NH at 14 dpi ($n = 5$; one-way ANOVA).



NeuroHeal modulates fiber regeneration and reduces collagen deposition

To determine the effect of NeuroHeal of muscle repair, we analyzed the lesion area, previously identified by H&E staining, with immunohistochemical labeling of markers of regenerating myofibers and of collagen deposition at 14 dpi. The number of total muscle fibers was not modified by the treatment (**Fig. 2A**). Then, we evaluated the regeneration state of the injured fibers. After the fusion of the myoblast coordinated by MyoG protein, the regenerating muscle fibers initially express developmental MyHC form and later on adult fast and slow MyHC forms (Sartore et al., 1982; Whalen et al., 1990; Esser et al., 1993). We observed that NeuroHeal did not promote a change in the number of developmental MyHC (**Fig. 2B**). In addition, we observed that NeuroHeal induced a non-significant increase in the number of fast MyHC fibers, and an increase of slow MyHC fibers (**Fig. 2C**) in the injured GA muscle. On the other side, NeuroHeal treatment did not modify the distribution of fast and slow MyHC in the contralateral GA muscle (**Fig. S2**). Finally, the NeuroHeal-treated group showed less collagen I levels in comparison to the untreated group (**Fig. 2D**).

Figure 2. NeuroHeal reduces collagen deposition and promotes slow-twitch fiber typing after muscle injury. Representative microphotographs of lesioned gastrocnemius (GA) muscle sections from the injured untreated (Unt.) and injured treated with NeuroHeal (NH) groups at 14 dpi. Scale bar 500 μm , for all corresponding microphotographs as represented in the first image panel, the untreated condition. **(A) Left**, representative microphotographs of GA muscle sections stained with H&E. **Right**, Bar graph of the average number of muscle fibers ($n = 4$; t-test). **(B) Left**, representative microphotographs of GA muscle sections immunostained for developmental MyHC. **Right**, bar graph of the average number of positive fibers for dMyHC ($n = 4$; t-test). **(C) Left**, representative microphotographs of GA muscle sections immunostained for fast and slow MyHC. **Right**, bar graph of the average number of positive fibers for fMyHC and sMyHC ($n = 3$; t-test, $*p < 0.01$). **(D) Left**, representative microphotographs of GA muscle sections immunostained for Collagen type I (Col I). **Right**, bar graph of the average of the area immunolabeled for Col I ($n = 4$; t-test, $*p < 0.05$).



NeuroHeal influences muscle satellite cells

We further investigated if NeuroHeal might influence the response of SC, which are the natural/endogenous way of muscle to recover after injury by regeneration, as they are able to differentiate into myofibers (Gayraud-Morel et al., 2009). At 14 dpi, the number of Pax7-positive cells (a classical marker of activated SCs) was similar in the untreated injured animals compared to uninjured controls, while NeuroHeal treatment significantly reduced the quantity (**Fig. 3**). In contrast, there was a significant increase in the number of MyoD- (myoblast marker) and MyoG-positive cells (Myogenin, myocyte marker) in injured animals regardless of the treatment, as expected, which suggests commitment of SCs in the myogenic process (**Fig. 3**).

We additionally analyzed the differentiation process of myoblasts in vitro to verify the implication of NeuroHeal in this process. The differentiation process of the myoblast cell line C2C12 occurs during 3-5 days of low-serum culture medium (Dugdale et al., 2018). The non-activated and non-quiescent SCs are positive for Ki-67 and negative for Pax7. The following day after the initiation of the differentiation process, the number of Ki-67 positive cells was similar to the non-differentiated cells, but it drastically dropped after 3 div culture (**Fig. S3B**). The use of Ex-527, a selective inhibitor of SIRT1, increased the number of Ki-67 positive and Pax7 positive cells, while the total number of cells was similar to the control (**Fig. S3C**), suggesting the arresting of the differentiation process at this stage in a proportion of cells (**Fig. 4A**). The relative intensity of MyoD within the cells treated with Ex-527 was similar to the control in agreement with normal low activity of SIRT1 at this stage. Treatment with NeuroHeal did not affect the number of Ki-67 positive cells but significantly diminished the number of Pax7 positive cells with respect to the control, suggesting that more cells entered into later stages of differentiation (**Fig. 4A**). Curiously, the number of MyoD positive cells was not affected by NeuroHeal treatment despite the lower intensity of its expression compared to the control (**Fig. 4A**). This observation is consistent with the fact that SIRT1 activation reduces the expression of MyoD (Amat et al., 2009). However, the coefficient of fusion of the formed mature myotubes was increased with NeuroHeal compared to the untreated condition, suggesting an acceleration of this differentiation process (**Fig. 4B**). All these effects produced by NeuroHeal were not observed if Ex-527 was concomitantly added to the wells, suggesting that the activation of SIRT1 might be involved, although other factors may play a role and compensating some effects. Finally, we analyzed parvalbumin levels in vivo and in vitro to verify the interaction between SIRT1 and parvalbumin in the differentiation process (Ducreux et al., 2012). NeuroHeal treatment showed a reduction in the relative intensity of parvalbumin on myotubes of C2C12 cells (**Fig. S4A**) and also in the in vivo analysis in the intact contralateral GA muscle (**Fig. S4B**). This reduction was reverted by the addition of Ex-527 (**Fig. S4A**). Altogether, these results suggest that NeuroHeal modulates the differentiation process of the myoblast C2C12 cell line in

in vitro increasing the fusion of the new formed matured myotubes, and that SIRT1 activation is involved on it.

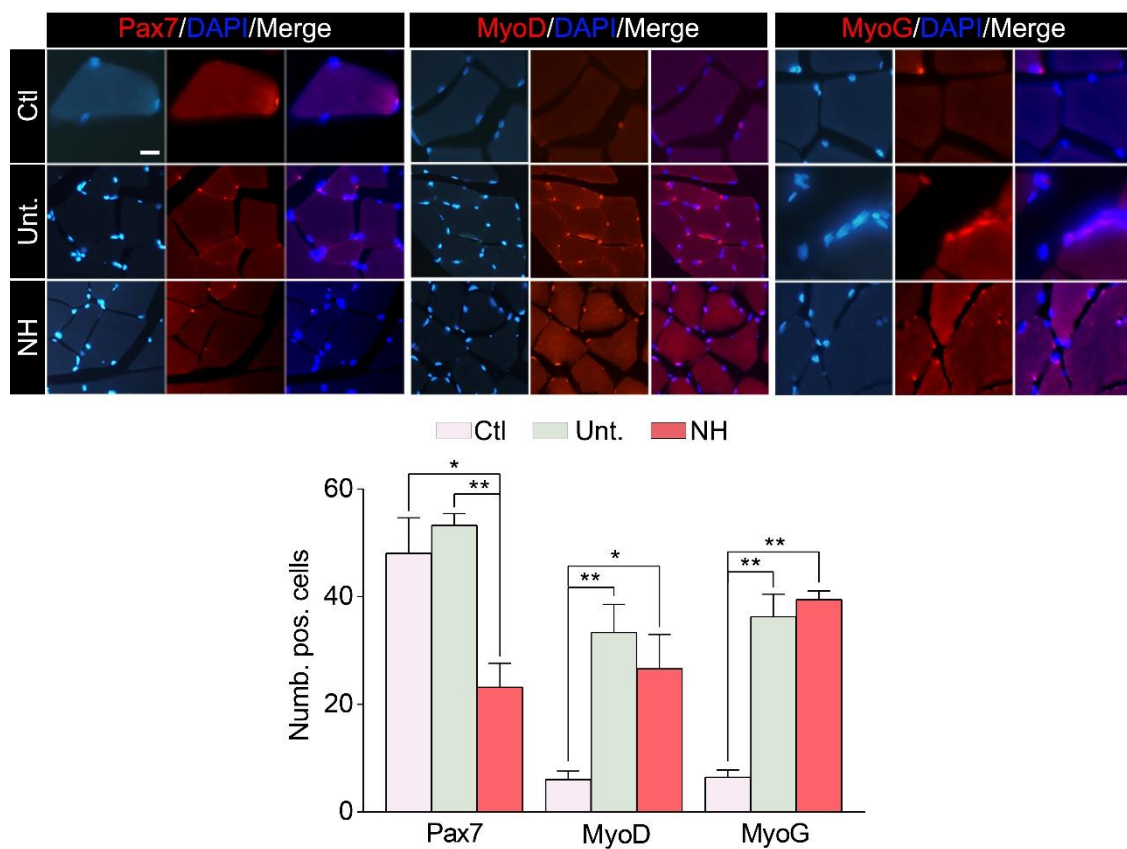


Figure 3. NeuroHeal accelerates satellite cell activation and differentiation after muscle injury. Up, representative microphotographs of the ipsi- and contralateral lesioned gastrocnemius muscle sections revealing the presence of Pax 7, MyoD, MyoG and stained with DAPI (blue) from the different experimental groups: control (CTL), injured untreated (Unt.), injured treated with NeuroHeal (NH) at 14 dpi. Scale bar 200 μ m and identical for all corresponding microphotographs as represented in the first image panel, the control condition. Down, bar graphs of the average number of positive satellite nuclei for Pax7, MyoD or Myogenin (n = 3; one-way ANOVA, *p < 0.05).

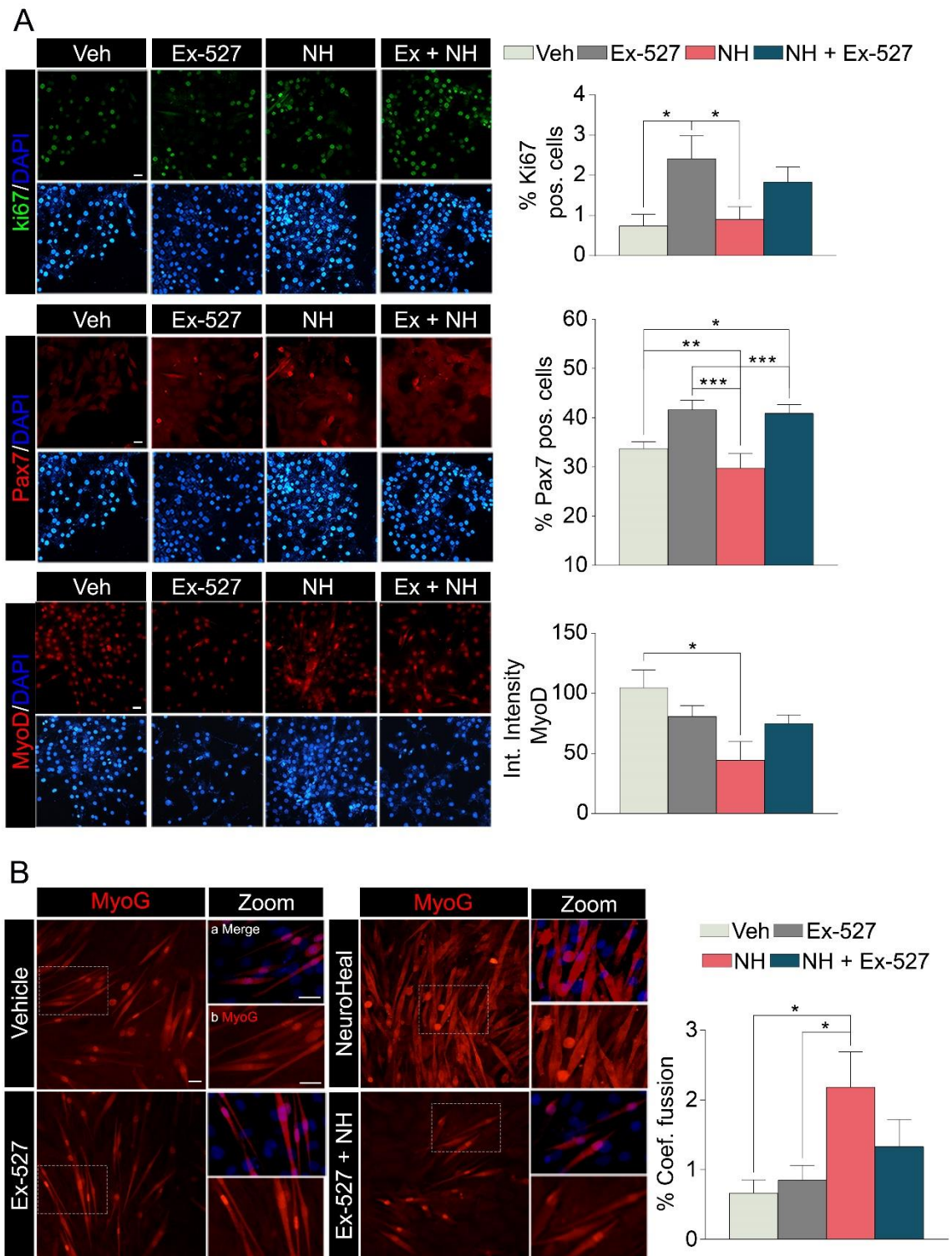


Figure 4. NeuroHeal modulates differentiation process and increases myoblast fusion *in vitro*. (A) Left, representative microphotographs of differentiated C2C12 myoblast cell line immunostained for Ki67, Pax7, MyoD and stained with DAPI from the different experimental groups at 3 days of differentiation: atrophy-induced treated with vehicle (Veh), atrophy-induced treated with Ex-527 (Ex-527), atrophy-induced treated with NeuroHeal (NH) and atrophy-induced treated with NH plus Ex-527. Scale bar 25 μ m and identical for all corresponding microphotographs as represented in the first image panel, the vehicle condition. Right, bar graph of the average number of positive nuclei for Ki67 and Pax7, and the relative intensity per

cell of MyoD ($n = 3$; one-way ANOVA, $*p < 0.05$). **(B) Up**, representative immunofluorescence microphotographs of differentiated C2C12 myoblast cell line immunostained for MyHC and stained with DAPI (blue) from the different experimental groups at 5 days of differentiation. At each condition, panels a-b are zoom images from the squared region of the images of the left. Scale bar 200 μm and identical for all corresponding microphotographs as represented in the first image panel, the vehicle condition, and zoomed images. **Down**, bar graph of the percentage of the number of positive myotubes with three or more nuclei ($n = 3$, one-way ANOVA, $*p < 0.05$).

DISCUSSION

The results of this work indicate that NeuroHeal affects muscle cell biology, improving muscle regeneration and accelerating myogenesis after injury. These beneficial effects are accompanied by reduced collagen deposition and an increased number of mature muscle fibers, preferentially of the slow-twitch type. Overall, NeuroHeal may be a promising treatment to improve skeletal muscle regeneration after damage and for some muscle-related diseases.

Although NeuroHeal was discovered to act on the nervous system, in previous studies we observed that it also reduces muscle atrophy caused by denervation (Romeo-Guitart et al., 2017) and by hindlimb immobilization (Marmolejo-Martínez-Artesero et al., 2020). For that reason we pursued to decipher whether it may act on muscle cell biology as well by using a rat model of sports-type muscle injury (Contreras-Muñoz et al., 2016). Surprisingly, we observed that the treatment with NeuroHeal advanced the recovery of the electrophysiological response, and promoted a tendency to increase the TetF of the damaged muscle. This was accompanied by observations in the histological analysis; less collagen deposition which contributes to form scar tissue, and an increasing number of mature muscle fibers, in particular slow-twitch fibers. These observations are in agreement with the known mechanism of action of NeuroHeal as a SIRT1 activator (Romeo-Guitart et al., 2018b, 2018a). Several studies have shown that activation of SIRT1 in muscle disease models promotes shifting from fast to slow-twitch fibers (Lagouge et al., 2006; Ljubicic et al., 2014; Zhang et al., 2015). However, we did not observe such an increase in this type of fibers in the uninjured muscles in our model, suggesting that more time of treatment is necessary under normal conditions or that this only occurs when the muscle is affected/lesioned. In any case, it would be worth exploring these possibilities.

In the muscular force analysis, there was an unexpected increase in the contraction and relaxation time produced by NeuroHeal treatment, due to a PF light increase. This may be attributed to an increase in the pulse of free Ca^{+2} in the cytoplasm. Two possible mechanisms may contribute to this action. First, it is reported that one action of NeuroHeal's compound ACA is the activation of VGCC channel (Feng et al., 2013),

which provides Ca^{+2} entry activating the RyR. This prolongation of the RyR activation could explain the increase in the CT parameter. A second reason may be related to the reduction of parvalbumin produced by NeuroHeal, which acts as a Ca^{+2} binding protein, extending the concentration of free Ca^{+2} . This would impede the muscle to relax, leading to a HRT increase. In addition, these low levels are in agreement with findings reported by Ducreux and collaborators (Ducreux et al., 2012). They reported that parvalbumin expression and mitochondrial volume in muscle cells are inversely regulated via a SIRT1/PGC-1 α signaling axis. We did not explore the action of NeuroHeal on mitochondria biogenesis, but considering the importance of parvalbumin in buffering Ca^{+2} during the relaxation/contraction process, this may explain why the times for contraction and relaxation were higher in the animals treated with NeuroHeal compared to controls in both contralateral and ipsilateral muscles.

Finally, we explored the effects of NeuroHeal on SCs, which normally remain in a quiescent state until they receive activating signals to begin proliferation (Brack and Rando, 2012; Yin et al., 2013). SC activation is metabolically highly demanding, and it is associated with a large increase in cellular ATP. Indeed, it was found that SIRT1, a key nutrient sensor, modulates autophagic flux during SC activation (Ng and Tang, 2013). The activation of the autophagic machinery by SIRT1 is necessary in order to generate nutrients, which are essential for the generation of ATP, to support the considerable increase in anabolic activity associated with the activation process. Inhibition of SIRT1 or autophagy causes a delay in SC activation (Tang and Rando, 2014). We have previously found that NeuroHeal activates SIRT1 and favors the autophagy flux (Romeo-Guitart et al., 2020), so these may be causing either the effect of a quick activation of myoblast observed in vitro or the diminished number of Pax7 positive SC in vivo compared to the untreated animals. Upon SC activation, the metabolic switch from fatty acid oxidation to glycolysis produces a drop in free NAD^{+} , and SIRT1 loses its catalytic activity which allows the expression of muscle-specific genes like MyoD (Ryall et al., 2016). We observed that NeuroHeal treatment did not prevent the ability of cells to finish myogenesis and even reduced MyoD expression, which is in agreement with what is reported on SIRT1 action (Ryall et al., 2016). Furthermore, we observed an increase in the fusion coefficient to form myotubes with NeuroHeal treatment which, again, could be related to the activation of SIRT1 and its favorable action in the respiration of mitochondria (Wu et al., 1999).

Overall, we conclude that NeuroHeal could be used clinically to accelerate muscle regeneration, and probably also as a treatment in various muscle diseases due to its ability to activate SIRT1 (Tonkin et al., 2012).

REFERENCES

- Amat R, Planavila A, Chen SL, Iglesias R, Giralt M, Villarroya F (2009) SIRT1 Controls the Transcription of the Peroxisome Proliferator-activated Receptor- γ Co-activator-1 α (PGC-1 α) Gene in Skeletal Muscle through the PGC-1 α Autoregulatory Loop and Interaction with MyoD. *J Biol Chem* 284:21872–21880.
- Brack AS, Rando TA (2012) Tissue-Specific Stem Cells: Lessons from the Skeletal Muscle Satellite Cell. *Cell Stem Cell* 10:504–514.
- Canata GL, D’Hooghe P, Hunt KJ (2017) Muscle and Tendon Injuries (Canata GL, D’Hooghe P, Hunt KJ, eds). Berlin, Heidelberg, Heidelberg: Springer Berlin Heidelberg.
- Chan O, Del Buono A, Best TM, Maffulli N (2012) Acute muscle strain injuries: a proposed new classification system. *Knee Surgery, Sport Traumatol Arthrosc* 20:2356–2362.
- Contreras-Muñoz P, Fernández-Martín A, Torrella R, Serres X, De La Varga M, Viscor G, Järvinen TAH, Martínez-Ibáñez V, Peiró JL, Rodas G, Marotta M (2016) A New Surgical Model of Skeletal Muscle Injuries in Rats Reproduces Human Sports Lesions. *Int J Sports Med* 37:183–190.
- Contreras-Muñoz P, Torrella JR, Serres X, Rizo-Roca D, De la Varga M, Viscor G, Martínez-Ibáñez V, Peiró JL, Järvinen TAH, Rodas G, Marotta M (2017a) Postinjury Exercise and Platelet-Rich Plasma Therapies Improve Skeletal Muscle Healing in Rats But Are Not Synergistic When Combined. *Am J Sports Med* 45:2131–2141.
- Contreras-Muñoz P, Torrella JR, Serres X, Rizo-Roca D, De La Varga M, Viscor G, Martínez-Ibáñez V, Peiró JL, Järvinen TAH, Rodas G, Marotta M (2017b) Postinjury Exercise and Platelet-Rich Plasma Therapies Improve Skeletal Muscle Healing in Rats but Are Not Synergistic When Combined. *Am J Sports Med* 45:2131–2141.
- Ducreux S, Gregory P, Schwaller B (2012) Inverse Regulation of the Cytosolic Ca²⁺ Buffer Parvalbumin and Mitochondrial Volume in Muscle Cells via SIRT1/PGC-1 α Axis Koch K-W, ed. *PLoS One* 7:e44837.
- Dugdale HF, Hughes DC, Allan R, Deane CS, Coxon CR, Morton JP, Stewart CE, Sharples AP (2018) The role of resveratrol on skeletal muscle cell differentiation and myotube hypertrophy during glucose restriction. *Mol Cell Biochem* 444:109–123.
- Esser K, Gunning P, Hardeman E (1993) Nerve-Dependent and -Independent Patterns of mRNA Expression in Regenerating Skeletal Muscle. *Dev Biol* 159:173–183.
- Feng Y, Wang B, Du F, Li H, Wang S, Hu C, Zhu C, Yu X (2013) The Involvement of PI3K-Mediated and L-VGCC-Gated Transient Ca²⁺ Influx in 17 β -Estradiol-Mediated Protection of Retinal Cells from H₂O₂-Induced Apoptosis with Ca²⁺ Overload Zhivotovsky B, ed. *PLoS One* 8:e77218.
- Gayraud-Morel B, Chrétien F, Tajbakhsh S (2009) Skeletal muscle as a paradigm for regenerative biology and medicine. *Regen Med* 4:293–319.
- Grassi A, Napoli F, Romandini I, Samuelsson K, Zaffagnini S, Candrian C, Filardo G (2018) Is Platelet-Rich Plasma (PRP) Effective in the Treatment of Acute Muscle Injuries? A Systematic Review and Meta-Analysis. *Sport Med* 48:971–989.

- Harriss D, Atkinson G (2013) Ethical Standards in Sport and Exercise Science Research: 2014 Update. *Int J Sports Med* 34:1025–1028.
- Huard J, Li Y, Fu FH (2002) Muscle injuries and repair: current trends in research. *J Bone Jt Surgery-American Vol* 84:822–832.
- Lagouge M, Argmann C, Gerhart-Hines Z, Meziane H, Lerin C, Daussin F, Messadeq N, Milne J, Lambert P, Elliott P, Geny B, Laakso M, Puigserver P, Auwerx J (2006) Resveratrol Improves Mitochondrial Function and Protects against Metabolic Disease by Activating SIRT1 and PGC-1 α . *Cell* 127:1109–1122.
- Lepper C, Partridge TA, Fan C-M (2011) An absolute requirement for Pax7-positive satellite cells in acute injury-induced skeletal muscle regeneration. *Development* 138:3639–3646.
- Ljubicic V, Burt M, Lunde JA, Jasmin BJ (2014) Resveratrol induces expression of the slow, oxidative phenotype in mdx mouse muscle together with enhanced activity of the SIRT1-PGC-1 α axis. *Am J Physiol Physiol* 307:C66–C82.
- Marmolejo-Martínez-Artesero S, Romeo-Guitart D, Mañas-García L, Barreiro E, Casas C (2020) NeuroHeal Reduces Muscle Atrophy and Modulates Associated Autophagy. *Cells* 9:1575.
- Ng F, Tang BL (2013) Sirtuins' modulation of autophagy. *J Cell Physiol* 228:2262–2270.
- Pallafacchina G, Blaauw B, Schiaffino S (2013) Role of satellite cells in muscle growth and maintenance of muscle mass. *Nutr Metab Cardiovasc Dis* 23:S12–S18.
- Qazi TH, Duda GN, Ort MJ, Perka C, Geissler S, Winkler T (2019) Cell therapy to improve regeneration of skeletal muscle injuries. *J Cachexia Sarcopenia Muscle* 10:501–516.
- Rocheteau P, Vinet M, Chretien F (2015) Dormancy and Quiescence of Skeletal Muscle Stem Cells. In: *Results and Problems in Cell Differentiation*, pp 215–235. Springer Verlag.
- Romeo-Guitart D, Casas C (2019) Network-centric medicine for peripheral nerve injury: Treating the whole to boost endogenous mechanisms of neuroprotection and regeneration. *Neural Regen Res* 14:1122.
- Romeo-Guitart D, Casas C (2020) NeuroHeal Treatment Alleviates Neuropathic Pain and Enhances Sensory Axon Regeneration. *Cells* 9:808.
- Romeo-Guitart D, Forés J, Herrando-Grabulosa M, Valls R, Leiva-Rodríguez T, Galea E, González-Pérez F, Navarro X, Petegnief V, Bosch A, Coma M, Mas JM, Casas C (2018a) Neuroprotective Drug for Nerve Trauma Revealed Using Artificial Intelligence. *Sci Rep* 8:1–15.
- Romeo-Guitart D, Forés J, Navarro X, Casas C (2017) Boosted Regeneration and Reduced Denervated Muscle Atrophy by NeuroHeal in a Pre-clinical Model of Lumbar Root Avulsion with Delayed Reimplantation. *Sci Rep* 7:1–12.
- Romeo-Guitart D, Leiva-Rodríguez T, Espinosa-Alcantud M, Sima N, Vaquero A, Domínguez-Martín H, Ruano D, Casas C, Domínguez-Martín H, Ruano D, Casas C (2018b) SIRT1 activation with neuroheal is neuroprotective but SIRT2 inhibition with AK7 is detrimental for disconnected motoneurons. *Cell Death Dis* 9:531.
- Romeo-Guitart D, Leiva-Rodríguez T, Forés J, Casas C (2019) Improved Motor Nerve

Regeneration by SIRT1/Hif1a-Mediated Autophagy. *Cells* 8:1354.

Romeo-Guitart D, Marcos-DeJuana C, Marmolejo-Martínez-Artesero S, Navarro X, Casas C (2020) Novel neuroprotective therapy with NeuroHeal by autophagy induction for damaged neonatal motoneurons. *Theranostics* 10:5154–5168.

Ryall JG, Orso SD, Derfoul A, Juan A, Zare H, Feng X, Clermont D, Koulis M, Gutierrez-cruz G, Sartorelli V (2016) The NAD⁺-Dependent SIRT1 Deacetylase Translates a Metabolic Switch into Regulatory Epigenetics in Skeletal Muscle Stem Cells. *16*:171–183.

Sambasivan R, Yao R, Kissenpfennig A, Van Wittenberghe L, Paldi A, Gayraud-Morel B, Guenou H, Malissen B, Tajbakhsh S, Galy A (2011) Pax7-expressing satellite cells are indispensable for adult skeletal muscle regeneration. *Development* 138:4333–4333.

Sartore S, Gorza L, Schiaffino S (1982) Fetal myosin heavy chains in regenerating muscle. *Nature* 298:294–296.

Starkey JD, Yamamoto M, Yamamoto S, Goldhamer DJ (2011) Skeletal Muscle Satellite Cells Are Committed to Myogenesis and Do Not Spontaneously Adopt Nonmyogenic Fates. *J Histochem Cytochem* 59:33–46.

Tang AH, Rando TA (2014) Induction of autophagy supports the bioenergetic demands of quiescent muscle stem cell activation. *EMBO J* 33:2782–2797.

Tonkin J, Villarroya F, Puri PL, Vinciguerra M (2012) SIRT1 signaling as potential modulator of skeletal muscle diseases. *Curr Opin Pharmacol* 12:372–376.

Whalen RG, Harris JB, Butler-Browne GS, Sesodia S (1990) Expression of myosin isoforms during notexin-induced regeneration of rat soleus muscles. *Dev Biol* 141:24–40.

Wu Z, Puigserver P, Andersson U, Zhang C, Adelmant G, Mootha V, Troy A, Cinti S, Lowell B, Scarpulla RC, Spiegelman BM (1999) Mechanisms Controlling Mitochondrial Biogenesis and Respiration through the Thermogenic Coactivator PGC-1. *Cell* 98:115–124.

Yin H, Price F, Rudnicki MA (2013) Satellite cells and the muscle stem cell niche. *Physiol Rev* 93:23–67.

Zhang C, Luo J, Yu B, Zheng P, Huang Z, Mao X, He J, Yu J, Chen J, Chen D (2015) Dietary resveratrol supplementation improves meat quality of finishing pigs through changing muscle fiber characteristics and antioxidative status. *Meat Sci* 102:15–21.

SUPPLEMENTARY FIGURES

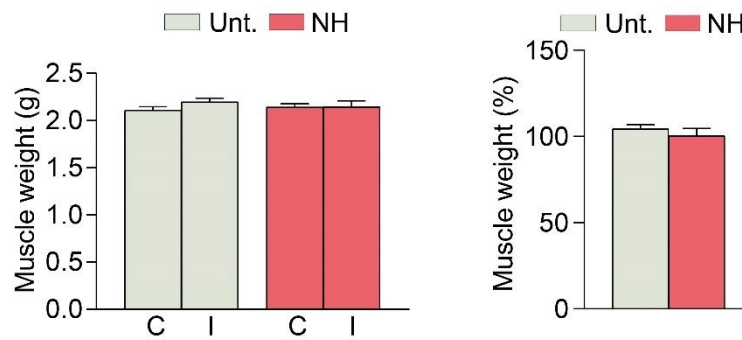


Figure S1. Muscle injury does not modify muscle weight. Left, bar graph of the average of the muscle weight from ipsi- and contralateral gastrocnemius (GA) muscle from the different experimental groups injured untreated (Unt.) and injured treated with NeuroHeal (NH) at 14 dpi (n = 5; t-test). Right, bar graph of the relative mean of muscle weight of the ipsilateral GA muscle respect to the contralateral one from Unt. and NH at 14 dpi (n = 5; t-test).

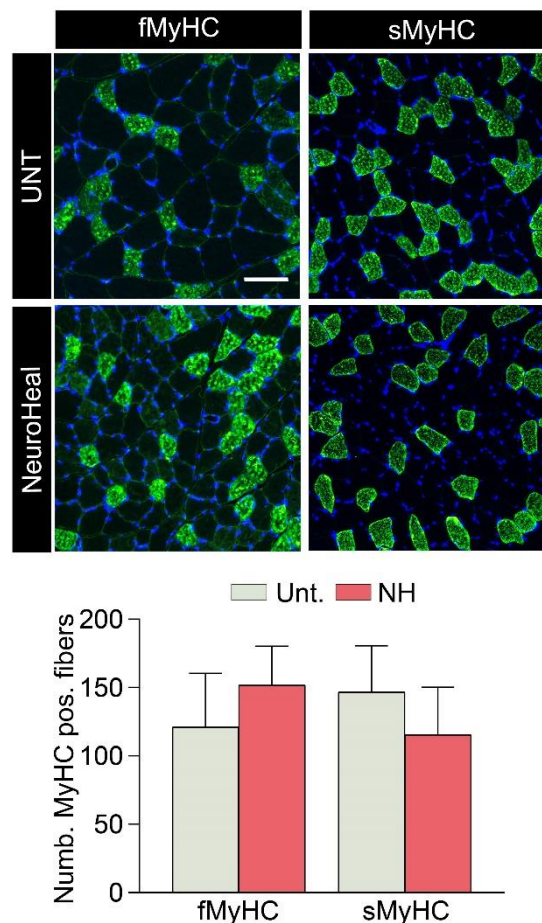


Figure S2. NeuroHeal does not modify the myosin-fiber pattern in healthy muscle. Top, representative microphotographs of the contralateral lesioned gastrocnemius muscle sections revealing the presence of fast and slow MyHC with DAPI (blue) from the different experimental groups injured untreated (Unt.) and injured treated with NeuroHeal (NH) at 14 dpi. Scale bar 100

μm and identical for all corresponding microphotographs as represented in the first image panel, the untreated condition. **Bottom**, bar graphs of the average of positive fibers for fast and slow MyHC ($n = 5$; t-test).

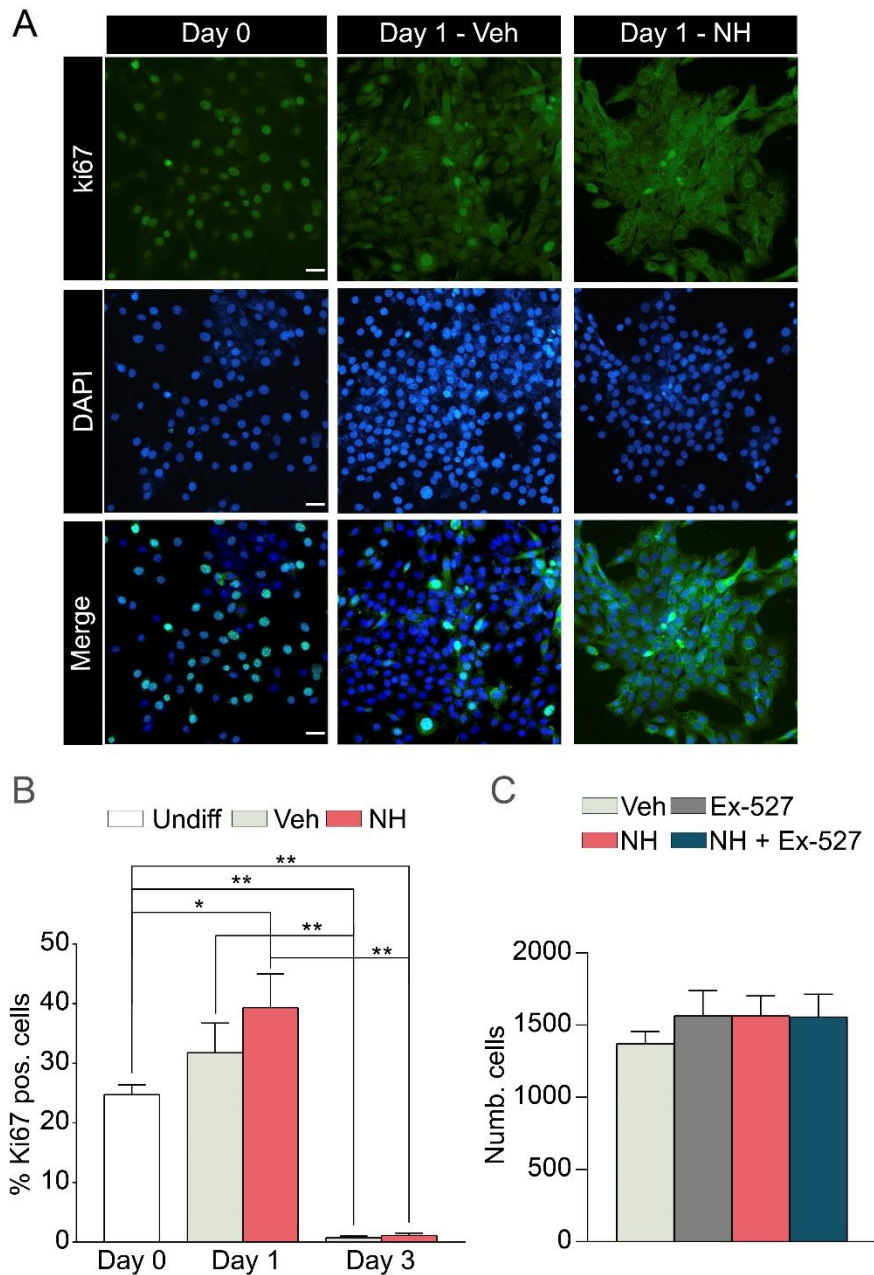


Figure S3. C2C12 cell line maintains high rate of proliferation 1 day after differentiation. (A) Representative microphotographs of differentiated C2C12 myoblast cell line immunostained for Ki67 and stained with DAPI from the different experimental groups at day 0 and 1 days of differentiation: atrophy-induced treated with vehicle (Veh) and atrophy-induced treated with NeuroHeal (NH). Scale bar 50 μm and identical for all corresponding microphotographs as represented in the first image panel, the day 0. (B) Bar graph of the average number of positive

nuclei for Ki67 ($n = 3$; one-way ANOVA, $*p < 0.0001$). (C) Bar graph of the average number of nuclei for condition ($n = 3$; one-way ANOVA).

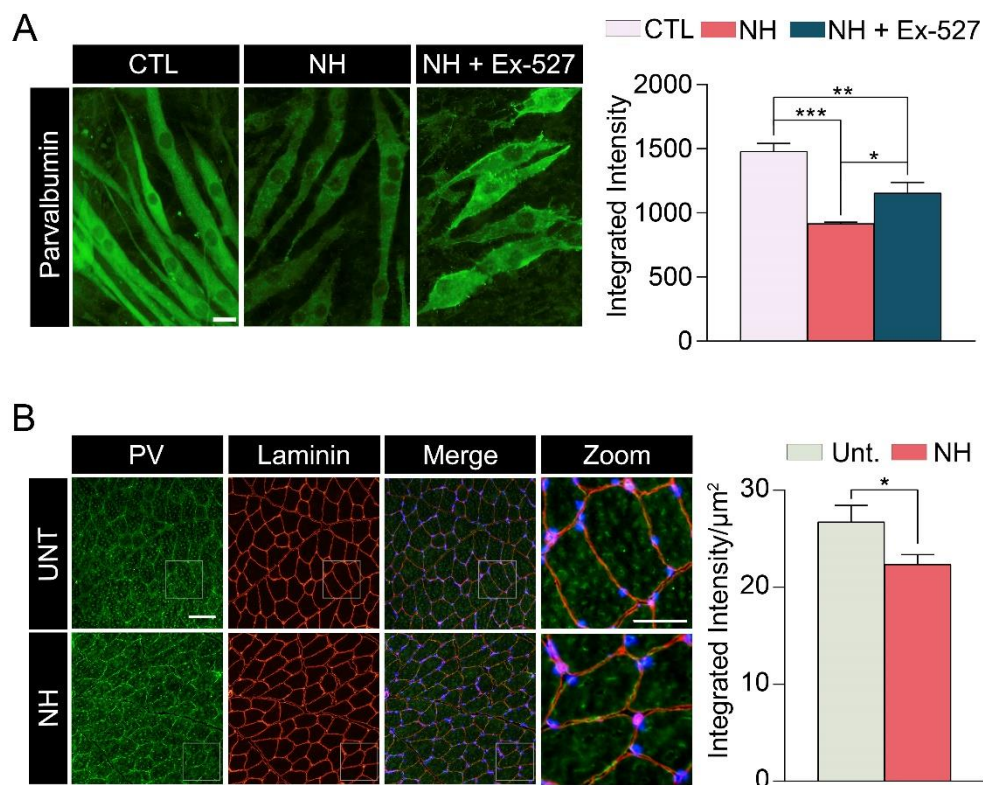


Figure S4. Parvalbumin is modulated by SIRT1 in vivo and in vitro. (A) Left, representative microphotographs of differentiated C2C12 myoblast cell line immunostained for parvalbumin and stained with DAPI from the different experimental groups at 3 days of differentiation: untreated (Ctl), treated with NeuroHeal (NH) and treated with NH plus Ex-527. Scale bar 25 μm and identical for all corresponding microphotographs as represented in the first image panel, the control. Right, bar graph of the relative intensity per cell of parvalbumin ($n = 5$; one-way ANOVA, $*p < 0.05$). (B) Left, representative microphotographs of the contralateral lesioned gastrocnemius muscle sections revealing the presence of parvalbumin, laminin with DAPI (blue) from the different experimental groups injured untreated (Unt.) and injured treated with NeuroHeal (NH) at 14 dpi. Scale bar 100 μm and identical for all corresponding microphotographs as represented in the first image panel, the untreated condition. Right, bar graphs of the relative intensity per fiber of parvalbumin ($n = 5$, t-test, $*p < 0.05$).

GENERAL DISCUSSION

This thesis aimed to decipher the novel therapeutic effect of NeuroHeal for muscle tissue disorders, focusing on muscle atrophy and acute muscle injury. The rationale behind arises from the ability of NeuroHeal to boost endogenous mechanisms of protection present in neurons (Romeo-Guitart et al., 2017, 2018b, 2019). Thus, we pursued to elucidate if NeuroHeal also endorsed these mechanisms in muscle tissue to promote its recovery after disuse or injury. First, we determined whether NeuroHeal could have a direct effect on muscle tissue, and we performed an initial characterization of the mechanisms by which NeuroHeal protects and promotes regenerative effects on the muscle. We used two *in vivo* models to study whether NeuroHeal could modulate muscle atrophy, by immobilization and denervation models, and the data was accompanied by the analysis on an *in vitro* model based on C2C12 cell line. In these models, we observed that NeuroHeal prevented myofiber atrophy promoted by a lack of motor activity. These protective effects were mediated by a reduction in the UB-proteasome activity and a correct resolution of the autophagy process. Regarding the regenerative effect, we studied it through muscle contraction and SCs biology, in an *in vivo* model of the GA muscle injury. Using this model, we observed that NeuroHeal modulated the biological response of the SCs, improving muscle regeneration, and accelerating myogenesis after injury. We demonstrated that NeuroHeal reduced muscle atrophy, as well as accelerated muscle regeneration. Altogether, NeuroHeal is a plausible therapy for a variety of muscle alterations, such as denervation due to peripheral nerve injuries, degenerative diseases, immobilization, and acute injuries.

Currently, there is no pharmacological therapy to prevent and improve muscle atrophy. Exercise, food supplementation, and physical therapy are the only available options to alleviate or prevent muscle atrophy. Unfortunately, exercise as a protocol is not a good option in patient under certain circumstances: immobilization, either by a cast or by bed-resting, or elderly patients whom their physical capacity is greatly weakened. Most of the current therapies are focused on diet supplementation, stem cells or autograph, gene therapy, and pharmacology. Therefore, pharmacological therapy, combined with the currently used treatments, would be beneficial for all types of patients with diverse muscular pathologies. On the other hand, therapies used for recovery after a muscle injury are very limited or without a solid scientific validation. Anti-inflammatory drugs, exercise, or surgery are the only approved therapies. Although in most cases recovery occurs spontaneously without any external intervention, the results are not always satisfactory, increasing the incidence of suffering a new injury in the same area. Find a therapy to accelerate muscle recovery and avoid the incidence is vitally important for health systems worldwide. Hence, NeuroHeal could be a feasible pharmacological treatment for all these muscle pathologies.

NeuroHeal was designed to overwhelm the paradigm one-target one-drug, aiming to threaten an unmet medical need: MN degeneration after nerve injury. The

rationale was to boost the endogenous mechanisms of neuroprotection intrinsically present in the neurons, in contrast to the most common workflow in drug discovery, based on the suppression of pathological pathways. NeuroHeal was discovered using a novel bioinformatic based on systems biology approach and artificial neural networks. From this bioinformatic analysis, NeuroHeal was the drug combination with the best results among all the analyzed (Romeo-Guitart et al., 2018a), because it promotes MN neuroprotection, is anti-inflammatory, enhances axonal regeneration after axotomy, and reduces muscle atrophy (Romeo-Guitart et al., 2017, 2018b, 2019, 2020). NeuroHeal is a combination of two repurposed drugs which are currently used in human medicine for long-lasting treatment: Acamprosate and Ribavirin. Drug repurposing reduces the time-lines in assays, because the behavior and the safety of the drugs within the human organism are well-described. Currently, there are other repurposed drugs under study to treat muscular pathologies, such as Liraglutide, an analog of glucagon-like peptide-1 (GLP-1), which induces protection and restored myofibrillar architecture in diverse models of muscle atrophy (Gurjar et al., 2020), or Alendronate, which is used to treat osteoporosis and Paget's disease of bone, improved muscle atrophy down-regulating SIRT3 (Chiu et al., 2018).

Muscle injury triggers the activation of the necrosis and the apoptosis pathways. Apoptosis induction leads to muscle atrophy, causing a reduction of the cytoplasm and the activation of the UPS (Marzetti et al., 2010; Carmeli et al., 2015). Promoting an activation of the anti-apoptosis pathways would be beneficial to reduce this atrophy. This induction can be boosted by NeuroHeal which activates as beneficial endogenous mechanisms the anti-apoptosis and anti-apoptosis pathways after nervous system injuries (Romeo-Guitart et al., 2018a). These helpful effects are promoted by the modulation of the NeuroHeal's target, NMDA-R, VGCC-R, and IMPDH enzyme (Romeo-Guitart et al., 2018a), which are also present in the skeletal muscle, and the synergy of Acamprosate and Ribavirin observed in our results, in which only animals treated with NeuroHeal showed a reduction in the weight loss of the GAs muscles. This synergy was also required in a root avulsion model to obtain neuroprotection and regenerative effects (Romeo-Guitart et al., 2018a). Preliminary studies in a root avulsion with a delayed reimplantation model treated with NeuroHeal reported a reduction in muscle atrophy (Romeo-Guitart et al., 2017). To exclude whether this effect was caused by nerve regeneration, we chose two *in vivo* models of muscle affectation no triggered by nervous system injury: denervation and hindlimb immobilization models. These models mimic situations caused by traumatic nerve injuries, such as accidents, neurodegenerative diseases, such as ALS, or immobilization, such as bedridden or sling use.

Knowing that NeuroHeal reduced muscle atrophy, we wanted to unravel which were the underlying mechanisms of this beneficial effect. Muscular atrophy is originated

after an imbalance in protein metabolism due to an increased protein degradation. Indeed, after denervation, the myofibers degenerate leading to an accumulation of misfolded ubiquitinated proteins which are normally degraded via the UPS. Thus, we analyzed how NeuroHeal modulated protein metabolism, by analyzing the pathways involved in protein synthesis and degradation. NeuroHeal diminished the catabolic response caused by reduced UPS response, thus decreasing the degradation of the proteins. The Akt-mTOR pathway was not altered, in agreement with previous reports which showed that atrophy is independent of this pathway (MacDonald et al., 2014). The misfolded ubiquitinated proteins can also be degraded by autophagy, which participates in muscle atrophy, increasing myofiber content degradation (Grumati and Bonaldo, 2012). This overactivation is followed by a blockage in the resolution, which induces toxicity and cellular degeneration. This blockage was resolved by NeuroHeal without an increase in autophagy induction, after muscle denervation. In previous studies, NeuroHeal led to fine regulation of the autophagic flux in the nervous system to promote neuroprotection (Romeo-Guitart et al., 2020). The UPS and the autophagy pathway are connected, mainly by the cargo-recognition protein p62. It is involved in the nucleation of protein aggregates labeled with Ub to be eliminated by the lysosome (Kageyama et al., 2014; Galluzzi et al., 2017). These same aggregates are also degraded by the proteasome. The preferential use of one of the two routes is mainly caused by the accumulation of the aggregates and the concentration of Ub-K48. The accumulation of protein aggregates promotes their elimination through autophagy by upregulating p62 and inhibiting UPS. Besides, p62-induced clustering can be inhibited by a high concentration of K48-linked ubiquitin chains, which can be accumulated upon proteasome deficiency (Kaiser et al., 2011). After denervation, we observed an increase in p62 and Ub K-48, suggesting dysfunction in both systems. NeuroHeal reestablished both pathways reducing both proteins, which leads to a decrease in aggregates accumulation by a correct elimination of autophagosomes and/or autophagolysosomes. Regarding current therapies, there are some molecules under study which modulate the UPS and autophagy activities. Conessine treatment reduces dexamethasone-induced muscle atrophy by regulating MuRF-1 and Atrogin-1 expression (Kim et al., 2018). Myricanol rescues atrophy by SIRT1 and reducing atrogenes in the same model (Shen et al., 2019). Finally, Salidroside alleviates skeletal muscle atrophy in a denervation model, through the suppression of oxidative stress and inflammation and reduction of the expression of atrogenes and autophagy genes (Huang et al., 2019).

Protective promotion in a tissue alteration, it is interesting to activate regenerative mechanisms to restore it. After a muscle injury or during exercise, the muscle resident stem cells, the SCs, are activated and are able to regenerate the tissue. To analyze whether NeuroHeal has muscle regenerative abilities, we chose an animal model which mimics skeletal muscle lesions detected in human athletes (Contreras-Muñoz et al.,

2016). It represents an excellent approach for the study of the mechanisms of muscle injury and repair. Using this model, we observed that NeuroHeal improved muscle regeneration and accelerated myogenesis. In homeostatic conditions, quiescent SCs require constitutive autophagy for their maintenance (García-Prat et al., 2016). But, upon injury, there is an induction of the autophagy by SIRT1 to provide nutrients to make the transition from a quiescent to an active state of the SC during myoblast differentiation to restore the damaged fiber (Gumucio et al., 2012; Tang and Rando, 2014; Nischenko et al., 2016, 2020; Call et al., 2017; McClung et al., 2017). Besides, the increase of autophagy activity promotes the clearance of damaged proteins and organelles in the fibers. Alterations in autophagy induction resulted in a slow recovery of muscle strength, as it is in the case of skeletal muscle-specific KO of Ulk1 (Call et al., 2017), or impaired muscle regeneration after injury in genetically altered Atg16l1 mice (Cadwell et al., 2008; Paolini et al., 2018). Proper elimination of the autophagosomes impairs the muscle strength in DMD mice treated with rapamycin (Bibee et al., 2014). These suggest that NeuroHeal could promote functional improvement through a correct resolution of autophagy flux. We observed a faster recovery in the injured muscle model, but we did not study if it was modulated by an autophagy response. This recovery was evidenced by the increase in CMAP amplitude, an expected result since it had been previously observed that NeuroHeal promoted the recovery of the motor endplates after denervation (Romeo-Guitart et al., 2017). Besides, NeuroHeal treatment showed a higher TetF with a slight increase in the PF by an increase in CT and HRT, regardless of the lesion. As there is a greater response, this may require more time of contraction and, consequently, a longer time of relaxation. These results suggested that NeuroHeal modulated the muscle response by increasing the intracellular $[Ca^{2+}]$. We hypothesized that NeuroHeal increased Ca^{2+} levels in the sarcoplasm by VGCC activation and Parvalbumin diminution. There are a few drugs under study which modulate the concentration of calcium in muscle atrophy due to denervation or immobilization. Most of them are oriented to Duchenne disease or cardiac pathologies. However, some molecules which activate the RyR have been proposed as potential therapeutic compounds, such as BIT molecules (Robinson et al., 2020) or FK506-binding protein 12 (FKBP12) (Witherspoon and Meilleur, 2016). Lastly, it was observed in a SOD1 model that the restoration of SERCA ATPase levels prevents oxidative stress-related muscle atrophy and weakness (Qaisar et al., 2019).

Ca^{2+} is involved in myogenesis and regeneration. When there is an increase in $[Ca^{2+}]$, there is an activation of the gene transcription of the slow fibers. We observed that NeuroHeal exerted a change in the pattern of expression of the slow muscle fibers. This phenomenon could be useful for other diseases which require the preservation of muscle fibers, for example, in neurodegenerative diseases such as ALS. This disease is characterized by neuromuscular denervation, MN death, and paralysis. This triggers

an early degeneration of the fast fibers, while no defects are observed in the slow. Therefore, by preventing degeneration of the surviving fibers, muscle activity may be prolonged and the quality of life of these patients improved. Currently, there are only two drugs, Riluzole (Bensimon et al., 1994) and Edaravone (Abe et al., 2017), approved for the treatment of ALS, which only extend the life expectancy by a few months. There are drugs under study with positive results, such as the PXT864 drug, which is a combination of Baclofen and Acamprosate (Boussicault et al., 2020). Impairment in several proteostatic mechanisms has been reported in skeletal muscle of patients with neuromuscular conditions such as ALS. In ALS, several lines of evidence suggest that the most vulnerable fast motor neurons are also the most dependent on autophagy (Kanning et al., 2010). Defects in autophagy in ALS has been described in all the steps: initiation, nucleation, and resolution. mSOD1 mice showed an upregulation of Beclin1, LC3, p62, and autophagosome formation (Dobrowolny et al., 2008; Crippa et al., 2013; Oliván et al., 2015; Xiao et al., 2018). Other mutation, in VCP gene, which can cause familial ALS, impairs autophagosome degradation but not biogenesis (Ching et al. 2013). All these show an impairment in resolution of the autophagy flux. This can be solved with proper removal of the ubiquitinated substrates and a correct degradation of the autolysosomes, effects promoted by NeuroHeal.

One of the NeuroHeal targets we seem to be involved in protecting against atrophy and inducing regeneration is SIRT1. Previously, it was shown that NeuroHeal exerted neuroprotective and regenerative effects in the nervous system through SIRT1 activation (Romeo-Guitart et al., 2018b, 2019). This is not the unique node of the protein interaction map by which NeuroHeal promoted protection, due to Akt was showed to have neuroprotective effects (Romeo-Guitart et al., 2020). Also, maintained normal activation levels of Akt by NeuroHeal allows it to continue inducing autophagy to reduce atrophy after denervation. In general, Sirtuins act as major players in linking changes in metabolism to transcription. There are different types of Sirtuins, but the most expressed in the skeletal muscle is SIRT1. In the skeletal muscle, SIRT1 controls muscle metabolism, fiber differentiation, and prevents muscle waste by the deacetylation of NF- κ B and the inhibition of TNF α (Ghosh and Karin, 2002; Fulco et al., 2003b, 2008; Yeung et al., 2004; Amat et al., 2009a; Salminen and Kaarniranta, 2009; Vinciguerra et al., 2010; Zorzano et al., 2010a). SIRT1 allows skeletal muscle fibers to adapt to the energetic demands with the deacetylation of PGC1 α (Gerhart-Hines et al., 2007; Cantó et al., 2010). This energy requirement modulates the differentiation by the inhibition of MyoD by SIRT1 (Fulco et al., 2003a, 2008; Amat et al., 2009b; Zorzano et al., 2010b; Cerletti et al., 2012). We observed that the inhibition of SIRT1 decreases the recovery of myofibers, produced by an increase in atrogenes protein levels and an autophagy blockage. SIRT1 modulates autophagy through FoxO3 (Huang and Tindall, 2007; Kroemer et al., 2010; Daitoku et al., 2011), p53 (Luo et al., 2001; Vaziri et al., 2001; Jin,

2005), and NFkB (Yeung et al., 2004; Criollo et al., 2010; Comb et al., 2011; Liu et al., 2012). We observed a delay in the SCs activation inhibiting SIRT1. This result can be contradictory since the inhibition of SIRT1 leads to an increase in MyoD allowing cell differentiation. As discussed before, myogenesis is modulated by many factors, among them autophagy, which is activated by NeuroHeal. It would be interesting to study the state of autophagy in myogenesis. SIRT1 can be related to Ca^{2+} due to SIRT/PGC1a axis inversely regulated Parvalbumin expression and mitochondrial volume. SIRT1 has been the target of studies in the search of new treatments, such as resveratrol that showed anti-atrophic effects modulating autophagy (Albani et al., 2010; Donmez, 2012; Park et al., 2012; Tennen et al., 2012; Bennett et al., 2013; Porquet et al., 2013; Hsu et al., 2020) and curcumin that attenuated atrophy reducing protein degradation (Thaloor et al., 1999; Mañas-García et al., 2020). Although positive results were obtained, more research is needed to determine the underlying mechanisms of both compounds.

In this thesis, we have shown that NeuroHeal has a protective and regenerative effect on the muscle. NeuroHeal prevents the reduction of myofibers, reduces the catalytic activity of the UPS, and induces a correct resolution of autophagy. Besides, NeuroHeal accelerates the recovery of grip strength and neuromuscular response. On the other hand, NeuroHeal promotes the regenerative response of the skeletal muscle, enhancing activation and differentiation of the SCs. This is accompanied by an increase in muscle contraction and a fast myosin fiber-switch. All these features are modulated by the action of a network, formed by the interaction between the different molecular mechanisms, being deacetylase activity of SIRT1 an essential node. Therefore, NeuroHeal is a feasible treatment for a wide variety of muscle pathologies.

CONCLUSIONS

Chapter I. NeuroHeal reduces Muscle Atrophy and modulates Associated Autophagy

- NeuroHeal reduces muscle fiber atrophy in the *in vivo* models, of denervation and hindlimb immobilization, and *in vitro*, in TNF α atrophy-induced C2C12 cell line.
- NeuroHeal improves recovery of grip strength in animals subjected to hindlimb immobilization.
- NeuroHeal sustains a normal activation of protein synthesis after denervation, without promoting hypertrophy in normal conditions.
- NeuroHeal reduces protein degradation through downregulation of the ubiquitin-protease activity and promotes amelioration of the autophagy flux, inducing its activation and a functional resolution.
- SIRT1 activation by NeuroHeal is necessary to prevent muscle atrophy.

Chapter II. NeuroHeal improves Muscle Regeneration after Injury

- NeuroHeal improves the recovery of the muscle response.
- NeuroHeal reduces collagen deposition and increases the number of mature muscle fibers.
- NeuroHeal accelerates myogenesis after injury, enhancing activation and differentiation of the muscle satellite cells with an increase in the fusion coefficient to form myotubes.
- SIRT1 activity is needed for NeuroHeal modulation of satellite cell activation and modulation.

REFERENCES

- Abe K et al. (2017) Safety and efficacy of edaravone in well defined patients with amyotrophic lateral sclerosis: a randomised, double-blind, placebo-controlled trial. *Lancet Neurol* 16:505–512.
- Adams L, Carlson BM, Henderson L, Goldman D (1995) Adaptation of nicotinic acetylcholine receptor, myogenin, and MRF4 gene expression to long-term muscle denervation. *J Cell Biol* 131:1341–1349.
- Albani D, Polito L, Signorini A, Forloni G (2010) Neuroprotective properties of resveratrol in different neurodegenerative disorders. *BioFactors* 36:370–376.
- Alter J, Rozentzweig D, Bengal E (2008) Inhibition of Myoblast Differentiation by Tumor Necrosis Factor α Is Mediated by c-Jun N-terminal Kinase 1 and Leukemia Inhibitory Factor. *J Biol Chem* 283:23224–23234.
- Amat R, Planavila A, Chen SL, Iglesias R, Giralt M, Villarroya F (2009a) SIRT1 Controls the Transcription of the Peroxisome Proliferator-activated Receptor- γ Co-activator-1 α (PGC-1 α) Gene in Skeletal Muscle through the PGC-1 α Autoregulatory Loop and Interaction with MyoD. *J Biol Chem* 284:21872–21880.
- Amat R, Planavila A, Chen SL, Iglesias R, Giralt M, Villarroya F (2009b) SIRT1 Controls the Transcription of the Peroxisome Proliferator-activated Receptor- γ Co-activator-1 α (PGC-1 α) Gene in Skeletal Muscle through the PGC-1 α Autoregulatory Loop and Interaction with MyoD. *J Biol Chem* 284:21872–21880.
- Arbogast F, Gros F (2018) Lymphocyte Autophagy in Homeostasis, Activation, and Inflammatory Diseases. *Front Immunol* 9:1801.
- Ashburn TT, Thor KB (2004) Drug repositioning: identifying and developing new uses for existing drugs. *Nat Rev Drug Discov* 3:673–683.
- Baehr LM, Furlow JD, Bodine SC (2011) Muscle sparing in muscle RING finger 1 null mice: response to synthetic glucocorticoids. *J Physiol* 589:4759–4776.
- Baehr LM, West DWD, Marshall AG, Marcotte GR, Baar K, Bodine SC (2017) Muscle-specific and age-related changes in protein synthesis and protein degradation in response to hindlimb unloading in rats. *J Appl Physiol* 122:1336–1350.
- Banerjee R, He J, Spaniel C, Quintana MT, Wang Z, Bain JR, Newgard CB, Muehlbauer MJ, Willis MS (2015) Non-targeted metabolomics analysis of cardiac Muscle Ring Finger-1 (MuRF1), MuRF2, and MuRF3 in vivo reveals novel and redundant metabolic changes. *Metabolomics* 11:312–322.
- Barabási A-L (2007) Network Medicine — From Obesity to the “Diseasome.” *N Engl J Med* 357:404–407.
- Batt J, Bain J, Goncalves J, Michalski B, Plant P, Fahnestock M, Woodgett J (2006) Differential gene expression profiling of short and long term denervated muscle. *FASEB J* 20:115–117.
- Baumann CW, Rogers RG, Gahlot N, Ingalls CP (2014) Eccentric contractions disrupt FKBP12 content in mouse skeletal muscle. *Physiol Rep* 2:e12081.
- Bechet D, Tassa A, Taillandier D, Combaret L, Attaix D (2005) Lysosomal proteolysis in skeletal muscle. *Int J Biochem Cell Biol* 37:2098–2114.
- Beehler BC, Sleph PG, Benmassaoud L, Grover GJ (2006) Reduction of Skeletal Muscle Atrophy by a Proteasome Inhibitor in a Rat Model of Denervation. *Exp Biol Med* 231:335–341.
- Bennett BT, Mohamed JS, Alway SE (2013) Effects of Resveratrol on the Recovery of Muscle Mass Following Disuse in the Plantaris Muscle of Aged Rats López Lluch G, ed. *PLoS One* 8:e83518.
- Bensimon G, Lacomblez L, Meininger V (1994) A Controlled Trial of Riluzole in Amyotrophic Lateral Sclerosis. *N Engl J Med* 330:585–591.
- Best TM, Hunter KD (2000) Muscle Injury and Repair. *Phys Med Rehabil Clin N Am* 11:251–266.
- Bibee KP, Cheng Y, Ching JK, Marsh JN, Li AJ, Keeling RM, Connolly AM, Golumbek PT, Myerson JW, Hu G, Chen J, Shannon WD, Lanza GM, Weihl CC, Wickline SA (2014) Rapamycin nanoparticles target defective autophagy in muscular dystrophy to enhance both strength and

- cardiac function. *FASEB J* 28:2047–2061.
- Bjornson CRR, Cheung TH, Liu L, Tripathi P V., Steeper KM, Rando TA (2012) Notch Signaling Is Necessary to Maintain Quiescence in Adult Muscle Stem Cells. *Stem Cells* 30:232–242.
- Bodine SC (2001) Identification of Ubiquitin Ligases Required for Skeletal Muscle Atrophy. *Science* (80-) 294:1704–1708.
- Bodine SC, Stitt TN, Gonzalez M, Kline WO, Stover GL, Bauerlein R, Zlotchenko E, Scrimgeour A, Lawrence JC, Glass DJ, Yancopoulos GD (2001a) Akt/mTOR pathway is a crucial regulator of skeletal muscle hypertrophy and can prevent muscle atrophy in vivo. *Nat Cell Biol* 3:1014–1019.
- Bodine SC, Stitt TN, Gonzalez M, Kline WO, Stover GL, Bauerlein R, Zlotchenko E, Scrimgeour A, Lawrence JC, Glass DJ, Yancopoulos GD (2001b) Akt/mTOR pathway is a crucial regulator of skeletal muscle hypertrophy and can prevent muscle atrophy in vivo. *Nat Cell Biol* 3:1014–1019.
- Boldrin L, Muntoni F, Morgan JE (2010) Are Human and Mouse Satellite Cells Really the Same? *J Histochem Cytochem* 58:941–955.
- Borden KLB, Freemont PS (1996) The RING finger domain: a recent example of a sequence—structure family. *Curr Opin Struct Biol* 6:395–401.
- Borisov AB, Dedkov EI, Carlson BM (2001) Interrelations of myogenic response, progressive atrophy of muscle fibers, and cell death in denervated skeletal muscle. *Anat Rec* 264:203–218.
- Borisov AB, Huang S-K, Carlson BM (2000) Remodeling of the vascular bed and progressive loss of capillaries in denervated skeletal muscle. *Anat Rec* 258:292–304.
- Boussicault L, Laffaire J, Schmitt P, Rinaudo P, Callizot N, Nabirotkin S, Hajj R, Cohen D (2020) Combination of acamprosate and baclofen (PXT864) as a potential new therapy for amyotrophic lateral sclerosis. *J Neurosci Res:jnr.24714*.
- Boutari C, Mantzoros CS (2017) Decreasing Lean Body Mass with Age: Challenges and Opportunities for Novel Therapies. *Endocrinol Metab* 32:422.
- Brack AS, Conboy IM, Conboy MJ, Shen J, Rando TA (2008) A Temporal Switch from Notch to Wnt Signaling in Muscle Stem Cells Is Necessary for Normal Adult Myogenesis. *Cell Stem Cell* 2:50–59.
- Brandon AE, Tid-Ang J, Wright LE, Stuart E, Suryana E, Bentley N, Turner N, Cooney GJ, Ruderman NB, Kraegen EW (2015) Overexpression of SIRT1 in Rat Skeletal Muscle Does Not Alter Glucose Induced Insulin Resistance Kanzaki M, ed. *PLoS One* 10:e0121959.
- Brocca L, Toniolo L, Reggiani C, Bottinelli R, Sandri M, Pellegrino MA (2017) FoxO-dependent atrogenes vary among catabolic conditions and play a key role in muscle atrophy induced by hindlimb suspension. *J Physiol* 595:1143–1158.
- Brockett CL, Morgan DL, Proske U (2004) Predicting Hamstring Strain Injury in Elite Athletes. *Med Sci Sport Exerc* 36:379–387.
- Brooks S V., Zerba E, Faulkner JA (1995) Injury to muscle fibres after single stretches of passive and maximally stimulated muscles in mice. *J Physiol* 488:459–469.
- Cadwell K, Liu JY, Brown SL, Miyoshi H, Loh J, Lennerz JK, Kishi C, Kc W, Carrero JA, Hunt S, Stone CD, Brunt EM, Xavier RJ, Sleckman BP, Li E, Mizushima N, Stappenbeck TS, Virgin IV HW (2008) A key role for autophagy and the autophagy gene Atg16l1 in mouse and human intestinal Paneth cells. *Nature* 456:259–263.
- Cai D, Frantz JD, Tawa NE, Melendez PA, Oh B-C, Lidov HGW, Hasselgren P-O, Frontera WR, Lee J, Glass DJ, Shoelson SE (2004) IKK β /NF- κ B Activation Causes Severe Muscle Wasting in Mice. *Cell* 119:285–298.
- Call JA, Wilson RJ, Laker RC, Zhang M, Kundu M, Yan Z (2017) Ulk1-mediated autophagy plays an essential role in mitochondrial remodeling and functional regeneration of skeletal muscle. *Am J Physiol Cell Physiol* 312:C724–C732.
- Campbell WG, Gordon SE, Carlson CJ, Pattison JS, Hamilton MT, Booth FW (2001) Differential global gene expression in red and white skeletal muscle. *Am J Physiol Physiol* 280:C763–C768.
- Cantó C, Jiang LQ, Deshmukh AS, Matakaki C, Coste A, Lagouge M, Zierath JR, Auwerx J (2010)

- Interdependence of AMPK and SIRT1 for Metabolic Adaptation to Fasting and Exercise in Skeletal Muscle. *Cell Metab* 11:213–219.
- Carmeli E, Aizenbud D, Rom O (2015) How Do Skeletal Muscles Die? An Overview. In: *Advances in Experimental Medicine and Biology*, pp 99–111. Springer New York LLC.
- Carpenter S, Karpati G (1982) Necrosis of capillaries in denervation atrophy of human skeletal muscle. *Muscle Nerve* 5:250–254.
- Carraro U, Rossini K, Mayr W, Kern H (2005) Muscle Fiber Regeneration in Human Permanent Lower Motoneuron Denervation: Relevance to Safety and Effectiveness of FES-Training, Which Induces Muscle Recovery in SCI Subjects. *Artif Organs* 29:187–191.
- Casas C, Isus L, Herrando-Grabulosa M, Mancuso FM, Borrás E, Sabidó E, Forés J, Aloy P (2015) Network-based proteomic approaches reveal the neurodegenerative, neuroprotective and pain-related mechanisms involved after retrograde axonal damage. *Sci Rep* 5:9185.
- Centner T, Yano J, Kimura E, McElhinny AS, Pelin K, Witt CC, Bang M-L, Trombitas K, Granzier H, Gregorio CC, Sorimachi H, Labeit S (2001) Identification of muscle specific ring finger proteins as potential regulators of the titin kinase domain. *J Mol Biol* 306:717–726.
- Cerletti M, Jang YC, Finley LWS, Haigis MC, Wagers AJ (2012) Short-Term Calorie Restriction Enhances Skeletal Muscle Stem Cell Function. *Cell Stem Cell* 10:515–519.
- Chan O, Del Buono A, Best TM, Maffulli N (2012) Acute muscle strain injuries: a proposed new classification system. *Knee Surgery, Sport Traumatol Arthrosc* 20:2356–2362.
- Chen D, Chen S, Wang W, Liu F, Zhang C, Zheng H (2010) Modulation of satellite cells in rat facial muscle following denervation and delayed reinnervation. *Acta Otolaryngol* 130:1411–1420.
- Chen S-E, Jin B, Li Y-P (2007) TNF- α regulates myogenesis and muscle regeneration by activating p38 MAPK. *Am J Physiol Physiol* 292:C1660–C1671.
- Cheng F, Liu C, Jiang J, Lu W, Li W, Liu G, Zhou W, Huang J, Tang Y (2012) Prediction of Drug-Target Interactions and Drug Repositioning via Network-Based Inference Altman RB, ed. *PLoS Comput Biol* 8:e1002503.
- Chiu H-C, Chiu C-Y, Yang R-S, Chan D-C, Liu S-H, Chiang C-K (2018) Preventing muscle wasting by osteoporosis drug alendronate in vitro and in myopathy models via sirtuin-3 down-regulation. *J Cachexia Sarcopenia Muscle* 9:585–602.
- Choi SJ (2014) Cellular mechanism of eccentric-induced muscle injury and its relationship with sarcomere heterogeneity. *J Exerc Rehabil* 10:200–204.
- Clarke BA, Drujan D, Willis MS, Murphy LO, Corpina RA, Burova E, Rakhilin S V., Stitt TN, Patterson C, Latres E, Glass DJ (2007a) The E3 Ligase MuRF1 Degrades Myosin Heavy Chain Protein in Dexamethasone-Treated Skeletal Muscle. *Cell Metab* 6:376–385.
- Clarke BA, Drujan D, Willis MS, Murphy LO, Corpina RA, Burova E, Rakhilin S V., Stitt TN, Patterson C, Latres E, Glass DJ (2007b) The E3 Ligase MuRF1 Degrades Myosin Heavy Chain Protein in Dexamethasone-Treated Skeletal Muscle. *Cell Metab* 6:376–385.
- Cohen S, Brault JJ, Gygi SP, Glass DJ, Valenzuela DM, Gartner C, Latres E, Goldberg AL (2009) During muscle atrophy, thick, but not thin, filament components are degraded by MuRF1-dependent ubiquitylation. *J Cell Biol* 185:1083–1095.
- Cohen S, Zhai B, Gygi SP, Goldberg AL (2012) Ubiquitylation by Trim32 causes coupled loss of desmin, Z-bands, and thin filaments in muscle atrophy. *J Cell Biol* 198:575–589.
- Colonna M, Butovsky O (2017) Microglia Function in the Central Nervous System During Health and Neurodegeneration. *Annu Rev Immunol* 35:441–468.
- Comb WC, Cogswell P, Sitcheran R, Baldwin AS (2011) IKK-dependent, NF- κ B-independent control of autophagic gene expression. *Oncogene* 30:1727–1732.
- Cong H, Sun L, Liu C, Tien P (2011) Inhibition of Atrogin-1/MAFbx Expression by Adenovirus-Delivered Small Hairpin RNAs Attenuates Muscle Atrophy in Fasting Mice. *Hum Gene Ther* 22:313–324.
- Contreras-Muñoz P, Fernández-Martín A, Torrella R, Serres X, De La Varga M, Viscor G,

- Järvinen TAH, Martínez-Ibáñez V, Peiró JL, Rodas G, Marotta M (2016) A New Surgical Model of Skeletal Muscle Injuries in Rats Reproduces Human Sports Lesions. *Int J Sports Med* 37:183–190.
- Criollo A et al. (2010) The IKK complex contributes to the induction of autophagy. *EMBO J* 29:619–631.
- Crippa V, Boncoraglio A, Galbiati M, Aggarwal T, Rusmini P, Giorgetti E, Cristofani R, Carra S, Pennuto M, Poletti A (2013) Differential autophagy power in the spinal cord and muscle of transgenic ALS mice. *Front Cell Neurosci* 7:234.
- Csibi A, Cornille K, Leibovitch M-P, Poupon A, Tintignac LA, Sanchez AMJ, Leibovitch SA (2010) The Translation Regulatory Subunit eIF3f Controls the Kinase-Dependent mTOR Signaling Required for Muscle Differentiation and Hypertrophy in Mouse Blagosklonny M V., ed. *PLoS One* 5:e8994.
- Csibi A, Leibovitch MP, Cornille K, Tintignac LA, Leibovitch SA (2009) MAFbx/Atrogin-1 Controls the Activity of the Initiation Factor eIF3-f in Skeletal Muscle Atrophy by Targeting Multiple C-terminal Lysines. *J Biol Chem* 284:4413–4421.
- Daitoku H, Sakamaki J, Fukamizu A (2011) Regulation of FoxO transcription factors by acetylation and protein–protein interactions. *Biochim Biophys Acta - Mol Cell Res* 1813:1954–1960.
- Daou HN (2020) Exercise as an anti-inflammatory therapy for cancer cachexia: a focus on interleukin-6 regulation. *Am J Physiol Integr Comp Physiol* 318:R296–R310.
- Davie JK, Cho J-H, Meadows E, Flynn JM, Knapp JR, Klein WH (2007) Target gene selectivity of the myogenic basic helix–loop–helix transcription factor myogenin in embryonic muscle. *Dev Biol* 311:650–664.
- Davis HL, Kiernan JA (1980) Neurotrophic effects of sciatic nerve extract on denervated extensor digitorum longus muscle in the rat. *Exp Neurol* 69:124–134.
- Day K, Shefer G, Richardson JB, Enikolopov G, Yablonka-Reuveni Z (2007) Nestin-GFP reporter expression defines the quiescent state of skeletal muscle satellite cells. *Dev Biol* 304:246–259.
- de Castro Rodrigues A, Schmalbruch H (1995) Satellite cells and myonuclei in long-term denervated rat muscles. *Anat Rec* 243:430–437.
- De Smet AA, Best TM (2000) MR Imaging of the Distribution and Location of Acute Hamstring Injuries in Athletes. *Am J Roentgenol* 174:393–399.
- de Theije CC, Langen RCJ, Lamers WH, Schols AMWJ, Köhler SE (2013) Distinct responses of protein turnover regulatory pathways in hypoxia- and semistarvation-induced muscle atrophy. *Am J Physiol Cell Mol Physiol* 305:L82–L91.
- Denegar CR, Saliba E, Foreman-Saliba S (2016) Therapeutic modalities for musculoskeletal injuries (Kinetics H, ed). *Human Kinetics*.
- Devor ST, Faulkner JA (1999) Regeneration of new fibers in muscles of old rats reduces contraction-induced injury. *J Appl Physiol* 87:750–756.
- Dikic I, Elazar Z (2018) Mechanism and medical implications of mammalian autophagy. *Nat Rev Mol Cell Biol* 19:349–364.
- Dobrowolny G, Aucello M, Rizzuto E, Beccafico S, Mammucari C, Boncompagni S, Belia S, Wannenes F, Nicoletti C, Del Prete Z, Rosenthal N, Molinaro M, Protasi F, Fanò G, Sandri M, Musarò A (2008) Skeletal Muscle Is a Primary Target of SOD1G93A-Mediated Toxicity. *Cell Metab* 8:425–436.
- Donmez G (2012) The neurobiology of sirtuins and their role in neurodegeneration. *Trends Pharmacol Sci* 33:494–501.
- Duchesne E, Tremblay M-H, Côté CH (2011) Mast cell tryptase stimulates myoblast proliferation; a mechanism relying on protease-activated receptor-2 and cyclooxygenase-2. *BMC Musculoskelet Disord* 12:235.
- Dugdale HF, Hughes DC, Allan R, Deane CS, Coxon CR, Morton JP, Stewart CE, Sharples AP (2017) The role of resveratrol on skeletal muscle cell differentiation and myotube hypertrophy

- during glucose restriction. *Mol Cell Biochem* 0:1–15.
- Dziki J, Badylak S, Yabroudi M, Sicari B, Ambrosio F, Stearns K, Turner N, Wyse A, Boninger ML, Brown EHP, Rubin JP (2016) An acellular biologic scaffold treatment for volumetric muscle loss: results of a 13-patient cohort study. *npj Regen Med* 1:16008.
- Esser K, Gunning P, Hardeman E (1993) Nerve-Dependent and -Independent Patterns of mRNA Expression in Regenerating Skeletal Muscle. *Dev Biol* 159:173–183.
- Fielitz J, Kim M-S, Shelton JM, Latif S, Spencer JA, Glass DJ, Richardson JA, Bassel-Duby R, Olson EN (2007) Myosin accumulation and striated muscle myopathy result from the loss of muscle RING finger 1 and 3. *J Clin Invest* 117:2486–2495.
- Files DC et al. (2012) A Critical Role for Muscle Ring Finger-1 in Acute Lung Injury–associated Skeletal Muscle Wasting. *Am J Respir Crit Care Med* 185:825–834.
- Finley D (2009) Recognition and Processing of Ubiquitin-Protein Conjugates by the Proteasome. *Annu Rev Biochem* 78:477–513.
- Fulco M, Cen Y, Zhao P, Hoffman EP, McBurney MW, Sauve AA, Sartorelli V (2008a) Glucose Restriction Inhibits Skeletal Myoblast Differentiation by Activating SIRT1 through AMPK-Mediated Regulation of Nampt. *Dev Cell* 14:661–673.
- Fulco M, Cen Y, Zhao P, Hoffman EP, McBurney MW, Sauve AA, Sartorelli V (2008b) Glucose Restriction Inhibits Skeletal Myoblast Differentiation by Activating SIRT1 through AMPK-Mediated Regulation of Nampt. *Dev Cell* 14:661–673.
- Fulco M, Schiltz RL, Iezzi S, King MT, Zhao P, Kashiwaya Y, Hoffman E, Veech RL, Sartorelli V (2003a) Sir2 Regulates Skeletal Muscle Differentiation as a Potential Sensor of the Redox State. *Mol Cell* 12:51–62.
- Fulco M, Schiltz RLL, Iezzi S, King MTT, Zhao P, Kashiwaya Y, Hoffman E, Veech RL, Sartorelli V (2003b) Sir2 Regulates Skeletal Muscle Differentiation as a Potential Sensor of the Redox State. *Mol Cell* 12:51–62.
- Galluzzi L et al. (2017) Molecular definitions of autophagy and related processes. *EMBO J* 36:1811–1836.
- Galluzzi L, Bravo-San Pedro JM, Blomgren K, Kroemer G (2016) Autophagy in acute brain injury. *Nat Rev Neurosci* 17:467–484.
- García-Prat L, Martínez-Vicente M, Perdiguero E, Ortet L, Rodríguez-Ubreva J, Rebollo E, Ruiz-Bonilla V, Gutarra S, Ballestar E, Serrano AL, Sandri M, Muñoz-Cánoves P (2016) Autophagy maintains stemness by preventing senescence. *Nature* 529:37–42.
- Gerhart-Hines Z, Rodgers JT, Bare O, Lerin C, Kim S-H, Mostoslavsky R, Alt FW, Wu Z, Puigserver P (2007) Metabolic control of muscle mitochondrial function and fatty acid oxidation through SIRT1/PGC-1 α . *EMBO J* 26:1913–1923.
- Germani A, Di Carlo A, Mangoni A, Straino S, Giacinti C, Turrini P, Biglioli P, Capogrossi MC (2003) Vascular Endothelial Growth Factor Modulates Skeletal Myoblast Function. *Am J Pathol* 163:1417–1428.
- Ghosh S, Karin M (2002) Missing Pieces in the NF- κ B Puzzle. *Cell* 109:S81–S96.
- Glickman MH, Ciechanover A (2002) The Ubiquitin-Proteasome Proteolytic Pathway: Destruction for the Sake of Construction. *Physiol Rev* 82:373–428.
- Gomes MD, Lecker SH, Jagoe RT, Navon A, Goldberg AL (2001) Atrogin-1, a muscle-specific F-box protein highly expressed during muscle atrophy. *Proc Natl Acad Sci* 98:14440–14445.
- Groll M, Ditzel L, Löwe J, Stock D, Bochtler M, Bartunik HD, Huber R (1997) Structure of 20S proteasome from yeast at 2.4Å resolution. *Nature* 386:463–471.
- Grounds MD (2008) Complexity of Extracellular Matrix and Skeletal Muscle Regeneration. In: *Skeletal Muscle Repair and Regeneration*, pp 269–302. Dordrecht: Springer Netherlands.
- Grumati P, Bonaldo P (2012) Autophagy in skeletal muscle homeostasis and in muscular dystrophies. *Cells* 1:325–345.

- Grumati P, Coletto L, Sabatelli P, Cescon M, Angelin A, Bertaglia E, Blaauw B, Urciuolo A, Tiepolo T, Merlini L, Maraldi NM, Bernardi P, Sandri M, Bonaldo P (2010) Autophagy is defective in collagen VI muscular dystrophies, and its reactivation rescues myofiber degeneration. *Nat Med* 16:1313–1320.
- Gumucio JP, Davis ME, Bradley JR, Stafford PL, Schiffman CJ, Lynch EB, Claflin DR, Bedi A, Mendias CL (2012) Rotator cuff tear reduces muscle fiber specific force production and induces macrophage accumulation and autophagy. *J Orthop Res* 30:1963–1970.
- Gundersen K, Leberer E, Lømo T, Pette D, Staron RS (1988) Fibre types, calcium-sequestering proteins and metabolic enzymes in denervated and chronically stimulated muscles of the rat. *J Physiol* 398:177–189.
- Gurjar AA, Kushwaha S, Chattopadhyay S, Das N, Pal S, China SP, Kumar H, Trivedi AK, Guha R, Chattopadhyay N, Sanyal S (2020) Long acting GLP-1 analog liraglutide ameliorates skeletal muscle atrophy in rodents. *Metabolism* 103:154044.
- Gutmann E (1948) EFFECT OF DELAY OF INNERVATION ON RECOVERY OF MUSCLE AFTER NERVE LESIONS. *J Neurophysiol* 11:279–294.
- Guttridge DC, Albanese C, Reuther JY, Pestell RG, Baldwin AS (1999) NF- κ B Controls Cell Growth and Differentiation through Transcriptional Regulation of Cyclin D1. *Mol Cell Biol* 19:5785–5799.
- Haigis MC, Sinclair DA (2010) Mammalian Sirtuins: Biological Insights and Disease Relevance. *Annu Rev Pathol Mech Dis* 5:253–295.
- Hawke TJ, Garry DJ (2001) Myogenic satellite cells: physiology to molecular biology. *J Appl Physiol* 91:534–551.
- Herrando-Grabulosa M, Mulet R, Pujol A, Mas JM, Navarro X, Aloy P, Coma M, Casas C (2016) Novel Neuroprotective Multicomponent Therapy for Amyotrophic Lateral Sclerosis Designed by Networked Systems Duce JA, ed. *PLoS One* 11:e0147626.
- Hsu Y-J, Ho C-S, Lee M-C, Ho C-S, Huang C-C, Kan N-W (2020) Protective Effects of Resveratrol Supplementation on Contusion Induced Muscle Injury. *Int J Med Sci* 17:53–62.
- Huang H, Tindall DJ (2007) Dynamic FoxO transcription factors. *J Cell Sci* 120:2479–2487.
- Huang Z, Fang Q, Ma W, Zhang Q, Qiu J, Gu X, Yang H, Sun H (2019) Skeletal Muscle Atrophy Was Alleviated by Salidroside Through Suppressing Oxidative Stress and Inflammation During Denervation. *Front Pharmacol* 10:997.
- Hurtgen BJ, Ward CL, Leopold Wager CM, Garg K, Goldman SM, Henderson BEP, McKinley TO, Greising SM, Wenke JC, Corona BT (2017) Autologous minced muscle grafts improve endogenous fracture healing and muscle strength after musculoskeletal trauma. *Physiol Rep* 5:e13362.
- Järvinen TAH, Järvinen TLN, Kääriäinen M, Äärimaa V, Vaittinen S, Kalimo H, Järvinen M (2007) Muscle injuries: optimising recovery. *Best Pract Res Clin Rheumatol* 21:317–331.
- Järvinen TAH, Järvinen TLN, Kääriäinen M, Kalimo H, Järvinen M (2005) Muscle Injuries. *Am J Sports Med* 33:745–764.
- Jeng S-F, Rau C-S, Liliang P-C, Wu C-J, Lu T-H, Chen Y-C, Lin C-J, Hsieh C-H (2009) Profiling Muscle-Specific MicroRNA Expression after Peripheral Denervation and Reinnervation in a Rat Model. *J Neurotrauma* 26:2345–2353.
- Jin S (2005) p53, Autophagy and Tumor Suppression. *Autophagy* 1:171–173.
- Joazeiro CAP (1999) The Tyrosine Kinase Negative Regulator c-Cbl as a RING-Type, E2-Dependent Ubiquitin-Protein Ligase. *Science* (80-) 286:309–312.
- Kageyama S, Sou Y, Uemura T, Kametaka S, Saito T, Ishimura R, Kouno T, Bedford L, Mayer RJ, Lee M-S, Yamamoto M, Waguri S, Tanaka K, Komatsu M (2014) Proteasome Dysfunction Activates Autophagy and the Keap1-Nrf2 Pathway. *J Biol Chem* 289:24944–24955.
- Kaiser SE, Riley BE, Shaler TA, Trevino RS, Becker CH, Schulman H, Kopito RR (2011) Protein standard absolute quantification (PSAQ) method for the measurement of cellular ubiquitin pools.

Nat Methods 8:691–696.

Kamura T (1999) Rbx1, a Component of the VHL Tumor Suppressor Complex and SCF Ubiquitin Ligase. *Science* (80-) 284:657–661.

Kanning KC, Kaplan A, Henderson CE (2010) Motor Neuron Diversity in Development and Disease. *Annu Rev Neurosci* 33:409–440.

Karpati G, Engel WK (1968) Correlative histochemical study of skeletal muscle after suprasegmental denervation, peripheral nerve section, and skeletal fixation. *Neurology* 18:681–681.

Kaur J, Debnath J (2015) Autophagy at the crossroads of catabolism and anabolism. *Nat Rev Mol Cell Biol* 16:461–472.

Kedar V, McDonough H, Arya R, Li H-H, Rockman HA, Patterson C (2004) Muscle-specific RING finger 1 is a bona fide ubiquitin ligase that degrades cardiac troponin I. *Proc Natl Acad Sci* 101:18135–18140.

Kern H, Boncompagni S, Rossini K, Mayr W, Fanò G, Zanin ME, Podhorska-Okolow M, Protasi F, Carraro U (2004) Long-Term Denervation in Humans Causes Degeneration of Both Contractile and Excitation-Contraction Coupling Apparatus, Which Is Reversible by Functional Electrical Stimulation (FES): A Role for Myofiber Regeneration? *J Neuropathol Exp Neurol* 63:919–931.

Kim H, Jang M, Park R, Jo D, Choi I, Choe J, Oh WK, Park J (2018) Conessine treatment reduces dexamethasone-induced muscle atrophy by regulating MuRF1 and atrogin-1 expression. *J Microbiol Biotechnol* 28:520–526.

Kravtsova-Ivantsiv Y, Ciechanover A (2012) Non-canonical ubiquitin-based signals for proteasomal degradation. *J Cell Sci* 125:539–548.

Kroemer G, Mariño G, Levine B (2010) Autophagy and the Integrated Stress Response. *Mol Cell* 40:280–293.

Kuang S, Kuroda K, Le Grand F, Rudnicki MA (2007) Asymmetric Self-Renewal and Commitment of Satellite Stem Cells in Muscle. *Cell* 129:999–1010.

Kujala UM, Orava S, Järvinen M (1997) Hamstring Injuries. *Sport Med* 23:397–404.

Labeit S, Kohl CH, Witt CC, Labeit D, Jung J, Granzier H (2010) Modulation of Muscle Atrophy, Fatigue and MLC Phosphorylation by MuRF1 as Indicated by Hindlimb Suspension Studies on MuRF1-KO Mice. *J Biomed Biotechnol* 2010:1–9.

Lafreniere JF, Mills P, Bouchentouf M, Tremblay JP (2006) Interleukin-4 improves the migration of human myogenic precursor cells in vitro and in vivo. *Exp Cell Res* 312:1127–1141.

Lagirand-Cantaloube J, Cornille K, Csibi A, Batonnet-Pichon S, Leibovitch MP, Leibovitch SA (2009) Inhibition of Atrogin-1/MAFbx Mediated MyoD Proteolysis Prevents Skeletal Muscle Atrophy In Vivo *Parise G, ed. PLoS One* 4:e4973.

Lagirand-Cantaloube J, Offner N, Csibi A, Leibovitch MP, Batonnet-Pichon S, Tintignac LA, Segura CT, Leibovitch SA (2008) The initiation factor eIF3-f is a major target for Atrogin1/MAFbx function in skeletal muscle atrophy. *EMBO J* 27:1266–1276.

Langen RCJ, Haegens A, Vernooy JHJ, Wouters EFM, de Winther MPJ, Carlsen H, Steele C, Shoelson SE, Schols AMWJ (2012) NF- κ B Activation Is Required for the Transition of Pulmonary Inflammation to Muscle Atrophy. *Am J Respir Cell Mol Biol* 47:288–297.

Lapalombella R, Kern H, Adami N, Biral D, Zampieri S, Scordari A, di Tullio S, Marini M (2008) Persistence of regenerative myogenesis in spite of down-regulation of activity-dependent genes in long-term denervated rat muscle. *Neurol Res* 30:197–206.

Lee D, Goldberg AL (2013) SIRT1 protein, by blocking the activities of transcription factors FoxO1 and FoxO3, inhibits muscle atrophy and promotes muscle growth. *J Biol Chem* 288:30515–30526.

Li HH, Willis MS, Lockyer P, Miller N, McDonough H, Glass DJ, Patterson C (2007) Atrogin-1 inhibits Akt-dependent cardiac hypertrophy in mice via ubiquitin-dependent coactivation of Forkhead proteins. *J Clin Invest* 117:3211–3223.

- Lin J, Wu H, Tarr PT, Zhang C-Y, Wu Z, Boss O, Michael LF, Puigserver P, Isotani E, Olson EN, Lowell BB, Bassel-Duby R, Spiegelman BM (2002) Transcriptional co-activator PGC-1 α drives the formation of slow-twitch muscle fibres. *Nature* 418:797–801.
- Liu S, Hartleben B, Kretz O, Wiech T, Igarashi P, Mizushima N, Walz G, Huber TB (2012) Autophagy plays a critical role in kidney tubule maintenance, aging and ischemia-reperfusion injury. *Autophagy* 8:826–837.
- Lluri G, Langlois GD, McClellan B, Soloway PD, Jaworski DM (2006) Tissue inhibitor of metalloproteinase-2 (TIMP-2) regulates neuromuscular junction development via a β 1 integrin-mediated mechanism. *J Neurobiol* 66:1365–1377.
- Loos B, Toit A du, Hofmeyr J-HS (2014) Defining and measuring autophagosome flux—concept and reality. *Autophagy* 10:2087–2096.
- Lu D-X, Huang S-K, Carlson BM (1997) Electron microscopic study of long-term denervated rat skeletal muscle. *Anat Rec* 248:355–365.
- Luo J, Nikolaev AY, Imai S, Chen D, Su F, Shiloh A, Guarente L, Gu W (2001) Negative Control of p53 by Sir2 α Promotes Cell Survival under Stress. *Cell* 107:137–148.
- MacDonald EM, Andres-Mateos E, Mejias R, Simmers JL, Mi R, Park J-S, Ying S, Hoke A, Lee S-J, Cohn RD (2014) Denervation atrophy is independent from Akt and mTOR activation and is not rescued by myostatin inhibition. *Dis Model Mech* 7:471–481.
- Mackey AL, Mikkelsen UR, Magnusson SP, Kjaer M (2012) Rehabilitation of muscle after injury - the role of anti-inflammatory drugs. *Scand J Med Sci Sports* 22:e8–e14.
- Maffulli N, Del Buono A, Oliva F, Giai Via A, Frizziero A, Barazzuol M, Brancaccio P, Freschi M, Galletti S, Lisitano G, Melegati G, Nanni G, Pasta G, Ramponi C, Rizzo D, Testa V, Valent A (2015) Muscle Injuries: A Brief Guide to Classification and Management. *Transl Med @ UniSa* 12:14–18.
- Mammucari C, Milan G, Romanello V, Masiero E, Rudolf R, Del Piccolo P, Burden SJ, Di Lisi R, Sandri C, Zhao J, Goldberg AL, Schiaffino S, Sandri M (2007) FoxO3 Controls Autophagy in Skeletal Muscle In Vivo. *Cell Metab* 6:458–471.
- Mañas-García L, Bargalló N, Gea J, Barreiro E (2020) Muscle Phenotype, Proteolysis, and Atrophy Signaling During Reloading in Mice: Effects of Curcumin on the Gastrocnemius. *Nutrients* 12:388.
- Mann CJ, Perdiguero E, Kharraz Y, Aguilar S, Pessina P, Serrano AL, Muñoz-Cánoves P (2011) Aberrant repair and fibrosis development in skeletal muscle. *Skelet Muscle* 1:1–20.
- Marzetti E, Privitera G, Simili V, Wohlgemuth SE, Aulisa L, Pahor M, Leeuwenburgh C (2010) Multiple Pathways to the Same End: Mechanisms of Myonuclear Apoptosis in Sarcopenia of Aging. *Sci World J* 10:340–349.
- Masiero E, Agatea L, Mammucari C, Blaauw B, Loro E, Komatsu M, Metzger D, Reggiani C, Schiaffino S, Sandri M (2009) Autophagy is required to maintain muscle mass. *Cell Metab* 10:507–515.
- Masiero E, Sandri M (2010) Autophagy inhibition induces atrophy and myopathy in adult skeletal muscles. *Autophagy* 6:307–309.
- Mauro A (1961) SATELLITE CELL OF SKELETAL MUSCLE FIBERS. *J Biophys Biochem Cytol* 9:493–495.
- McClung JM, McCord TJ, Ryan TE, Schmidt CA, Green TD, Southerland KW, Reinardy JL, Mueller SB, Venkatraman TN, Lascola CD, Keum S, Marchuk DA, Spangenburg EE, Dokun A, Annex BH, Kontos CD (2017) BAG3 (Bcl-2-Associated Athanogene-3) Coding Variant in Mice Determines Susceptibility to Ischemic Limb Muscle Myopathy by Directing Autophagy. *Circulation* 136:281–296.
- McCully KK, Faulkner JA (1985) Injury to skeletal muscle fibers of mice following lengthening contractions. *J Appl Physiol* 59:119–126.
- McElhinny AS, Kakinuma K, Sorimachi H, Labeit S, Gregorio CC (2002) Muscle-specific RING finger-1 interacts with titin to regulate sarcomeric M-line and thick filament structure and may have

- nuclear functions via its interaction with glucocorticoid modulatory element binding protein-1. *J Cell Biol* 157:125–136.
- Midrio M (2006) The denervated muscle: facts and hypotheses. A historical review. *Eur J Appl Physiol* 98:1–21.
- Mitchell PO, Pavlath GK (2004) Skeletal muscle atrophy leads to loss and dysfunction of muscle precursor cells. *Am J Physiol Physiol* 287:C1753–C1762.
- Mizushima N, Levine B, Cuervo AM, Klionsky DJ (2008) Autophagy fights disease through cellular self-digestion. *Nature* 451:1069–1075.
- Mizushima N, Yamamoto A, Matsui M, Yoshimori T, Ohsumi Y (2004) In Vivo Analysis of Autophagy in Response to Nutrient Starvation Using Transgenic Mice Expressing a Fluorescent Autophagosome Marker. *Mol Biol Cell* 15:1101–1111.
- Mizushima N, Yoshimori T, Levine B (2010) Methods in Mammalian Autophagy Research. *Cell* 140:313–326.
- Mochizuki Y, Ojima K, Uezumi A, Masuda S, Yoshimura K, Takeda S (2005) Participation of Bone Marrow-Derived Cells in Fibrotic Changes in Denervated Skeletal Muscle. *Am J Pathol* 166:1721–1732.
- Moore-Carrasco R, Busquets S, Almendro V, Palanki M, López-Soriano F, Argilés J (2007) The AP-1/NF- κ B double inhibitor SP100030 can revert muscle wasting during experimental cancer cachexia. *Int J Oncol* 30:1239–1245.
- Moresi V, Williams AH, Meadows E, Flynn JM, Potthoff MJ, McAnally J, Shelton JM, Backs J, Klein WH, Richardson JA, Bassel-Duby R, Olson EN (2010) Myogenin and Class II HDACs Control Neurogenic Muscle Atrophy by Inducing E3 Ubiquitin Ligases. *Cell* 143:35–45.
- Mourikis P, Sambasivan R, Castel D, Rocheteau P, Bizzarro V, Tajbakhsh S (2012) A Critical Requirement for Notch Signaling in Maintenance of the Quiescent Skeletal Muscle Stem Cell State. *Stem Cells* 30:243–252.
- Mozdziak PE, Pulvermacher PM, Schultz E (2001) Muscle regeneration during hindlimb unloading results in a reduction in muscle size after reloading. *J Appl Physiol* 91:183–190.
- Mulder E, Clément G, Linnarsson D, Paloski WH, Wuyts FP, Zange J, Frings-Meuthen P, Johannes B, Shushakov V, Grunewald M, Maassen N, Buehlmeier J, Rittweger J (2015) Musculoskeletal effects of 5 days of bed rest with and without locomotion replacement training. *Eur J Appl Physiol* 115:727–738.
- Murphy MM, Lawson JA, Mathew SJ, Hutcheson DA, Kardon G (2011) Satellite cells, connective tissue fibroblasts and their interactions are crucial for muscle regeneration. *Development* 138:3625–3637.
- Mutsaers SE, Bishop JE, McGrouther G, Laurent GJ (1997) Mechanisms of tissue repair: from wound healing to fibrosis. *Int J Biochem Cell Biol* 29:5–17.
- Nagata Y, Kobayashi H, Umeda M, Ohta N, Kawashima S, Zammit PS, Matsuda R (2006) Sphingomyelin Levels in the Plasma Membrane Correlate with the Activation State of Muscle Satellite Cells. *J Histochem Cytochem* 54:375–384.
- Napolitano LM, Jaffray EG, Hay RT, Meroni G (2011) Functional interactions between ubiquitin E2 enzymes and TRIM proteins. *Biochem J* 434:309–319.
- Nichenko AS, Southern WM, Atuan M, Luan J, Peissig KB, Foltz SJ, Beedle AM, Warren GL, Call JA (2016) Mitochondrial maintenance via autophagy contributes to functional skeletal muscle regeneration and remodeling. *Am J Physiol Physiol* 311:C190–C200.
- Nichenko AS, Southern WM, Tehrani KF, Qualls AE, Flemington AB, Mercer GH, Yin A, Mortensen LJ, Yin H, Call JA (2020) Mitochondrial-specific autophagy linked to mitochondrial dysfunction following traumatic freeze injury in mice. *Am J Physiol Cell Physiol* 318:242–252.
- Oliván S, Calvo AC, Gasco S, Muñoz MJ, Zaragoza P, Osta R (2015) Time-Point Dependent Activation of Autophagy and the UPS in SOD1G93A Mice Skeletal Muscle Musaro A, ed. *PLoS One* 10:e0134830.

- Otis JS, Niccoli S, Hawdon N, Sarvas JL, Frye MA, Chicco AJ, Lees SJ (2014) Pro-Inflammatory Mediation of Myoblast Proliferation Lluich GL, ed. *PLoS One* 9:e92363.
- Paolini A, Omairi S, Mitchell R, Vaughan D, Matsakas A, Vaiyapuri S, Ricketts T, Rubinsztein DC, Patel K (2018) Attenuation of autophagy impacts on muscle fibre development, starvation induced stress and fibre regeneration following acute injury. *Sci Rep* 8:9062.
- Park I-H, Chen J (2005) Mammalian Target of Rapamycin (mTOR) Signaling Is Required for a Late-stage Fusion Process during Skeletal Myotube Maturation. *J Biol Chem* 280:32009–32017.
- Park I-H, Erbay E, Nuzzi P, Chen J (2005) Skeletal myocyte hypertrophy requires mTOR kinase activity and S6K1. *Exp Cell Res* 309:211–219.
- Park S-J, Ahmad F, Philp A, Baar K, Williams T, Luo H, Ke H, Rehmann H, Taussig R, Brown AL, Kim MK, Beaven MA, Burgin AB, Manganiello V, Chung JH (2012) Resveratrol Ameliorates Aging-Related Metabolic Phenotypes by Inhibiting cAMP Phosphodiesterases. *Cell* 148:421–433.
- Parzych KR, Klionsky DJ (2014) An overview of autophagy: morphology, mechanism, and regulation. *Antioxid Redox Signal* 20:460–473.
- Passmore LA, Barford D (2004) Getting into position: the catalytic mechanisms of protein ubiquitylation. *Biochem J* 379:513–525.
- Pelosi L, Giacinti C, Nardis C, Borsellino G, Rizzuto E, Nicoletti C, Wannenes F, Battistini L, Rosenthal N, Molinaro M, Musar A (2007) Local expression of IGF-1 accelerates muscle regeneration by rapidly modulating inflammatory cytokines and chemokines. *FASEB J* 21:1393–1402.
- Perdan K, Lipnik-Štangelj M, Kržan M (2009) Chapter 8 The Impact of Astrocytes in the Clearance of Neurotransmitters by Uptake and Inactivation. In, pp 211–235.
- Perdiguer E, Ruiz-Bonilla V, Serrano AL, Muñoz-Cánoves P (2007) Genetic Deficiency of p38 α Reveals its Critical Role in Myoblast Cell Cycle Exit: The p38 α -JNK Connection. *Cell Cycle* 6:1298–1303.
- Perera S, Mankoo B, Gautel M (2012) Developmental regulation of MURF E3 ubiquitin ligases in skeletal muscle. *J Muscle Res Cell Motil* 33:107–122.
- Pickart CM, Cohen RE (2004) Proteasomes and their kin: proteases in the machine age. *Nat Rev Mol Cell Biol* 5:177–187.
- Pocock JM, Kettenmann H (2007) Neurotransmitter receptors on microglia. *Trends Neurosci* 30:527–535.
- Porquet D, Casadesús G, Bayod S, Vicente A, Canudas AM, Vilaplana J, Pelegrí C, Sanfeliu C, Camins A, Pallàs M, del Valle J (2013) Dietary resveratrol prevents Alzheimer's markers and increases life span in SAMP8. *Age (Omaha)* 35:1851–1865.
- Prentice WE (2020) Rehabilitation techniques for Sports Medicine and Athletic training.
- Qaisar R, Bhaskaran S, Ranjit R, Sataranatarajan K, Premkumar P, Huseman K, Van Remmen H (2019) Restoration of SERCA ATPase prevents oxidative stress-related muscle atrophy and weakness. *Redox Biol* 20:68–74.
- Raben N, Hill V, Shea L, Takikita S, Baum R, Mizushima N, Ralston E, Plotz P (2008) Suppression of autophagy in skeletal muscle uncovers the accumulation of ubiquitinated proteins and their potential role in muscle damage in Pompe disease. *Hum Mol Genet* 17:3897–3908.
- Rall J (1996) Role of Parvalbumin in Skeletal Muscle Relaxation. *Physiology* 11:249–255.
- Ramírez C, Russo TL, Sandoval MC, Dentillo AA, Couto MAS, Durigan JLQ, Salvini TF (2011) Joint Inflammation Alters Gene and Protein Expression and Leads to Atrophy in the Tibialis Anterior Muscle in Rats. *Am J Phys Med Rehabil* 90:930–939.
- Ravikumar B, Acevedo-Arozena A, Imarisio S, Berger Z, Vacher C, O'Kane CJ, Brown SDM, Rubinsztein DC (2005) Dynein mutations impair autophagic clearance of aggregate-prone proteins. *Nat Genet* 37:771–776.
- Rawls A, Valdez MR, Zhang W, Richardson J, Klein WH, Olson EN (1998) Overlapping functions of the myogenic bHLH genes MRF4 and MyoD revealed in double mutant mice. *Development*

125:2349–2358.

Reggiori F, Ungermann C (2017) Autophagosome Maturation and Fusion. *J Mol Biol* 429:486–496.

Relaix F, Zammit PS (2012) Satellite cells are essential for skeletal muscle regeneration: the cell on the edge returns centre stage. *Development* 139:2845–2856.

Robinson K, Culley D, Waring S, Lamb GD, Easton C, Casarotto MG, Dulhunty AF (2020) Peptide mimetic compounds can activate or inhibit cardiac and skeletal ryanodine receptors. *Life Sci* 260:118234.

Rodrigues ADC, Andreo JC, Júnior GMR, dos Santos NB, Moraes LHR, Lauris JRP (2007) Fat cell invasion in long-term denervated skeletal muscle. *Microsurgery* 27:664–667.

Romanello V, Guadagnin E, Gomes L, Roder I, Sandri C, Petersen Y, Milan G, Masiero E, Del Piccolo P, Foretz M, Scorrano L, Rudolf R, Sandri M (2010) Mitochondrial fission and remodelling contributes to muscle atrophy. *EMBO J* 29:1774–1785.

Romeo-Guitart D, Forés J, Herrando-Grabulosa M, Valls R, Leiva-Rodríguez T, Galea E, González-Pérez F, Navarro X, Petegnief V, Bosch A, Coma M, Mas JM, Casas C (2018a) Neuroprotective Drug for Nerve Trauma Revealed Using Artificial Intelligence. *Sci Rep* 8:1–15.

Romeo-Guitart D, Forés J, Navarro X, Casas C (2017) Boosted Regeneration and Reduced Denervated Muscle Atrophy by NeuroHeal in a Pre-clinical Model of Lumbar Root Avulsion with Delayed Reimplantation. *Sci Rep* 7:1–12.

Romeo-Guitart D, Leiva-Rodríguez T, Espinosa-Alcantud M, Sima N, Vaquero A, Domínguez-Martín H, Ruano D, Casas C, Domínguez-Martín H, Ruano D, Casas C (2018b) SIRT1 activation with neuroheal is neuroprotective but SIRT2 inhibition with AK7 is detrimental for disconnected motoneurons. *Cell Death Dis* 9:531.

Romeo-Guitart D, Leiva-Rodríguez T, Forés J, Casas C (2019) Improved Motor Nerve Regeneration by SIRT1/Hif1a-Mediated Autophagy. *Cells* 8:1354.

Romeo-Guitart D, Marcos-DeJuana C, Marmolejo-Martínez-Artesero S, Navarro X, Casas C (2020) Novel neuroprotective therapy with NeuroHeal by autophagy induction for damaged neonatal motoneurons. *Theranostics* 10:5154–5168.

Russell RC, Tian Y, Yuan H, Park HW, Chang Y-Y, Kim J, Kim H, Neufeld TP, Dillin A, Guan K-L (2013) ULK1 induces autophagy by phosphorylating Beclin-1 and activating VPS34 lipid kinase. *Nat Cell Biol* 15:741–750.

Ryall JG (2012) The role of sirtuins in the regulation of metabolic homeostasis in skeletal muscle. *Curr Opin Clin Nutr Metab Care* 15:561–566.

Sacheck JM, Hyatt J-PK, Raffaello A, Jagoe RT, Roy RR, Edgerton VR, Lecker SH, Goldberg AL (2007) Rapid disuse and denervation atrophy involve transcriptional changes similar to those of muscle wasting during systemic diseases. *FASEB J* 21:140–155.

Salminen A, Kaarniranta K (2009) NF- κ B Signaling in the Aging Process. *J Clin Immunol* 29:397–405.

Sanchez AMJ, Csibi A, Raibon A, Docquier A, Lagirand-Cantaloube J, Leibovitch MP, Leibovitch SA, Bernardi H (2013) eIF3f: A central regulator of the antagonism atrophy/hypertrophy in skeletal muscle. *Int J Biochem Cell Biol* 45:2158–2162.

Sandri M (2008) Signaling in Muscle Atrophy and Hypertrophy. *Physiology* 23:160–170.

Sandri M, Lin J, Handschin C, Yang W, Arany ZP, Lecker SH, Goldberg AL, Spiegelman BM (2006) PGC-1 protects skeletal muscle from atrophy by suppressing FoxO3 action and atrophy-specific gene transcription. *Proc Natl Acad Sci* 103:16260–16265.

Sandri M, Sandri C, Gilbert A, Skurk C, Calabria E, Picard A, Walsh K, Schiaffino S, Lecker SH, Goldberg AL (2004) Foxo Transcription Factors Induce the Atrophy-Related Ubiquitin Ligase Atrogin-1 and Cause Skeletal Muscle Atrophy. *Cell* 117:399–412.

Sartore S, Gorza L, Schiaffino S (1982) Fetal myosin heavy chains in regenerating muscle. *Nature* 298:294–296.

- Saurin AJ, Borden KLB, Boddy MN, Freemont PS (1996) Does this have a familiar RING? Trends Biochem Sci 21:208–214.
- Scharner J, Zammit PS (2011) The muscle satellite cell at 50: the formative years. Skelet Muscle 1:28.
- Schiaffino S, HanzlíkováVěra (1972) Studies on the effect of denervation in developing muscle. II. The lysosomal system. J Ultrastruct Res 39:1–14.
- Schmalbruch H, Al-Amood WS, Lewis DM (1991) Morphology of long-term denervated rat soleus muscle and the effect of chronic electrical stimulation. J Physiol 441:233–241.
- Schug TT, Xu Q, Gao H, Peres-da-Silva A, Draper DW, Fessler MB, Purushotham A, Li X (2010) Myeloid Deletion of SIRT1 Induces Inflammatory Signaling in Response to Environmental Stress. Mol Cell Biol 30:4712–4721.
- Schultz E, Jaryszak DL, Valliere CR (1985) Response of satellite cells to focal skeletal muscle injury. Muscle Nerve 8:217–222.
- Schwaller B (2012) The use of transgenic mouse models to reveal the functions of Ca²⁺ buffer proteins in excitable cells. Biochim Biophys Acta - Gen Subj 1820:1294–1303.
- Schwaller B, Dick J, Dhoot G, Carroll S, Vrbova G, Nicotera P, Pette D, Wyss A, Bluethmann H, Hunziker W, Celio MR (1999) Prolonged contraction-relaxation cycle of fast-twitch muscles in parvalbumin knockout mice. Am J Physiol Physiol 276:C395–C403.
- Serrano AL, Baeza-Raja B, Perdiguero E, Jardí M, Muñoz-Cánoves P (2008) Interleukin-6 Is an Essential Regulator of Satellite Cell-Mediated Skeletal Muscle Hypertrophy. Cell Metab 7:33–44.
- Shen S, Liao Q, Liu J, Pan R, Lee SM, Lin L (2019) Myricanol rescues dexamethasone-induced muscle dysfunction via a sirtuin 1-dependent mechanism. J Cachexia Sarcopenia Muscle 10:429–444.
- Shen W, Li Y, Tang Y, Cummins J, Huard J (2005) NS-398, a Cyclooxygenase-2-Specific Inhibitor, Delays Skeletal Muscle Healing by Decreasing Regeneration and Promoting Fibrosis. Am J Pathol 167:1105–1117.
- Sicari BM, Rubin JP, Dearth CL, Wolf MT, Ambrosio F, Boninger M, Turner NJ, Weber DJ, Simpson TW, Wyse A, Brown EHP, Dziki JL, Fisher LE, Brown S, Badyak SF (2014) An Acellular Biologic Scaffold Promotes Skeletal Muscle Formation in Mice and Humans with Volumetric Muscle Loss. Sci Transl Med 6:234ra58-234ra58.
- Smith C, Kruger MJ, Smith RM, Myburgh KH (2008) The Inflammatory Response to Skeletal Muscle Injury. Sport Med 38:947–969.
- Smith HK, Maxwell L, Martyn JA, Bass JJ (2000) Nuclear DNA fragmentation and morphological alterations in adult rabbit skeletal muscle after short-term immobilization. Cell Tissue Res 302:235–241.
- Song S, Kong X, Acosta S, Sava V, Borlongan C, Sanchez-Ramos J (2016) Granulocyte-colony stimulating factor promotes brain repair following traumatic brain injury by recruitment of microglia and increasing neurotrophic factor expression. Restor Neurol Neurosci 34:415–431.
- Squecco R, Carraro U, Kern H, Pond A, Adami N, Biral D, Vindigni V, Boncompagni S, Pietrangelo T, Bosco G, Fanò G, Marini M, Abruzzo PM, Germinario E, Danieli-Betto D, Protasi F, Francini F, Zampieri S (2009) A Subpopulation of Rat Muscle Fibers Maintains an Assessable Excitation-Contraction Coupling Mechanism After Long-Standing Denervation Despite Lost Contractility. J Neuropathol Exp Neurol 68:1256–1268.
- Takekura H, Kasuga N, Kitada K, Yoshioka T (1996) Morphological changes in the triads and sarcoplasmic reticulum of rat slow and fast muscle fibres following denervation and immobilization. J Muscle Res Cell Motil 17:391–400.
- Tang AH, Rando TA (2014) Induction of autophagy supports the bioenergetic demands of quiescent muscle stem cell activation. EMBO J 33:2782–2797.
- Tennen RI, Michishita-Kioi E, Chua KF (2012) Finding a Target for Resveratrol. Cell 148:387–389.

- Thaloor D, Miller KJ, Gephart J, Mitchell PO, Pavlath GK (1999) Systemic administration of the NF- κ B inhibitor curcumin stimulates muscle regeneration after traumatic injury. *Am J Physiol Physiol* 277:C320–C329.
- Tintignac LA, Lagirand J, Batonnet S, Sirri V, Leibovitch MP, Leibovitch SA (2005) Degradation of MyoD Mediated by the SCF (MAFbx) Ubiquitin Ligase. *J Biol Chem* 280:2847–2856.
- Tonkin J, Villarroya F, Puri PL, Vinciguerra M (2012) SIRT1 signaling as potential modulator of skeletal muscle diseases. *Curr Opin Pharmacol* 12:372–376.
- Torres R, Ribeiro F, Alberto Duarte J, Cabri JMH (2012) Evidence of the physiotherapeutic interventions used currently after exercise-induced muscle damage: Systematic review and meta-analysis. *Phys Ther Sport* 13:101–114.
- Tower SS (1935) Atrophy and degeneration in skeletal muscle. *Am J Anat* 56:1–43.
- Tyml K (2001) Structural and functional changes in the microvasculature of disused skeletal muscle. *Front Biosci* 6:d45.
- Vaziri H, Dessain SK, Eaton EN, Imai S-I, Frye RA, Pandita TK, Guarente L, Weinberg RA (2001) hSIR2/SIRT1 Functions as an NAD-Dependent p53 Deacetylase. *Cell* 107:149–159.
- Vergne I, Roberts E, Elmaoued RA, Tosch V, Delgado MA, Proikas-Cezanne T, Laporte J, Deretic V (2009) Control of autophagy initiation by phosphoinositide 3-phosphatase jumpy. *EMBO J* 28:2244–2258.
- Viguie CA, Lu D-X, Huang S-K, Rengen H, Carlson BM (1997) Quantitative study of the effects of long-term denervation on the extensor digitorum longus muscle of the rat. *Anat Rec* 248:346–354.
- Vinciguerra M, Fulco M, Ladurner A, Sartorelli V, Rosenthal N (2010a) SirT1 in muscle physiology and disease: lessons from mouse models. *Dis Model Mech* 3:298–303.
- Vinciguerra M, Musaro A, Rosenthal N (2010b) Regulation of Muscle Atrophy in Aging and Disease. In: *Advances in Experimental Medicine and Biology*, pp 211–233. Springer, Boston, MA.
- Walton M, Rothwell AG (1963) Reactions of thigh tissues of sheep to blunt trauma. *Clin Orthop Relat Res* 176:273–281.
- Whalen RG, Harris JB, Butler-Browne GS, Sesodia S (1990) Expression of myosin isoforms during notexin-induced regeneration of rat soleus muscles. *Dev Biol* 141:24–40.
- White GE, Wells GD (2013) Cold-water immersion and other forms of cryotherapy: physiological changes potentially affecting recovery from high-intensity exercise. *Extrem Physiol Med* 2:26.
- Witherspoon JW, Meilleur KG (2016) Review of RyR1 pathway and associated pathomechanisms. *Acta Neuropathol Commun* 4:121.
- Wohlgemuth SE, Seo AY, Marzetti E, Lees HA, Leeuwenburgh C (2010) Skeletal muscle autophagy and apoptosis during aging: Effects of calorie restriction and life-long exercise. *Exp Gerontol* 45:138–148.
- Woo JH, Shimon Y, Yang WS, Subramaniam P, Iyer A, Nicoletti P, Rodríguez Martínez M, López G, Mattioli M, Realubit R, Karan C, Stockwell BR, Bansal M, Califano A (2015) Elucidating Compound Mechanism of Action by Network Perturbation Analysis. *Cell* 162:441–451.
- Xiao Y, Karam C, Yi J, Zhang L, Li X, Yoon D, Wang H, Dhakal K, Ramlow P, Yu T, Mo Z, Ma J, Zhou J (2018) ROS-related mitochondrial dysfunction in skeletal muscle of an ALS mouse model during the disease progression. *Pharmacol Res* 138:25–36.
- Yablonka-Reuveni Z, Day K, Vine A, Shefer G (2008) Defining the transcriptional signature of skeletal muscle stem cells^{1,2}. *J Anim Sci* 86:E207–E216.
- Yeung F, Hoberg JE, Ramsey CS, Keller MD, Jones DR, Frye RA, Mayo MW (2004) Modulation of NF- κ B-dependent transcription and cell survival by the SIRT1 deacetylase. *EMBO J* 23:2369–2380.
- Zammit PS, Partridge TA, Yablonka-Reuveni Z (2006) The Skeletal Muscle Satellite Cell: The Stem Cell That Came in From the Cold. *J Histochem Cytochem* 54:1177–1191.

Zelena D, Demeter K, Haller J, Balázsfői D (2017) Considerations for the use of virally delivered genetic tools for in-vivo circuit analysis and behavior in mutant mice. *Behav Pharmacol* 28:598–609.

Zhang J, Yu Y, Wang J (2020) Protein Nutritional Support: The Classical and Potential New Mechanisms in the Prevention and Therapy of Sarcopenia. *J Agric Food Chem* 68:4098–4108.

Zhao J, Brault JJ, Schild A, Cao P, Sandri M, Schiaffino S, Lecker SH, Goldberg AL (2007) FoxO3 Coordinately Activates Protein Degradation by the Autophagic/Lysosomal and Proteasomal Pathways in Atrophying Muscle Cells. *Cell Metab* 6:472–483.

Zorzano A, Hernández-Alvarez MI, Palacín M, Mingrone G (2010a) Alterations in the mitochondrial regulatory pathways constituted by the nuclear co-factors PGC-1 α or PGC-1 β and mitofusin 2 in skeletal muscle in type 2 diabetes. *Biochim Biophys Acta - Bioenerg* 1797:1028–1033.

Zorzano A, Hernández-Alvarez MI, Palacín M, Mingrone G (2010b) Alterations in the mitochondrial regulatory pathways constituted by the nuclear co-factors PGC-1 α or PGC-1 β and mitofusin 2 in skeletal muscle in type 2 diabetes. *Biochim Biophys Acta - Bioenerg* 1797:1028–1033.

ACKNOWLEDGEMENTS
